Eva Thaler, Bakk. rer. nat.

Secretion of human and bacterial model proteins via the sec- or tat-pathway in *Ralstonia eutropha* H16

MASTER'S THESIS

to achieve the university degree of

Diplom-Ingenieurin

Master's degree programme: Biotechnology

submitted to

Graz University of Technology

Supervisors

Univ.-Prof. Dipl.-Ing. Dr.techn. Helmut Schwab

Mag.rer.nat. Dr.rer.nat. Petra Köfinger

Institute of Molecular Biotechnology

Graz, February 2015

AFFIDAVIT

I declare that I have authored this thesis independently, that I have not used other than the declared sources/resources, and that I have explicitly indicated all material which has been quoted either literally or by content from the sources used. The text document uploaded to TUGRAZonline is identical to the present master‘s thesis.

_____ _____

Date Signature

Acknowledgement

First of all I want to thank Prof. Helmut Schwab for giving me the opportunity and necessary support to complete my master thesis in the institute of molecular biotechnology. Furthermore, I want to thank my supervisors Dr. Petra Köfinger and Steffen Gruber for their constant aid and encouraging supervision.

Moreover, I would like to thank all my colleagues from the first floor with special thanks to Daniel Schwendenwein, Zalina Magomedova, Melanie Hirz and Simone Scharl for their friendship and assistance. It was a pleasure working with you.

Finally I want to thank my family and friends for their unconditional encouragement and support throughout my whole education.

Abstract

Ralstonia eutropha H16 is a Gram-negative soil bacterium, which has sparked great interest as a recombinant production organism in recent years. To date, heterologous gene expression was accomplished by plasmid and integration based systems and numerous well-known promoters (e.g. P_{T5}, P_{T7} and P_{tac}) were shown to be active. However, little is known about the functionality of secretion mechanisms of *R. eutropha* H16. Thus, the aim of this work was to examine if *R. eutropha* H16 is capable of recombinant protein secretion based on the examples of the three model proteins hGH, CelA and Lev.

Therefore, 20 signal peptides from identified exoproteins from *R. solanacearum* and 1 signal peptide from the known periplasmic protein NosZ of *R. eutropha* H16 were chosen and fused to the N-terminal end of the reporter proteins. The fusion constructs were cloned into expression vectors suitable for the expression in *R. eutropha* H16 and the secretion efficiencies of the individual signal peptides were measured in respect of the activity of the reporter proteins in the cell-free supernatants.

The secretory assays revealed that hGH could not be detected in the extracellular medium of *R. eutropha* H16 transconjugants. However, it could not be determined whether the lacking detectability was due to inefficient translocation of hGH or due to limitations in the detection assay. In contrast to the results of hGH secretion, 2 different CelA activity assays proved that 4 Sec- and 6 Tat- specific signal peptides were able to secrete CelA into the extracellular medium in *R. eutropha* H16 transconjugants. The best secretory yield of CelA could be achieved with the Tat- specific signal peptide F504_2793. Similar CelA secretion levels could also be achieved by the Sec- specific signal peptides CbhA and Aac. Moreover, 5 signal peptides were able to secrete Lev across the inner and outer membrane of *R. eutropha* H16. From those five, only 1 signal sequence was specific for the Sec translocase, while the others were specific for the Tat-pathway. The best signal peptide for the secretion of Lev was the Tat- specific F504_2199.

Thus, the functionality of the Sec- and Tat- translocase in *R. eutropha* H16 could be proven to be used for the secretion of heterologous proteins of prokaryotic origin. Therefore, a huge step in the establishment of *R. eutropha* H16 as an alternative secretory production host could be achieved.

Zusammenfassung

Das Gram-negative Bakterium *Ralstonia eutropha* H16 hat in den letzen Jahren große Aufmerksamkeit als rekombinanter Proteinproduzent auf sich gezogen. Zum jetzigen Zeitpunkt wurde die heterologe Genexpression durch Plasmid- oder Integrations-basierende Systeme ermöglicht und viele bekannte Promotoren (z.B. P_{T5}, P_{T7} und P_{tac}) konnten gute Expressionsraten aufweisen. Über die Funktionalität der Sekretionsmechanismen in *R. eutropha* H16 ist jedoch wenig bekannt. Das Ziel dieser Masterarbeit war es daher, die Funktionalität des TypII- Sekretionsweges anhand der rekombinanten Proteinsekretion von drei heterologen Proteinen (hGH, CelA und Lev) zu beweisen.

Dafür wurden 20 Signalsequenzen von bereits identifizierten Exoproteinen aus *R. solanacearum* und 1 Signalsequenz von einem bereits bekannten periplasmatischen Protein aus *R. eutropha* H16 ausgewählt und an das N- terminale Ende der Modellproteine fusioniert. Die Sekretionsproduktivität der einzelnen Signalsequenzen wurde anhand der Aktivität der Modellproteine im zellfreien Fermentationsüberstand gemessen.

Die sekretorischen Analysen ergaben, dass hGH im extrazellulären Medium von *R. eutropha* H16 Transkonjuganten nicht nachgewiesen werden konnte. Es konnte jedoch nicht festgestellt werden, ob die mangelnde Nachweisbarkeit aufgrund der zu geringen Sekretion von hGH oder aufgrund Limitierungen der Detektionstests hervorgeht. Im Gegensatz dazu konnten 2 unterschiedliche CelA Aktivitätstests beweisen, dass CelA durch 4 Sec- und 6 Tat- spezifische Signalpeptide in das extrazelluläre Medium von *R. eutropha* H16 Transkonjuganten sekretiert wurde. Der beste CelA Ertrag im zellfreien Überstand konnte durch das Tat- spezifische Signalpeptid F504_2793 erreicht werden. Ähnliche CelA Sekretionsausbeuten konnten durch die Sec-spezifischen Signalpeptide CbhA und Aac erreich werden. Weiters konnte bewiesen werden, dass Lev durch 1 Sec-spezifische und 4 Tat- spezifische Signalsequenzen in das extrazelluläre Medium sekretiert werden konnte. Die beste Lev Ausbeute im zellfreien Überstand konnte durch das Tat- spezifische Signalpeptid F504_2199 erreicht werden.

Anhand dieser Masterarbeit konnte die Funktionalität der Sec- und Tat- Translocase für die sekretorische Produktion von heterologen Proteinen bestätigt werden. Damit konnte

eine gute Basis für die Anwendung von *R. eutropha* H16 als alternativer Produktionsorganismus für sekretorische Proteine gelegt werden.

Table of Contents

II. List of abbreviatons

ABC	ATP-binding cassette
ADP	adenosine-5'-diphosphate
APS	ammonium persulfate
ATP	adenosine-5'-triphosphate
Bp	base pairs
BSA	bovine serum albumin
CelA	Cellulase A
CMC	Carboxymethylcellulose
CP	coupling protein
EDTA	Ethylenediaminetetraacetic acid
ELISA	Enzyme linked immunosorbent assay
FSB	final sample buffer
Fwd	forward
G-6-P	glucose-6-phosphate
G-6-P-DH	glucose-6-phosphate dehydrogenase
HCl	hydrochloric acid
hGH	human growth hormone
HK	hexokinase
HMM	Hidden Markov Model
IM	inner membrane
IMP	inner membrane protein
LB	lysogeny broth
Lev	Levanase
NaCl	sodium chloride
NAD	nicotinamide adenine dinucleotide
NB	nutrient broth
OD	optical density
oePCR	overlap extension PCR
OM	outer membrane
OMP	outer membrane protein
PC	positive control
PCR	polymerase chain reaction
pHBAH	*para*-hydrobenzoic acid hydrazide
P_{tac}	tac promoter
Rev	reverse
SDS	sodium dodecyl sulfate
SDS-PAGE	sodium dodecyl sulfate polyacrylamide gel electrophoresis
SP	signal peptide
SRP	signal recognition particle
T1SS	type I secretion system
T2SS	type II secretion system
T3SS	type III secretion system
T4SS	type IV secretion system
T5SS	type V secretion system
T6SS	type VI secretion system
Tat	Twin-arginine translocation
TEMED	Tetramethylethylenediamine
TBS	Tris buffered saline
Tm	melting temperature
TMP	Tris buffered milk protein
TSB	tryptic soy broth
TY	tryptone broth
ΔS	without signal peptide

III. List of figures

IV. List of tables

1 Introduction

1.1 *Ralstonia eutropha* H16

Ralstonia eutropha H16 (now named *Cupriavidus necator* H16), a ubiquitous inhabitant of soil and fresh water, is a Gram-negative bacterium belonging to the β-subdivision of *Proteobacteria* [1, 2]. The organism consists of a 7.4 Mbp multi replicon genome, which is comprised of three circular replicons: chromosome 1 (4,052,032 bp), chromosome 2 (2,912,490 bp) and the megaplasmid pHG1 (452,156 bp). Chromosome 1 carries genes responsible for most key functions of DNA replication, transcription and translation as well as genes for translocation, whereas genes for the degradation of aromatic compounds and different genes for alternative carbohydrate metabolism are located on chromosome 2 [2]. *R. eutropha* H16 has been well studied for its ability to accumulate the biodegradable polymer poly-3-hydroxybutyrate (PHB) in intracellular storage granules under growth-limiting conditions in the presence of excessive carbon sources and has become a well-known model organism for the oxidation of molecular hydrogen (H_2) and the fixation of carbon dioxide (CO_2) [2, 3, 4]. Furthermore, in the absence of O_2 *R. eutropha* H16 is capable to switch to anaerobic respiration by using NO_3^- and NO_2^- as alternative electron acceptors [2].

R. eutropha H16 is also capable of switching between heterotrophic growth using organic compounds as the source of energy, and lithoautotrophic CO_2 fixation, where H_2 is utilized as the energy source [5]. Under heterotrophic cultivation conditions, it is able to use various carbon and energy sources, such as fructose, N-acetylglucosamine and various organic acids and the sugars are metabolized via the Entner-Doudoroff (KPDG) pathway [2]. In the absence of organic compounds, *R. eutropha* H16 is capable to fix CO_2 via the Calvin-Benson-Bassham (CBB) cycle and oxidize H_2 to meet the energy demand [5]. The reversible oxidation of H_2 is catalysed by a membrane-bound hydrogenase, coupled to the respiratory chain, and a cytoplasmic soluble NAD^+-reducing hydrogenase [6]. Both [NiFe] hydrogenases are encoded on the megaplasmid pHG1 [2].

In recent years, *R. eutropha* H16 has sparked great interest as an alternative bacterial expression host as the system permits high-cell-density growth (up to 230 g L^{-1}) in large-scale bioreactors [7]. Furthermore, using *R. eutropha* H16 as a recombinant expression host allows overcoming some disadvantages of the traditional *Escherichia coli* based

expression systems. The problem of inclusion body formation, which limits the spectrum of heterologous proteins expressable in *E. coli*, has not been observed in *R. eutropha* H16 yet [7]. Several studies examined the expression of foreign genes based on plasmid or integration systems and numerous well-known promoters were shown to be active in *R. eutropha* H16 including P_{tac}, P_{lac}, P_{BAD}, P_{T7}, P_{T5} and P_{J5} [8, 9, 10, 11, 12]. So far, heterologous gene expression was achieved by either complex inducible or constitutive expression systems [9, 10, 11]. P_{tac} and P_{lac} are strong promoters that can only be used under constitutive conditions as it is not possible yet to induce gene expression with IPTG (isopropyl-β-D-thiogalactopyranoside) or lactose [10]. *R. eutropha* H16 lacks the galactose permease gene *lacY*, which is responsible for the transport of lactose or IPTG into *E. coli* [11]. Gruber et al. developed a number of stable plasmid based expression systems with varying promoters and origins of replication for protein production in *R. eutropha* H16. Different promoters were examined comparing their expression levels of eGFP and P_{J5} was characterized as the strongest promoter under constitutive conditions [10].

To date, there is little data available if *R. eutropha* H16 has a functional secretion mechanism. So far, only three perplasmic enzymes carrying a N-terminal signal peptide are known to be synthesized by *R. eutropha* H16: the nitrous oxide reductase (NosZ), the membrane-bound hydrogenase (MBH) and the periplasmic nitrate reductase (Nap) [13]. Furthermore, analysis of the genome sequence revealed that *R. eutropha* H16 possesses genes for four of the six secretion pathways (type I, II, IV and VI), but their functionality has not been examined yet [14].

1.2 *Ralstonia solanacearum*

Ralstonia solanacearum is a widely distributed soil-borne pathogen belonging to the β-subclass of *Proteobacteria* and shares 93 % identity with *R. eutropha* H16. As one of the causes of lethal wilting disease in more than 200 plant species including tomatoes, potatoes and bananas, several studies have focused on the pathogenesis of bacterial wilt. While plant pathogenesis is not fully understood yet, secreted proteins play a key element in the course of disease [15, 16, 17]. *R. solanacearum* has been reported to secrete more than 100 proteins into the extracellular medium and analysis of the

genome sequence revealed that all the major secretion pathways described in Gram-negative bacteria are present in the model strain *R. solanacearum* GMI1000 [15]. Exoproteins, such as cell wall degrading enzymes and other additional proteins, secreted through the type II secretion system (T2SS) contribute to the disease development [15, 17, 18]. Zuleta examined further exoproteins secreted by *R. solanacearum* and 44 exoproteins were identified as T2SS substrates, which are more than reported in any other Gram-negative bacteria [19].

1.3 Recombinant secretory protein production

The production of recombinant proteins in bacteria and yeast has become increasingly valuable in a wide range of applicable areas, such as structural analysis, diagnostic investigation, as well as, for the production of pharmaceutical proteins. Recombinant proteins synthesized by Gram-negative bacteria may agglomerate in one of the three compartments: cytoplasm, periplasm or extracellular milieu [20]. If possible, the secretory protein production is the strategy of choice as it allows simplified downstream processing at reduced costs. Compared to cytoplasmic protein production, the isolation and purification of proteins secreted into the extracellular medium is much easier due to reduced impurity with cellular components [21]. Furthermore, the contamination with liposaccharides can be avoided, as well as, the potential of proteolytic degradation can be decreased [21, 22]. If glycosylation or other post-translational modifications are not necessary, *E. coli* is the host of choice. However, the disadvantages of *E. coli* include incorrect protein folding due to reducing intracytosolic conditions, production of non-functional proteins, accumulation of insoluble proteins in the form of inclusion bodies and intracellular degradation of proteins [23, 24, 25]. Another drawback of *E. coli* as an expression host in the secretory protein production is the limited capacity of its secretion pathways and compared to other expression hosts (i.e. the Gram-positive bacteria *Bacillus subtilis*), the yields of secreted recombinant proteins is low [23]. Successful protein secretion in Gram-negative bacteria requires the effective translocation of the protein across the inner and the outer membranes and depends on naturally occurring secretion systems adapted by genetic modifications [26]. The translocation across the inner membrane (IM) can be achieved by either the general secretory pathway (Sec) or the twin-arginine (Tat) pathway. By fusing secretion signals to reporter genes,

recombinant secretory protein production has been demonstrated in a wide range of expression hosts (i.e. *E. coli, Streptomyces lividans, Pseudoalteromonas haloplanktis* etc.) [25, 27, 28]. Further adapted strategies to enhance the secretion of recombinant proteins include the use of cell envelope mutants, the co-expression of lysis promoting proteins or translocase elements and the manipulation of culture conditions (growth rate, rate of induction) [23, 25, 29].

1.4 Secretory pathways in Gram-negative bacteria

In all living organisms, protein export systems mediate the passage of macromolecules across the cellular membranes. In bacteria, secretion plays a central role in their virulence and survival. Gram-negative bacteria contain numerous, apparently independent, systems for protein secretion and to date, six distinct protein secretion systems have been identified. These secretion pathways, types I – VI, facilitate the transport of chemical messages from the bacterial cytoplasm to the outside of the cell or, in some cases, directly into the cell of a eukaryotic host [30]. The cell envelope of Gram-negative bacteria is composed of two membranes, which are separated by the peptidoglycan-containing periplasm. Therefore, bacterial protein secretion systems can be broadly categorized as either one- or two-step.

One-step secretion systems, including types I, III, IV and VI (Figure 1), serve as direct channels through the bacterial cell envelope [30]. The type I secretion machinery (T1SS) is composed of only three proteins residing in the inner and outer membrane. One of these proteins is a specific outer membrane channel protein (OMP), TolC (H16_A2879 in *R. eutropha* H16), and the other two are cytoplasmic membrane proteins: the ATP-binding cassette (ABC), HlyB (H16_B2312), and the membrane fusion protein HlyD (H16_B2311) that spans the periplasm and connect the OMP and ABC components. Almost all T1SS substrates are polypeptides, usually toxins or enzymes, containing a C-terminal secretion signal, which targets them to the T1SS secretion apparatus. As the secreted protein does not experience a periplasmic intermediate the signal sequence is not cleaved off during secretion. The C-terminal position of the signal peptide implies that the transport of the substrate can only occur after translation leading to possible challenges during T1SS secretion due to premature folding of the protein [31].

The type-III secretion system (T3SS), also named injectisomes, is an export machine exclusively used by pathogenic Gram-negative bacteria to deliver proteins across the bacterial cell envelope into the host cell. By utilizing T3SS, Gram-negative bacteria, such as *Yersinia spp., Salmonella spp., Pseudomonas aeruginosa* and *R. solanacearum* are able to directly inject bacterial proteins (effectors) across the two bacterial membranes and the host membranes, where they can manipulate host cell function and thereby, contribute to the pathogenic relationship between bacterium and host [15, 32, 33]. Other proteins released by the T3SS machinery include so called “translocators”, which aid the effectors to cross the membrane of the host cell [32]. The T3SS apparatus is a large complex structure composed of several subunits, which in turn are composed of more than 20 bacterial proteins [34]. The basic structure is composed of two rings that span across the inner and outer membranes and a needle-like structure, which associates with the outer membrane (OM) ring and emerges from the bacterial cell surface [28].

The type-IV secretion system (T4SS) is another export mechanism used by pathogenic and symbiotic bacteria to transfer a wide range of macromolecules, such as single proteins, protein-protein or DNA-protein complexes, from the bacterial cell into host cells. It can also be used by the bacteria for the uptake of those T4SS substrates [35]. The T4SS translocation family is closely related to the conjugation machinery and can be divided into three subfamilies. The largest subfamily is found in most Gram-negative and Gram-positive bacteria, and mediates the conjugative DNA transfer within a wide range of bacteria species and sometimes even to fungi, plants and human cells [36]. The second subfamily is found in some Gram-negative bacteria, such as *Helicobacter pylori* and *Neisseria gonorrhoeae* and can facilitate DNA uptake and release into the extracellular milieu [35]. The third subfamily, also called “effector translocator systems”, are reminiscent to T3SS because they can deliver their effector substrates into the eukaryotic target cell through direct contact [36]. Despite the wide range of diverse substrates and functions, all T4SSs are evolutionary related and share several components arranged in a single or a few operons. Many of the T4SSs found in Gram-negative bacteria are comprised of 12 proteins, namely VirB1 to VirB11 and VirD4. In principle, T4SSs consists of an extracellular T-pilus that is associated with a transport apparatus that spans the cell envelope. The pilus is composed of the major pilin subunit VirB2 and the minor pilin subunit VirB5 [37]. Additional VirB proteins form an IM conduit and a pore at the OM

that allows the substrate to reach the extracellular milieu. The protein secretion by T4SS is energised by three ATPases, called VirB4, VirB11 and VirD4. VirD4 and its related proteins function as “coupling proteins” (CP) that bind the T4SS substrates and mediate their translocation. In a few cases, substrate binding can also be mediated by the Sec translocase and then the substrate further engages with the T4SS for the export across the OM [35].

In recent years, type-VI secretion systems (T6SS) have been described as novel one-step protein export mechanisms that are used by Gram-negative bacteria, such as *P. aeruginosa* and *Vibrio cholera* to target proteins into a host cell [38]. The function and characteristics of the T6SS still have to be fully understood but there appears to be an evolutionary relationship between bacteriophage tails and T6SS [30]. The composition and organization of the T6SS clusters contain 12 to more than 20 genes and vary greatly between species [39]. A functional T6SS can be recognized by the translocation of two proteins: haemolysin coregulated protein (Hcp) and Valin-Glycine repeat protein G (VgrG) [36]. The core components that have been partially characterised include an IcmF homologue, the ATPase ClpV, a regulatory FHA domain protein and the secreted VgrG and Hcp proteins [39]. In vitro studies identified the two proteins VgrG and Hcp as two substrates for the T6SS machinery and revealed a co-dependency for the secretion of each other, suggesting that both might not only be secreted effectors but also be part of the secretion apparatus [41]. Hcp1 forms a hexameric ring structure that spans the cell envelope (similar to the major tail protein of phage λ) and forms a channel through which the other proteins can be transferred into the extracellular milieu. The simplified scheme of T6SS, which shows the formation of the Hcp1 channel, is indicated in Figure 1. In addition to the structural similarity, the sequence of Hcp1 is similar to the sequence of gene product (gp) 19 of the bacteriophage T4, which forms a phage tail tube for DNA delivery into bacterial cells. VgrG proteins are structurally similar to the gp27/gp5 complex, the tailspike of bacteriophage T4 [30]. On the basis of a phage model of the T6SS, a physical interaction between Hcp and VgrG at the tip of the Hcp tube is predicted. Upon speculation following the bacteriophage T4 model, VgrG is released from the tube upon entering the target cell membrane and substrates can be delivered through the open Hcp conduit [36].

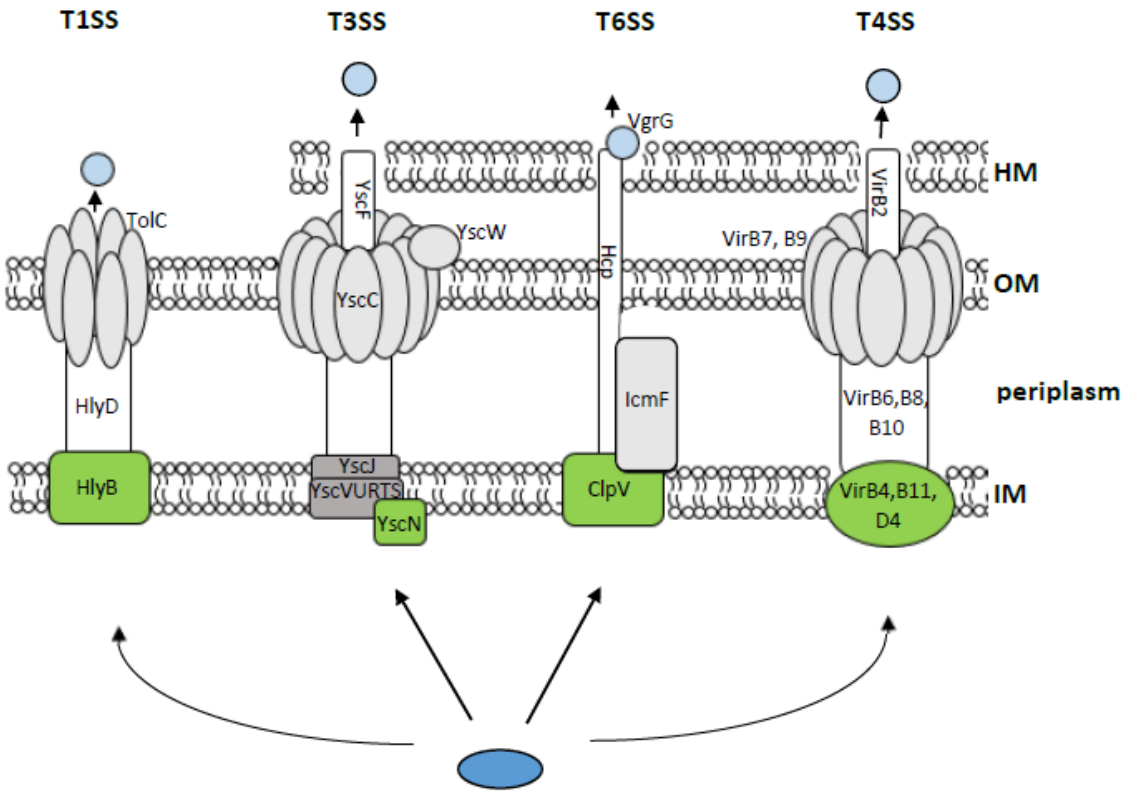

Figure 1 Simplified scheme of one-step secretion pathways in Gram-negative bacteria
One-step secretion systems (T1SS, T3SS, T4SS, and T6SS) serve as direct channels through which proteins can be secreted from the cytoplasm into the extracellular medium or into a host cell. T1SS consists of only three proteins (HlyB, Hly, and TolC) and T1SS substrates are targeted by a C-terminal signal peptide. T3SS, T4SS, and T6SS are secrection machineries used by pathogenic bacteria to deliver proteins across the bacterial cell envelope (IM, periplasm, OM) and across the membrane of the host cells (HM). Blue shapes mark the proteins to be exported, and green shapes mark the ATPases, that drive the effective translocation. Modified from [14]

Two-step secretion systems require that a precursor protein is first translocated across the IM via either the general secretory pathway (the Sec translocon) or the twin-arginine translocation (Tat) pathway. Following arrival in the periplasm, the N-terminal signal sequences of the preproteins are cleaved off by one of the two signal peptidases, LepB (H16_A2557) responsible for the cleavage of Sec- and Tat- specific signal peptides, or LspA (H16_A3047) responsible for the processing of signal peptides from lipoproteins [42]. In a second step the proteins are delivered to the extracellular milieu via the type II or type V secretion apparatus [43, 44] (Figure 2).

The type II secretion machinery (T2SS), also known as secreton, is responsible for the translocation of the periplasmic intermediates across the OM. The secreton is broadly conserved in Gram-negative bacteria and involves a set of 12 – 16 different protein components, named general secretion proteins Gsp [43]. The T2SS apparatus consists of

a putative pore in the OM, which is composed of 12 – 14 subunits of GspD, and a secretion pilus made up of GspG, GspH, GspI, GspJ and GspK. Due to the similarity of the pilin subunits to the subunits of the T4SS pilus, it has been suggested that the two systems are evolutionary related and that the type II pilus structure assists the secretion of substrates in a directly or indirectly manner. GspS is a small OM lipoprotein that can stabilize GspD, but has only been documented in the T2SS of *Klebsiella* and *Erwinia* [45]. Other T2SS, such as *R. eutropha* H16's, do not appear to feature GspS [14]. Although the T2SS has an IM component, this complex is not involved in the translocation across the IM and the type II secreton is supplied with substrates by either the Sec-dependent pathway or the Tat-system [46]. Most of the *gsp* genes appear to be essential for the OM translocation as mutations in these genes have shown to abort the secretion process resulting in the accumulation of exoproteins in the periplasm [43].

Type V secretion (T5SS) describes the secretory pathway via the monomeric autotransporter system (type V_a), the two-partner secretion pathway (type V_b) and the type V_c system [44]. More recently, two other subclasses, patatin-like autotransporters (type V_d) and type V_e, are classified. Type V_e is comprised of the intimin/invasin family of proteins that resemble the classical autotransporters, but have their domains in reverse order [47]. In Gram-negative bacteria, autotransport describes the ability of surface-localized proteins to pass the OM autonomously. Autotransporters are multi-domain proteins that are defined by their three functional domains: the signal peptide at the N-terminal end of the preprotein, the passenger domain and the β-domain at the C-terminal end, which consists of a short α-helical linker region and a β-core [44, 48]. A large number of proteins, such as adhesins, toxins, proteases and S-layer proteins, are secreted via the T5SS and they all are exported into the periplasm via the Sec translocase during the first step of translocation [46]. Following their arrival in the periplasm, the signal peptide is cleaved off and the C-terminal β-domains are inserted into the OM in a β-barrel structure that forms a pore. After the formation of the β-barrel, the passenger domain, which imparts the diverse effector functions of the autotransporters, is secreted through the translocation channel [44]. At the bacterial cell surface, most autotransporter passengers are proteolytically cleaved and then either remain attached to the cell surface via non-covalent interactions, or are released into the extracellular milieu [47].

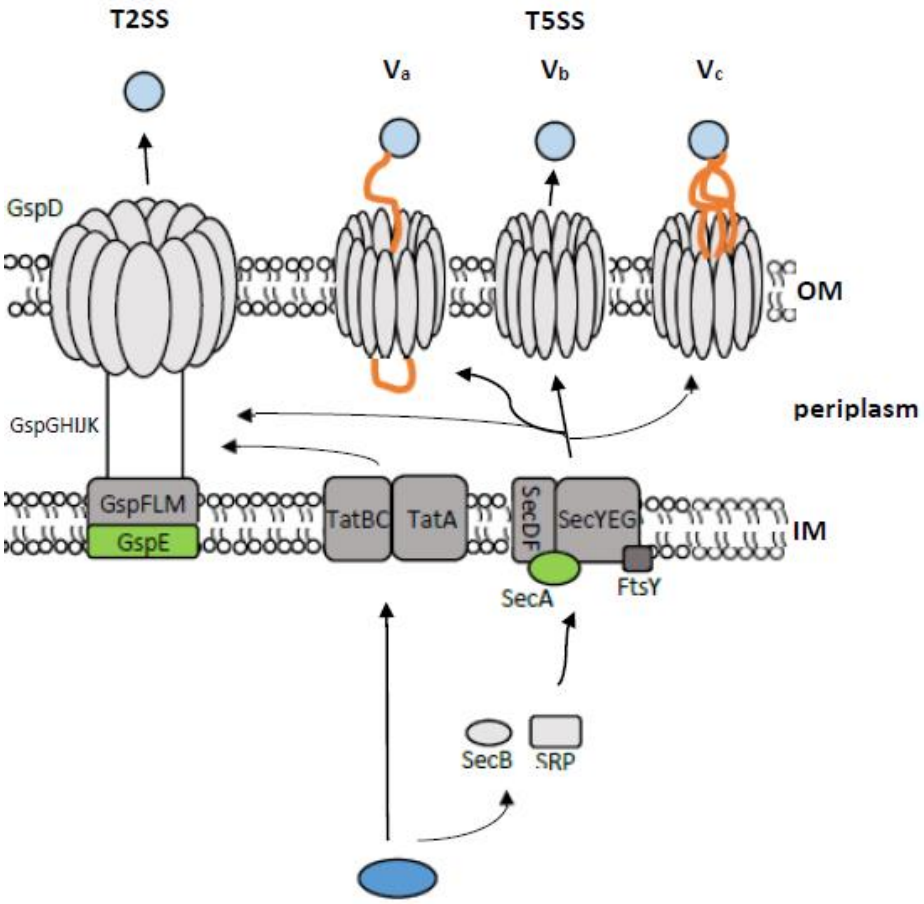

Figure 2 Simplified scheme of two-step secretion systems in Gram-negative bacteria
In two-step secretion systems, the precursor proteins are first exported across the IM. T2SS and T5SS substrates are targeted by N-terminal signal sequences, which facilitate the first transclocation via either the Sec-dependent or the Tat- pathway. In the periplasm, the signal peptides are cleaved off and the second translocation across the OM is achieved through either the T2SS or T5SS apparatus. Blue shapes mark the proteins to be exported, and green shapes mark the ATPases, that are involved in the effective translocation of proteins. Modified from [14]

1.5 The Sec-dependent translocase

The majority of proteins, more than 90 % in *E. coli*, are travelling across or into the bacterial IM via the evolutionary conserved Sec translocon [23, 49]. The Sec-dependent pathway, also called the "general secretion pathway", transports newly synthesized unfolded proteins across the cytoplasmic membrane and is also involved in the insertion of membrane proteins into the IM [50]. The substrates of the Sec translocase range from very hydrophilic to very hydrophobic proteins, but all contain a hydrophobic N-terminal region, i.e. signal sequence for secretory proteins (precursor proteins) and a membrane anchor signal for inserted inner membrane proteins (IMPs) [49]. Signal peptides consist of three domains: the positively charged N-terminal domain (or n-region), the

hydrophobic domain (h-region) and the C-terminal domain (c-region) [51]. The translocation across or integration of proteins into the IM can occur in a co-translational or post-translational manner. In bacteria, the co-translational pathway is mainly used for the integration of IMPs, while the post-translational pathway is utilized by proteins that are secreted into the extracellular milieu [49, 52]. For post-translational translocation, the cytosolic chaperone SecB (H16_A033) binds to an unfolded precursor protein harboring an N-terminal signal peptide and delivers the proteins to the IM-bound SecA (H16_A3264). During co-translational translocation the unfolded preprotein is bound by the signal recognition particle (SRP) Ffh (H16_A3241) and moved to SecA with the help of the signal recognition particle receptor FtsY (H16-A0363) [50]. In bacteria, the Sec translocase is composed of three proteins, namely SecY (H16_A3464), SecE (H16_3503) and SecG (H16_A1048), which form a heterotrimeric channel, named SecYEG, through which proteins are translocated across the IM [49, 50, 53]. SecA, a preprotein-stimulated translocation ATPase, functions as an ATP-dependent molecular motor that drives the secretory protein across the IM [49, 53]. SecA associates peripherally with SecYEG, where it accepts proteins from chaperones like SecB or the ribosome to translocate the unfolded proteins in a 'threading' mechanism through the small transmembrane channel formed by SecYEG [50]. The release of the preprotein from SecA appears to be driven by ATP hydrolysis, which leads to a conformational change of SecA and furthermore leads to the recycling of SecA [54]. Additional Sec proteins, SecD (H16_A3115), SecF (H16_A3116) and YajC (H16_A3114), work in conjunction with the SecYEG to facilitate higher secretion levels [49, 53].

1.6 The twin-arginine translocation pathway

The Tat-pathway is another protein transport system in Gram-negative bacteria for the export of substrates across the IM. This pathway differs from the Sec pathway because it translocates folded and cofactor-containing proteins across the IM using the transmembrane proton electrochemical gradient [50, 55]. It is therefore a Sec-independent and ATP-independent mechanism of protein translocation. Substrates of the Tat pathway contain a N-terminal signal peptide with consecutive, essentially invariant, arginine residues within an S-R-R-x-F-L-K consensus motif, where x is any polar amino acid [55]. Additionally, Tat signal sequences are typically longer and the h-region

of the Tat signal peptide is generally less hydrophobic than the Sec-specific signal due to the presence of more glycine and threonine residues [50, 51]. Initially, substrates secreted through the Tat pathway were thought to include only cofactor-carrying proteins, but more recent studies showed that the Tat pathway is also important for the translocation of 'non-cofactor' substrates that already are folded in the cytoplasm [55]. *R. eutropha* H16 possesses the same minimal set of components found in the *E. coli* Tat translocation system: the integral membrane proteins TatA (H16_A3405), TatB (H16_A3404) and TatC (H16_A3403) [55]. TatA and TatB are sequence-related proteins, especially in their functionally important N-terminal region, but perform distinct functions in the Tat pathway. TatB associates with TatC to form a functional TatBC complex that is able to bind Tat substrates in an energy-independent step [55, 56]. TatC seems to be the primary site of signal peptide recognition in the Tat pathway that TatC binds the consensus motif of the Tat signal peptide [57]. The TatBC-complex then associates with TatA in a proton gradient-dependent step and the association appears to persist until the substrate molecule has reached the periplasm [55]. For the production of recombinant proteins, the Tat pathway might have advantages over the Sec system since many proteins cannot be exported via the Sec-translocase because of premature folding resulting in the toxic accumulation of all secreted proteins due to the blocking of the secretion machinery [25, 29]. Another example of the disqualification of the Sec pathway for the export of some proteins, is the secretion of green fluorescent protein (GFP) in *E. coli*. When fused to a Sec-specific signal sequence, inactive GFP was accumulated in the periplasm. Contrary to those findings, when fused to a Tat-specific signal peptide, GFP was translocated to the periplasm in an active, fluorescent form [58]. The efficiency of this pathway has first been reported to be too low for industrial protein production [29]. However, Fisher et al. observed that the yield for relatively small and well-folded proteins is comparable for both the Sec- and the Tat- pathway and the yield of the Tat export seems to be only lower for larger, soluble fusion proteins [25].

1.7 Objective of this work

The aim of this study was to investigate if *R. eutropha* H16 is capable of secreting recombinant proteins into the extracellular media. Therefore, the recombinant secretion of proteins was examined by fusing signal sequences, specific for the Sec- and the Tat-pathway, to the N-terminal end of three model proteins. Recombinant secretory protein production has several advantages over intracellular production. These advantages include simplified downstream processing, higher product stability due to reduced possibilities of degradation and enhanced biological functionality. Several factors can influence the efficiency of protein secretion, such as protein size and amino acid compositions of the signal peptide and the target protein and thus, the examination of secretory recombinant protein production is often a trial-and-error evaluation [22]. To cover all of the above mentioned interactions, three model proteins varying in their molecular size and their native origin were chosen for the examination of their secretion in *R. eutropha* H16: human growth hormone (hGH), levanase (Lev) and cellulase A (CelA).

The eukaryotic hGH, also known as somatotropin, is a polypeptide hormone with a central role in growth, development and sexual maturation. It is used therapeutically for various growth and metabolic disorders, as well as for the relief from excessive burns or other thermal injuries. The protein has a molecular weight of 22 kDa and contains two disulphide bonds that are essential for the maintenance of a receptor structure necessary for hGH binding and for the stability of hGH [59, 60]. Two immunodetection methods were used to detect the hGH protein in the cell-free supernatant of *R. eutropha* H16 transconjugants.

Cellulase A is a novel endo-β-1,4-cellulase (EC 3.2.1.4) isolated from *Sorangium cellulosum*. The protein has a molecular weight of 42.9 kDa and contains a putative signal sequence of about 35 amino acids followed by repetition of Serine, Alanine, Threonine and Glycine (80 amino acids) and the functional GH5 core enzyme. It has been characterized intensively in the Christian-Doppler laboratory for genetically engineered lactic acid bacteria of TU Graz and several cloning variants were created, thereby [61]. For this study, the variant celAoCΔS (33 kDa) was used which is missing its native signal sequence and the amino acid repeats. A qualitative and a quantitative enzyme activity

assay based on the hydrolyzation of carboxymethylcelloluse (CMC) were used to detect active CelA in the cell-free supernatant of *R. eutropha* H16 transconjugants.

The enzyme levanase (Lev) (E.3.2.1.80), belonging to the family of β-D-Fructofuranosidases, is encoded by the *sacC* gene from *Bacillus subtilis* [62]. It has a molecular weight of 73 kDa and harbors a native Sec signal peptide. Lev is capable to hydrolyze sucrose and the polyfructans levan and inulin [63, 62]. For this work, a *sacC* gene variant without the native signal sequence designated as levΔS was used. The detection of functional levanase is based on the liberated glucose molecules after hydrolyzation of sucrose.

The primary factor for efficient secretion of a recombinant protein is the selection of a signal peptide. Altogether 20 signal peptides from identified exoproteins of *R. solancaearum* and one from a identified periplasmic protein (NosZ) of *R. eutropha* H16 were chosen for this study. The signal sequences were predicted using a method based on the Hidden Markov Model. Ten of the signal peptides from *R. solanacearum* were Sec-specific signal sequences and the rest (10+1) were signal sequences specific for the Tat-pathway.

Another very important factor to achieve high-level secretion of heterologous proteins is the rate of translation. High translation rates may prohibit protein secretion due to the physically limited periplasmic volume resulting in an increased cellular burden and reduced cell growth [21]. It is therefore important to choose a promoter strong enough to express good protein levels, but is not too strong to put any additional stress on the bacterial cells and thus, P_{tac} under constitutive conditions, was chosen as the promoter of choice.

In summary, this study was performed to prove if *R. eutropha* H16 is capable of recombinant protein secretion based on the examples of the three model proteins hGH, CelA and Lev.

2 Materials and Methods

2.1 Materials

The following chapter provides all the strains, signal peptides, primers and plasmids used in this study.

2.1.1 Strains

All strains used in this work are listed in Table 1.

Table 1. Strains used in this work

Strain	Description	References / Source	IMBT's Culture collection No.
E. coli Top10	F'(proAB, lacIq, lacZΔM15, Tn10(tet-R), mcrA, Δ(mrr-hsdRMS-mcrBC), Φ80ΔlacZΔM15, ΔlacX74, deoR, recA1, araD139(ara, leu), 7697, galU, galK, λ-, rpsL(streptomycin-r), endA1, nupG	Invitrogen	1482
E. coli S17-1	recA pro hsdR RP4-2-Tc::Mu-Km::Tn7 integrated into the chromosome	Invitrogen	446
E. coli HB101	F- supE44 lacY1 ara-14 galK2 xyl-5 mtl-1 leuB6 proA2 hsd20 mcrB recA13 rpsL20 thi-1 λ-	ATCC® 37159™	339
R. eutropha H16	Wild-type, gentamicin resistant	DSMZ428[a]	1
R. solanacearum F74	Wild-type	DSMZ1993[a]	625

a DSMZ, Deutsche Sammlung für Mikroorganismen und Zellkulturen

2.1.2 Signal peptides

All signal sequences used in this study are listed in Table 2. The prediction of the secretory pathway was conducted with Hidden Markov Models using the online tool PRED-TAT of the computational genetics research group of the University of Thessaly [65, 66]. The amino acid sequences of the signal peptides can be found in the appendix (see 7.2).

Table 2 Signal peptides used in this study

No.	Name	Size	Locus[1]
SP's for sec-dependent pathway			
S1	pehB	79 aa	F504_1633
S2	Pme	26 aa	F504_3589
S3	Egl	30 aa	F504_3606
S4	cbhA	46 aa	F504_4041
S5	Tek	34 aa	F504_4201
S6	Aac	28 aa	F504_2493
S7	treA	45 aa	F504_3718
S8	pqaA	23 aa	F504_3605
S9	F504_4738	27 aa	F504_4738
S10	F504_2783	20 aa	F504_2783
SP's for Tat-pathway			
T1	NosL	31 aa	F504_4829
T2	F504_2199	38 aa	F504_2199
T3	F504_2437	35 aa	F504_2437
T4	RlpB	30 aa	F504_2669
T5	F504_2793	27 aa	F504_2793
T6	amiC	48 aa	F504_2485
T7	nasF	41 aa	F504_402
T8	iorB2	42 aa	F504_1888
T9	ReH16NosZ	45 aa	PHG252
T10	pehC	57 aa	F504_4386
T12	RscNosZ	51 aa	F504_4824

1 gene locus of exoproteins in *R. solanacearum* FQY-4, except for T9: gene locus in *R. eutropha* H16

2.1.3 Plasmids

All plasmids used in this study are listed in Table 3. The column IMBT No. shows the number of the plasmids forwarded to the strain collection of the Institute of molecular biotechnogy (IMBT). The selected plasmids were chosen due to their observed positive secretion potential. Furthermore, all signal peptides were cloned into the pJET1.2 vector and then forwarded to the IMBT's strain collection. The numbers with the superscripted "c" mark the signal sequences, which are cloned into pJET1.2. The column PK No. shows the numbers of each plasmid in the internal plasmid list of the research group of Petra Köfinger.

Table 3 Plasmids used in this work

Plasmid	Description	Source	IMBT No.[a]	PK No.[b]
pKRep-P_{tac}-eGFP	Kan^r, *P_{tac}*, Rep, *egfp*, *par*, *mobRK2*	Steffen Gruber [10]	7360	236
pKRSF1010-P_{tac}-eGFP	Kan^r, *P_{tac}*, RSF1010, *egfp*, *par*	Steffen Gruber [10]	7361	49
pJET1.2/blunt cloning vector	Bla (amp^r), *P_{lacUV5}*, *P_{T7}*, Rep (pMB1), *eco47IR*	Thermo Scientific	-	-
pRK2013 (mobilization helper plasmid)	Kan^r, RK2	ATCC® 37159™ [65]	339	-
pCRep-P_{tac}-eGFP-reverse	Cm^r, *P_{tac}*, Rep, *egfp*, *par*, *mobRK2*	This study	-	-
pCRSF1010-P_{tac}-eGFP-reverse	Cm^r, *P_{tac}*, RSF1010, *egfp*, *par*, *mobRK2*	This study	-	252
pKRep-P_{tac}-eGFP-reverse	Kan^r, *P_{tac}*, Rep, *egfp*, *par*, *mobRK2*	This study	-	-
pCRep-P_{tac}-hGHΔS	Cm^r, *P_{tac}*, Rep, *hGHΔS*, *par*, *mobRK2*	This study	-	-
pCRep-P_{tac}-celAoCΔS	Cm^r, *P_{tac}*, Rep, *celAoCdS*, *par*, *mobRK2*	This study	-	-
pCRep-P_{tac}-levΔS	Cm^r, *P_{tac}*, Rep, *LevΔS*, *par*, *mobRK2*	This study	-	-
pCRSF1010-P_{tac}-hGHΔS	Cm^r, *P_{tac}*, RSF1010, *hGHΔS*, *par*	This study	-	253
pCRSF1010-P_{tac}-celAoCΔS	Cm^r, *P_{tac}*, RSF1010, *celAoCdS*, *par*	This study	-	254
pCRSF1010-P_{tac}-levΔS	Cm^r, *P_{tac}*, RSF1010, *LevΔS*, *par*	This study	-	255
pKRep-P_{tac}-pme-hGH	Kan^r, *P_{tac}*, Rep, *par*, *mobRK2, hGH, SP[1] of pme[2]*	This study	-	-
pKRep-P_{tac}-egl-hGH	Kan^r, *P_{tac}*, Rep, *par*, *mobRK2, hGH, SP[1]*	This study	-	-

	of egl²			
pKRep-P$_{tac}$-cbhA-hGH	Kan^r, *P$_{tac}$*, Rep, *par*, *mobRK2, hGH, SP¹ of cbhA²*	This study	-	-
pKRep-P$_{tac}$-pme-celA	Kan^r, *P$_{tac}$*, Rep, *par*, *mobRK2, celA, SP¹ of pme²*	This study	-	-
pKRep-P$_{tac}$-egl-celA	Kan^r, *P$_{tac}$*, Rep, *par*, *mobRK2, celA, SP¹ of egl²*	This study	-	-
pKRep-P$_{tac}$-pme-lev	Kan^r, *P$_{tac}$*, Rep, *par*, *mobRK2, Lev, SP¹ of pme²*	This study	-	-
pKRep-P$_{tac}$-egl-lev	Kan^r, *P$_{tac}$*, Rep, *par*, *mobRK2, Lev, SP¹ of egl²*	This study	-	-
pKRSF1010-P$_{tac}$-pme-hGH	Kan^r, *P$_{tac}$*, RSF1010, *par, hGH, SP¹ of pme²*	This study	-	256
pKRSF1010-P$_{tac}$-egl-hGH	Kan^r, *P$_{tac}$*, RSF1010, *par, hGH, SP¹ of egl²*	This study	-	257
pKRSF1010-P$_{tac}$-cbhA-hGH	Kan^r, *P$_{tac}$*, RSF1010, *par, hGH, SP¹ of cbhA²*	This study	-	258
pKRSF1010-P$_{tac}$-aac-hGH	Kan^r, *P$_{tac}$*, RSF1010, *par, hGH, SP¹ of aac²*	This study	7365[c]	259
pKRSF1010-P$_{tac}$-treA-hGH	Kan^r, *P$_{tac}$*, RSF1010, *par, hGH, SP¹ of treA²*	This study	7366[c]	260
pKRSF1010-P$_{tac}$-F504_4738-hGH	Kan^r, *P$_{tac}$*, RSF1010, *par, hGH, SP¹ of F504_4738²*	This study	7368[c]	261
pKRSF1010-P$_{tac}$-F504_2437-hGH	Kan^r, *P$_{tac}$*, RSF1010, *par, hGH, SP¹ of F504_2437²*	This study	7372[c]	262
pKRSF1010-P$_{tac}$-rlpB-hGH	Kan^r, *P$_{tac}$*, RSF1010, *par, hGH, SP¹ of rlpB²*	This study	7373[c]	263
pKRSF1010-P$_{tac}$-amiC-hGH	Kan^r, *P$_{tac}$*, RSF1010, *par, hGH, SP¹ of amiC²*	This study	7375[c]	264
pKRSF1010-P$_{tac}$-nasF-hGH	Kan^r, *P$_{tac}$*, RSF1010, *par, hGH, SP¹ of nasF²*	This study	7376[c]	265
pKRSF1010-P$_{tac}$-iorB2-hGH	Kan^r, *P$_{tac}$*, RSF1010, *par, hGH, SP¹ of iorB2²*	This study	7377[c]	266
pKRSF1010-P$_{tac}$-RscNosZ-hGH	Kan^r, *P$_{tac}$*, RSF1010, *par, hGH, SP¹ of NosZ²*	This study	7380[c]	267
pKRSF1010-P$_{tac}$-pme-celA	Kan^r, *P$_{tac}$*, RSF1010, *par, celA, SP¹ of pme²*	This study	7381	268
pKRSF1010-P$_{tac}$-egl-celA	Kan^r, *P$_{tac}$*, RSF1010, *par, celA, SP¹ of egl²*	This study	7382	269
pKRSF1010-P$_{tac}$-cbhA-celA	Kan^r, *P$_{tac}$*, RSF1010, *par, celA, SP¹ of cbhA²*	This study	7383	270
pKRSF1010-P$_{tac}$-aac-celA	Kan^r, *P$_{tac}$*, RSF1010, *par, celA, SP¹ of aac²*	This study	7384	271

pKRSF1010-P_{tac}-treA-celA	Kan^r, P_{tac}, RSF1010, *par, celA, SP[1] of treA[2]*	This study	7385	272
pKRSF1010-P_{tac}-F504_4738-celA	Kan^r, P_{tac}, RSF1010, *par, celA, SP[1] of F504_4738[2]*	This study	7386	273
pKRSF1010-P_{tac}-NosL-celA	Kan^r, P_{tac}, RSF1010, *par, celA, SP[1] of NosL[2]*	This study	-	274
pKRSF1010-P_{tac}-F504_2437-celA	Kan^r, P_{tac}, RSF1010, *par, celA, SP[1] of F504_2437[2]*	This study	7387	275
pKRSF1010-P_{tac}-rlpB-celA	Kan^r, P_{tac}, RSF1010, *par, celA, SP[1] of rlpB[2]*	This study	-	276
pKRSF1010-P_{tac}-F504_2793-celA	Kan^r, P_{tac}, RSF1010, *par, celA, SP[1] of F504_2793[2]*	This study	7388	277
pKRSF1010-P_{tac}-amiC-celA	Kan^r, P_{tac}, RSF1010, *par, celA, SP[1] of amiC[2]*	This study	7389	278
pKRSF1010-P_{tac}-nasF-celA	Kan^r, P_{tac}, RSF1010, *par, celA, SP[1] of nasF[2]*	This study	7390	279
pKRSF1010-P_{tac}-iorB2-celA	Kan^r, P_{tac}, RSF1010, *par, celA, SP[1] of iorB2[2]*	This study	-	280
pKRSF1010-P_{tac}-RscNosZ-celA	Kan^r, P_{tac}, RSF1010, *par, celA, SP[1] of NosZ[2]*	This study	7390	281
pKRSF1010-P_{tac}-ReH16NosZ-celA	Kan^r, P_{tac}, RSF1010, *par, celA, SP[1] of NosZ[3]*	This study	7391	282
pKRSF1010-P_{tac}-pme-lev	Kan^r, P_{tac}, RSF1010, *par, lev, SP[1] of pme[2]*	This study	-	283
pKRSF1010-P_{tac}-egl-lev	Kan^r, P_{tac}, RSF1010, *par, lev, SP[1] of egl[2]*	This study	-	284
pKRSF1010-P_{tac}-tek-lev	Kan^r, P_{tac}, RSF1010, *par, lev, SP[1] of tek[2]*	This study	7364[c]	285
pKRSF1010-P_{tac}-pqaA-lev	Kan^r, P_{tac}, RSF1010, *par, lev, SP[1] of pqaA[2]*	This study	7367[c]	286
pKRSF1010-P_{tac}-F504_4738-lev	Kan^r, P_{tac}, RSF1010, *par, lev, SP[1] of F504_4738[2]*	This study	7368[c]	287
pKRSF1010-P_{tac}-F504_2783-lev	Kan^r, P_{tac}, RSF1010, *par, lev, SP[1] of F504_2783[2]*	This study	7369[c]	288
pKRSF1010-P_{tac}-NosL-lev	Kan^r, P_{tac}, RSF1010, *par, lev, SP[1] of NosL[2]*	This study	7370[c]	289
pKRSF1010-P_{tac}-F504_2199-lev	Kan^r, P_{tac}, RSF1010, *par, lev, SP[1] of F504_2199[2]*	This study	7371[c]	290
pKRSF1010-P_{tac}-rlpB-lev	Kan^r, P_{tac}, RSF1010, *par, lev, SP[1] of rlpB[2]*	This study	7373[c]	291
pKRSF1010-P_{tac}-amiC-lev	Kan^r, P_{tac}, RSF1010, *par, lev, SP[1] of amiC[2]*	This study	7375[c]	292
pKRSF1010-P_{tac}-	Kan^r, P_{tac}, RSF1010, *par, lev, SP[1] of*	This study	7376[c]	293

nasF-lev	*nasF*[2]			
pKRSF1010-P_{tac}-iorB2-lev	Kan^r, *P_{tac}*, RSF1010, *par, lev, SP*[1] *of* *iorB2*[2]	This study	7377[c]	294
pKRSF1010-P_{tac}-RscNosZ-lev	Kan^r, *P_{tac}*, RSF1010, *par, lev, SP*[1] *of* *NosZ*[2]	This study	7380[c]	295

[1] SP – Signal peptide [2] of *R. solanacearum* [3] of *R. eutropha* H16

[a] No. in IMBT's culture collection [b] No. in the internal plasmid list of the research group of Petra Köfinger

[c] No. of pJET1.2 plasmid with SP-KAN fragment

2.1.4 Primer

All primers were ordered at Integrated DNA technology Inc. (Leuven, Belgium). The primer sequences and melting temperature are shown in Table 4 to Table 9. The highlighted parts are the recognition sites for the restriction enzymes used for cloning. The underlined parts are the overhang needed for the overlap extension PCR. The melting temperatures (Tm) were calculated using the online tool "Tm Calculator v1.6" from New Englands Biolabs® Inc. [68].

Table 4. Primer used for construction of turnaround vector

Name	No.[1]	Sequence (5' – 3')	Tm [°C]	Restriction sites
CMRfwd_XhoI_NotI	533	cag**gcggccgc**ttcgacaccataccgactcgtc**ctcgag**tcatgacgaataaatacctgt	54	*Xho*I, *Not*I
Rev-cmR-SpeI	338	**actagt**taactggcctcaggcattt	62	*Spe*I
KANfwd_XhoI_NotI	534	cag**gcggccgc**ttcgacaccataccgactcgtc**ctcgag**tcatgacgaataaatacctgt	54	*Xho*I, *Not*I
Rev-kanR-SpeI	69	cgg**actagt**gtctgacgctcagtggaacgaa	68	*Spe*I
pTac_XhoI	536	Cag**ctcgag**caggcagccatcggaagctg	70	*Xho*I
rrnBrev_NotI	535	Cag**gcggccgc**aaggccatccgtcaggatgg	68	*Not*I

[1] Primer number refers to the internal primer list of the research group of Petra Köfinger

Table 5 Primer used for amplification of reporter genes

Name	No.[1]	Sequence (5' – 3')	Tm [°C]	Restriction sites
hGH_fwd_NdeI	539	cgag**catatg**aaaagattcccaaccattccc	61	*Nde*I
hGH_rev_HindIII	540	cgc**aagctt**ctagaagccacagctgccctc	69	*Hind*III
celAoCdS_fwd_NdeI	537	cgag**catatg**actgatggtacgccagttgaa	64	*Nde*I
celAoCdS_rev_HindIII	538	cgc**aagctt**ttattcagcaattttcgcctt	68	*Hind*III
Lev_fwd_NdeI	541	**catatg**gccgattcaagctactatgat	60	*Nde*I
Lev_rev_HindIII	542	**aagctt**ttaagactccttcgttacatt	56	*Hind*III

[1] Primer number refers to the internal primer list of the research group of Petra Köfinger.

Table 6 Primer used for amplification of sec signal sequences

Name	No.[1]	Sequence (5′ – 3′)	Tm [°C]	Restriction site
pehB-Sec-fwd	544	tttgtttaactttaagaaggagatatacacatgcgacaaagaaaaatggggcgt	68	-
pehB-Sec-rev-NdeI	545	**catatg**gtcataggcgagcgccggaac	72	*Nde*I
pme-Sec-fwd	546	tttgtttaactttaagaaggagatatacacatgggcacgaccccgatccgt	75	-
pme-Sec-rev-NdeI	547	***catatg****tttgatagggatgtgcaactgatgg*	65	*Nde*I
egl-Sec-fwd	548	tttgtttaactttaagaaggagatatacacatgccgctggttgccgcttc	73	-
egl-Sec-rev-NdeI	549	**catatg**gtcggtagcggccgccgtgct	79	*Nde*I
cbhA-Sec-fwd	550	tttgtttaactttaagaaggagatatacacatgccgcctatccaacattatc	63	-
cbhA-Sec-rev-NdeI	551	**catatg**ggcttcggcgtgaacagctggag	63	*Nde*I
tek-Sec-fwd	552	tttgtttaactttaagaaggagatatacacatgcaagcacagttcaagaagcgag	74	-
tek-Sec-rev-NdeI	553	**catatg**cgaggcccccgattccgagc	73	*Nde*I
aac-Sec-fwd	554	tttgtttaactttaagaaggagatatacacatgacgcacggattcgcactgcg	74	-
aac-Sec-rev-NdeI	555	**catatg**acggctgccgtgcgccgtgc	81	*Nde*I
treA-Sec-fwd	556	tttgtttaactttaagaaggagatatacacatgctcgatccccgtggcttg	71	-
treA-Sec-rev-NdeI	557	**catatg**gacatcggcacaggcaggca	72	*Nde*I
PqaA-Sec-fwd	558	tttgtttaactttaagaaggagatatacacatgatgaaacgacctctcgtcgcg	70	-
PqaA-Sec-rev-NdeI	559	**catatg**ggccctggccagggccag	76	*Nde*I
F504_4738-Sec-fwd	560	tttgtttaactttaagaaggagatatacacatgtcaaaattaccttcatttaa	53	-
F504_4738-Sec-rev-	561	**catatg**gtcttgtccatgtgccgtgac	67	*Nde*I
F504_2783-Sec-fwd	562	tttgtttaactttaagaaggagatatacacatgaagaaatcgctgcttgcgat	66	-
F504_2783-Sec-rev-	563	**catatg**ggattgggcatgcgctgca	70	*Nde*I
NdeI				

[1] Primer number refers to the internal primer list of the research group of Petra Köfinger.

Table 7 Primer used for amplification of tat signal sequences

Name	No[1]	Sequence (5′ – 3′)	Tm [°C]	Restriction sites
NosL-Sec-fwd	564	tttgtttaactttaagaaggagatatacacatgaacgccgaccgtcgccgc	77	-
NosL-Sec-rev-NdeI	565	**catatg**gggcgcagcggcatcctgcct	80	*Nde*I
F504_2199-Sec-fwd	566	tttgtttaactttaagaaggagatatacacatgttggaaaccaaagcagcacaa	66	-
F504_2199-Sec-rev-	567	**catatg**cgcctgcgcggacgcact	76	*Nde*I
NdeI				
F504_2437-Sec-fwd	568	tttgtttaactttaagaaggagatatacacatgcaagctttcgacaacaaccg	67	-
F504_2437-Sec-rev-	569	**catatg**cgtcgcccgcgaggcca	76	*Nde*I
NdeI				
RlpB-Sec-fwd	570	tttgtttaactttaagaaggagatatacacatgccgtctcgtcgccgtttcg	73	-
RlpB-Sec-rev-NdeI	571	**catatg**gttgttgccgcgcaggtgaaagc	73	*Nde*I
F504_2793-Sec-fwd	572	tttgtttaactttaagaaggagatatacacatgcaacgacgcagcatcatcggat	72	-
F504_2793-Sec-rev-	573	**catatg**ggtctcggcctgtgcgccgaagg	78	*Nde*I
NdeI				
amiC-Sec-fwd	574	tttgtttaactttaagaaggagatatacacatgctgatcaagcatctgccgac	68	-
amiC-Sec-rev-NdeI	575	**catatg**gttggcgccgaaggcgatctgc	75	*Nde*I
nasF-Sec-rev-NdeI	576	tttgtttaactttaagaaggagatatacacatggccgcgccgagcaagaccga	79	-
	577	**catatg**gccggccgcccaggcccc	83	*Nde*I

iorB2-Sec-fwd	578	tttgtttaactttaagaaggagatatacacatgacggccgacgcaaccgc	75	-
iorB2-Sec-rev-NdeI	579	**catatg**gtccgccgcgtcgcccag	76	*Nde*I
ReH16-NosZ-Sec-fwd	580	tttgtttaactttaagaaggagatatacacatgagcaaagagaaggcatcgatcgg	69	-
ReH16-NosZ-Sec-rev-NdeI	581	**catatg**aacggccgccgccgcgggc	85	*Nde*I
pehC-Sec-fwd	582	tttgtttaactttaagaaggagatatacacatgcccaaacagaaacactccagc	69	-
pehC-Sec-rev-NdeI	583	**catatg**cgtggcggccgtggcactgct	80	*Nde*I
Rsc-NosZ-Sec-fwd	584	tttgtttaactttaagaaggagatatacacatgatgagcaagcacccgcatt	68	-
Rsc-NosZ-Sec-rev-NdeI	585	**catatg**ggttgcggcagcggacccc	76	*Nde*I

[1] Primer number refers to the internal primer list of the research group of Petra Köfinger.

Table 8 Primer used for amplifying the fragment needed for overlap extension PCR, thereby fusing the signal sequences to the *kan*^{r} cassette

Name	No[1]	Sequence (5' – 3')	Tm [°C]	Restriction sites
Signal_oe_rev	543	Gtgtatatctccttcttaaagttaaacaaaattatt	60	-

[1] Primer number refers to the internal primer list of the research group of Petra Köfinger.

Table 9 Primer used for sequencing

Name	No[1]	Sequence (5' – 3')
pMS_prom for	39	Gcataattcgtgtcgctcaagg
Tac pMS470 Stop_neu (rev)	40	Gcaaattctgttttatcagacc

[1] Primer number refers to the internal primer list of the research group of Petra Köfinger.

2.1.5 Antibodies

The antibodies and their concentration used in this study are listed in Table 10.

Table 10 Antibodies used in this work

Antibody	No.	Dilution	Working conc.	Source
GH (T-20)	sc-10365	1:300	33,4 µg	Santa Cruz Biotechnology, Inc.
Donkey anti-goat IgG, F(ab')$_2$-AP	sc-3852	1:5000	4 µg	Santa Cruz Biotechnology, Inc.
Self-made 2nd antibody	-	1:4170	5,3 µg	Florian Krainer

2.2 General methods

The following chapter describes general methods, as well as particular techniques, that were carried out during this work.

2.2.1 Isolation of Plasmid DNA

Isolation of plasmid DNA from *E. coli* Top 10 cells was carried out according to the manual of the GeneJET™ Plasmid Miniprep Kit from Thermo Fisher Scientific Inc. (Massachusetts, USA). For each miniprep, *E. coli* cells harboring the plasmids were freshly streaked out on LB plates and grown overnight at 37°C. On the next day, the cells were first resuspended in 250 µL Resuspension solution, then 250 µL Lysis solution were added and mixed by inverting of the tube. After the addition of 350 µL of Neutralization solution and inverting the tube, the tube was centrifuged at full speed for 10 min at room temperature (RT) using Eppendorf centrifuge 5415R (Eppendorf AG; Hamburg, Germany). The supernatant was loaded onto a GeneJET™ spin column and centrifuged for 1 min using prior conditions. The spin column was subsequently washed twice with 500 µL Wash solution and centrifuged for 1 min using prior conditions. After centrifugation of the empty spin column, it was transferred into a new 1.5 mL microcentrifuge tube (Eppendorf AG) and 50 µL ddH_2O were added to the purified DNA. After an incubation of 5 min, the column was centrifuged for 2 min using prior conditions and the flow-through was collected and stored at -20 °C until use.

2.2.2 Polymerase chain reaction

2.2.2.1. General set up for gene amplification

PCR reactions were performed using Q5® High-Fidelity DNA Polymerase (New England Biolabs Inc.; Massachusetts, USA) following the recommended protocol of the manufacturer. A standard PCR reaction was carried out as shown in Table 11.

Table 11 General PCR reaction mixture

5 x Q5® Reaction Buffer	5 µL
10 mM dNTP's	0.5 µL
10 µM Forward Primer	1.25 µL
10 µM Reverse Primer	1.25 µL
Template DNA (10 ng)	X
Q5 High-Fidelity DNA Polymerase	0.2 µL
5X Q5 High GC Enhancer (optional)	5 µL
ddH_2O	Y
	25 µL

The PCR reaction was carried out in the GeneAmp® PCR System 2700 thermocycler (Applied Biosciences; Connecticut, USA). The general PCR program is shown below (Table 12).

Table 12 General PCR program

Step	**Temperatur [°C]**	**Time [s]**	
Initial Denaturation	98	30	
Denaturation	98	10	25 - 35 cycles
Annealing	58	30	
Elongation	72	30 seconds/kb	
Final Elongation	72	120	

PCR reactions were always performed with 25 - 30 cycles until specified otherwise. All conducted PCRs are summarized in Table 13.

Table 13. Summary of PCR conditions using Q5® High-Fidelity DNA Polymerase

PCR fragment	Primer pair	No.	Annealingtemp. / -time	Extensiontemp. / -time	Cycles	Fragment size
cm^r	CMRfwd_XhoI_NotI	533	59°C, 30 sec	72°C, 35 sec	25	1138 bp
	Rev_cmR:SpeI	338				
kan^r	KANfwd_XhoI_NotI	534	61°C, 30 sec	72°C, 30 sec	25	1036 bp
	Rev-kanR-SpeI	69				
P_{tac}-egfp-rrnb	pTac_XhoI	536	71°C, 30 sec	72°C, 40 sec	30	1433 bp
	rrnBrev_NotI	535				
hGHΔS	hGH_fwd_NdeI	539	64°C, 30 sec	72°C, 20 sec	25	601 bp
	hGH_rev_HindIII	540				
celAoCΔS	celAoCdS_fwd_NdeI	537	61°C, 30 sec	72°C, 30 sec	25	916 bp

	celAoCdS_rev_HindIII	538				
LevΔS	Lev_fwd_NdeI	541	58°C, 20 sec	72°C, 50 sec	25	1974 bp
	Lev_rev_HindIII	542				
pehB	pehB-Sec-fwd	544	58°C, 20 sec	72°C, 10 sec	25	313 bp
	pehB-Sec-rev-NdeI	545				
Pme	pme-Sec-fwd	546	58°C, 20 sec	72°C, 10 sec	25	121 bp
	pme-Sec-rev-NdeI	547				
Egl	egl-Sec-fwd	548	58°C, 20 sec	72°C, 10 sec	25	133 bp
	egl-Sec-rev-NdeI	549				
cbhA	cbhA-Sec-fwd	550	58°C, 20 sec	72°C, 10 sec	25	214 bp
	cbhA-Sec-rev-NdeI	551				
Tek	tek-Sec-fwd	552	58°C, 20 sec	72°C, 10 sec	25	176 bp
	tek-Sec-rev-NdeI	553				
Aac	aac-Sec-fwd	554	58°C, 20 sec	72°C, 10 sec	30	157 bp
	aac-Sec-rev-NdeI	555				
TreA	treA-Sec-fwd	556	58°C, 20 sec	72°C, 10 sec	30	208 bp
	treA-Sec-rev-NdeI	557				
PqaA	PqaA-Sec-fwd	558	58°C, 20 sec	72°C, 10 sec	30	142 bp
	PqaA-Sec-rev-NdeI	559				
F504_4738	F504_4738-Sec-fwd	560	58°C, 20 sec	72°C, 10 sec	30	154 bp
	F504_4738-Sec-rev-NdeI	561				
F503_2783	F504_2783-Sec-fwd	562	58°C, 20 sec	72°C, 10 sec	30	133 bp
	F504_2783-Sec-rev-NdeI	563				
NosL	NosL-Sec-fwd	564	58°C, 20 sec	72°C, 10 sec	30	166 bp
	NosL-Sec-rev-NdeI	565				
F504_2199	F504_2199-Sec-fwd	566	58°C, 20 sec	72°C, 10 sec	30	187 bp
	F504_2199-Sec-rev-NdeI	567				
F504_2437	F504_2437-Sec-fwd	568	58°C, 20 sec	72°C, 10 sec	30	178 bp
	F504_2437-Sec-rev-NdeI	569				
RlpB	RlpB-Sec-fwd	570	58°C, 20 sec	72°C, 10 sec	30	163 bp
	RlpB-Sec-rev-NdeI	571				
F504_2793	F504_2793-Sec-fwd	572	58°C, 20 sec	72°C, 10 sec	30	154 bp
	F504_2793-Sec-rev-NdeI	573				
amiC	amiC-Sec-fwd	574	58°C, 20 sec	72°C, 10 sec	30	217 bp
	amiC-Sec-rev-NdeI	575				
NasF	nasF-Sec-fwd	576	58°C, 20 sec	72°C, 10 sec	30	196 bp
	nasF-Sec-rev-NdeI	577				
iorB2	iorB2-Sec-fwd	578	58°C, 20 sec	72°C, 10 sec	30	199 bp
	iorB2-Sec-rev-NdeI	579				

Rsc NosZ	Rsc-NosZ-Sec-fwd	584	58°C, 20 sec	72°C, 10 sec	30	196 bp
	Rsc-NosZ-Sec-rev-NdeI	585				
pehC	pehC-Sec-fwd	582	58°C, 20 sec	72°C, 10 sec	30	214 bp
	pehC-Sec-rev-NdeI	583				
ReH16 NosZ	ReH16-NosZ-Sec-fwd	580	58°C, 20 sec	72°C, 10 sec	30	208 bp
	ReH16-NosZ-Sec-rev-NdeI	581				
KANoeSS	*Rev-kanR-SpeI*	69	58°C, 30 sec	72°C, 45 sec	25	1285 bp
	Signal_oe_rev	543				

2.2.2.2. Overlap extension PCR

Overlap extension PCRs (oePCR) were performed to construct larger DNA fragments without the need of restriction sites and is based on the principle of the annealing of two complementary sequences. All overlap extension PCR reactions were performed with Q5® High-Fidelity DNA Polymerase. First, two standard PCRs were performed to amplify the desired DNA fragments (see 2.2.2.1 for a standard PCR reaction mix). Thereby, the reverse primer of the first DNA fragment and the forward primer of the second primer introduced the complementary overlap of 20 bp. These amplified fragments served as the templates for the overlap extension PCR. The setup of the overlap extension PCRs was conducted as described in the previous passage, but with the exception of having two templates instead of only one. The two templates were added in an equimolar ratio, whereas at least 10 ng of each template were used. All conducted overlap extension PCRs are summarized in Table 14.

Table 14 Summary of oePCR conditions using Q5® High-Fidelity DNA Polymerase.

The two templates used for each oePCR were the *kan*^{r} fragment and the fragment of each signal peptide

oePCR fragment	Primer pair	Annealingtemp. / -time	Extensiontemp. / -time	Cycles	Fragment size
pehBKAN	*KanR-SpeI-rev* *pehB-Sec-rev-NdeI*	58°C, 20 sec	72°C, 45 sec	30	1563 bp
PmeKAN	*KanR-SpeI-rev* *pme-Sec-rev-NdeI*	58°C, 20 sec	72°C, 45 sec	30	1371 bp
EglKAN	KanR-SpeI-rev *egl-Sec-rev-NdeI*	58°C, 20 sec	72°C, 45 sec	30	1383 bp
cbhAKAN	KanR-SpeI-rev	58°C, 20 sec	72°C, 45 sec	30	1464 bp

	cbhA-Sec-rev-NdeI				
TekKAN	KanR-SpeI-rev tek-Sec-rev-NdeI	58°C, 20 sec	72°C, 45 sec	30	1428 bp
AacKAN	KanR-SpeI-rev *aac-Sec-rev-NdeI*	58°C, 20 sec	72°C, 45 sec	30	1407 bp
TreAKAN	KanR-SpeI-rev treA-Sec-rev-NdeI	58°C, 20 sec	72°C, 45 sec	30	1458 bp
PqaAKAN	KanR-SpeI-rev PqaA-Sec-rev-NdeI	58°C, 20 sec	72°C, 45 sec	30	1392 bp
F504_4738KAN	KanR-SpeI-rev F504_4738-Sec-rev-NdeI	58°C, 20 sec	72°C, 45 sec	30	1404 bp
F503_2783KAN	KanR-SpeI-rev F504_2783-Sec-rev-NdeI	58°C, 20 sec	72°C, 45 sec	30	1383 bp
NosLKAN	KanR-SpeI-rev NosL-Sec-rev-NdeI	58°C, 20 sec	72°C, 45 sec	30	1416 bp
F504_2199KAN	KanR-SpeI-rev F504_2199-Sec-rev-NdeI	58°C, 20 sec	72°C, 45 sec	30	1437 bp
F504_2437KAN	KanR-SpeI-rev F504_2437-Sec-rev-NdeI	58°C, 20 sec	72°C, 45 sec	30	1428 bp
RlpBKAN	KanR-SpeI-rev RlpB-Sec-rev-NdeI	58°C, 20 sec	72°C, 45 sec	30	1413 bp
F504_2793KAN	KanR-SpeI-rev F504_2793-Sec-rev-NdeI	58°C, 20 sec	72°C, 45 sec	30	1404 bp
amiCKAN	KanR-SpeI-rev amiC-Sec-rev-NdeI	58°C, 20 sec	72°C, 45 sec	30	1467 bp
NasFKAN	KanR-SpeI-rev nasF-Sec-rev-NdeI	58°C, 20 sec	72°C, 45 sec	30	1446 bp
iorB2KAN	KanR-SpeI-rev iorB2-Sec-rev-NdeI	58°C, 20 sec	72°C, 45 sec	30	1449 bp
Rsc NosZKAN	KanR-SpeI-rev Rsc-NosZ-Sec-rev-NdeI	58°C, 20 sec	72°C, 45 sec	30	1446 bp
pehCKAN	KanR-SpeI-rev pehC-Sec-rev-NdeI	58°C, 20 sec	72°C, 45 sec	30	1464 bp
ReH16 NosZKAN	KanR-SpeI-rev ReH16-NosZ-Sec-rev-NdeI	58°C, 20 sec	72°C, 45 sec	30	1458 bp

2.2.2.3. Colony PCR

Colony PCR reactions were performed using DreamTaq DNA polymerase (Thermo Fisher Scientific Inc.) with the Green GoTaq® reaction buffer (Promega; Madison, USA) . Small amounts of cell materials were picked up with a toothpick and resuspended in the Colony PCR reaction mix. The breakage of the cells and the subsequent release of DNA was accomplished through the initial denaturation step of the PCR reaction. Table 15 describes the general setup for a Colony PCR reaction.

Table 15 General setup for a colony PCR reaction

Green GoTaq (5x)	5 µL
10mM dNTPs	0.6 µL
Forward Primer (10 mM)	1.25 µL
Reverse Primer (10 mM)	1.25 µL
DreamTaq Polymerase	0.2 µL
ddH_2O	x µL
	25 µL

The general PCR program is shown below (Table 16). The conducted colony PCRs, which confirmed the presence of plasmid DNA in *R. eutropha* H16 transconjugants are summarized in Table 17.

Table 16 General colony PCR program

Step	**Temperatur [°C]**	**Time [s]**	
Initial Denaturation	95	60	
Denaturation	95	30	25 - 35 cycles
Annealing	58	30	
Elongation	72	60 seconds/kb	
Final Elongation	72	300	
	4	∞	

Table 17 Summary of colony PCR conditions to verify the presence of plasmid DNA in *R. eutropha* H16 transconjugants

PCR fragment	Primer pair	No.	Extensiontemp. / -time	Cycles	Fragment size
SP-hGH	SP-Sec-fwd	546 - 585	72°C, 60 sec	30	685 - 781 bp
	hGH_rev_HindIII	540			
SP-lev	SP-Sec-fwd	546 - 585	72°C, 130 sec	30	2058 - 2154 bp
	hGH_rev_HindIII	540			

2.2.3 Agarose gel electrophoresis

Agarose gel electrophoresis was used to separate DNA fragments according to their size. A 1 % gel was poured by dissolving 2 g of agarose (Biozyme; Vienna, Austria) in 200 mL of 1 x TAE buffer (4.84 g L^{-1} Tris, 0.292 g L^{-1} EDTA, 1.142 mL L^{-1} acetic acid). The agarose was solubilized by heating it in the microwave for approximately 3 min and after rinsing the flask with water to cool down the solution, Ethidium bromide (EtBr) was added to make DNA bands visible. Control gels were run for 45 min at 120 V, whereas preparative agarose gels were run for 1.5 h at 90 V until a proper separation of DNA could be observed. Five µL of the standard GeneRuler™ DNA Ladder Mix (Thermo Fisher Scientific Inc.) were loaded onto the gel to determine the size and concentration of the DNA bands (Figure 3).

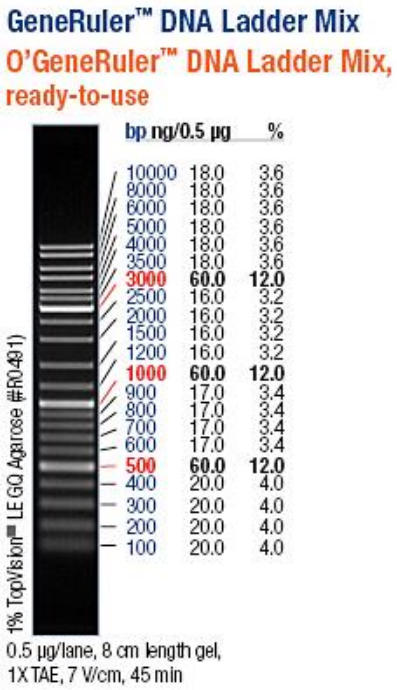

Figure 3 GeneRulerTM DNA Ladder Mix (Thermo Fisher Scientific Inc.) for agarose gels

2.2.4 Restriction digestion

Restriction digests were performed with restriction enzymes and the appropriate buffers from Thermo Fisher Scientific Inc. The optimal reaction conditions for the digestion with two enzymes were determined with the DoubleDigest web tool of Thermo Fisher Scientific [69]. The restriction reactions were prepared as described in Table 18.

Table 18 Preparation of restriction digests

	Control cuts	**Preparative digests**
DNA (200 – 500 ng)	x µL	x µL
Restriction enzymes (10 U / µL)	0.5 - 1 µL	1 – 2 µL
Reaction buffer (10 x)	3 µL	5 – 10 µL
ddH_2O	-	y µL
	30 µL	50 – 100 µL

A restriction reaction with the conventional enzymes was carried out at 37 °C for 4 h for control restrictions and overnight for preparative digestions. The incubation time could be reduced to 30 – 60 min for digestions using FastDigest restriction enzymes. In the

following, the reactions were heat inactivated at 65 °C or 80 °C for 20 min according to the thermal inactivation temperature of the used restriction enzyme. If necessary, the digested vector backbone was dephosphorylated using 2 µL Fast AP Thermosensitive Phosphatase (Thermo Fisher Scientific Inc.).

2.2.5 Purification of DNA gel slices and PCR products

The Wizard® SV Gel and PCR Clean-Up System Kit (Promega) was used to dissolve an agarose gel slice or to clean up a PCR product or a restriction digest. The kit was used as recommended by the manufacturer. To dissolve the gel slice, 10 µL of membrane binding solution was added to 10 mg of gel slice. The sample was incubated at 65 °C and 700 rpm until the gel slice was completely dissolved. When processing PCR reactions or restriction digests an equal volume of membrane binding solution was added to the reaction mix. For the binding of the DNA, the dissolved gel mixture or the prepared PCR reaction was then transferred into the SV minicolumn, which was inserted into a collection tube and incubated at RT for 1 min. The minicolumn was then centrifuged at 16,000 x g for 1 min and the flow-through was discarded. After that, the DNA was washed with 700 µL membrane wash solution, centrifuged using prior conditions for 1 min and the flow-through was discarded. The washing step was repeated with 500 µL of membrane wash solution, centrifuged using prior conditions for 5 min and the flow-through was discarded. After another centrifugation step, the minicolumn was transferred into a clean 1.5 mL microcentrifuge tube and 30 µL ddH_2O were added to the spin column. After an incubation for 5 min at RT, the minicolumn was centrifuged using prior conditions for 2 min and the flow-through was collected and stored at -20 °C until use.

2.2.6 Measurement of DNA concentration

The concentration of purified DNA was measured at a wavelength of 260 nm by NanoDrop2000c (Thermo Fisher Scientific Inc.).

2.2.7 Ligation

For ligation, the T4 DNA Ligase from Promega was used. A ligation mixture was set up to a total volume of 15 µL. It contained 1.5 µL of T4 DNA Ligase buffer, 0.5 µL of T4 DNA Ligase, a variable volume of vector backbone DNA (40 - 80 ng) and a variable amount of insert DNA to reach a vector to insert ratio of 1:3. The ligation mixture was filled up with ddH_2O to the total volume of 15 µL. The ligation reaction mixture was incubated overnight at 16 °C. Prior electroporation, the ligation reaction was thermal inactivated by heating it at 65 °C for 20 min and a subsequent desalting step was performed. The ligation was desalted on nitrocellulose filter plates (Millipore GSWP2500, pore size 0.22 µm) against ddH_2O for 30 min. An amount of 3.5 µL was then used for transformation.

2.2.8 Electrocompetent cells

Overnight cultures of *E. coli* TOP10 or *E. coli* S17-1 cells were set up in 30 mL of LB media and grown overnight at 37 °C and 220 rpm. For the main culture, 500 mL of LB media were inoculated to an OD of 0.1 in 2 L baffled flasks and incubated at 37 °C and 170 rpm until an OD_{600} value between 0.5 and 0.9 was reached. The cells were then pre-chilled on ice for 60 min before being harvested by centrifugation for 15 min at 3000 x *g* and 4 °C. Pellets were washed twice with 500 mL of ice-cold H_2O containing 1 mM hepes buffer and centrifuged as above. The cells were resuspended in 100 mL of pre-chilled, sterile 10 % glycerol and centrifuged for 15 min at 4500 x *g* and 4 °C. Finally, cells were resuspended in 500 µL per 500 mL of media of ice-cold 10 % glycerol. Aliquots containing 90 µL of electrocompetent cells were quick-frozen with liquid nitrogen and stored at -80 °C until use.

2.2.9 Electrotransformation

For electroporation of *E. coli* cells, 45 µL of electrocompetent cells were mixed with 2 µL of plasmid DNA or 3.5 µL of the ligation reaction mix and transferred to pre-chilled electroporation cuvettes. Cells were pulsed for 5-6 ms with the electroporator (Bio-Rad MicroPulser™; Hercules, USA) set to program EC2 at 2.5 kV. Immediately after transformation, one mL of LB medium was added and cells were regenerated at 600 rpm

and 37 °C for 60 min. The cells were then briefly spun down in the microcentrifuge and resuspended in 100 µL of LB media. The whole suspension was plated out on LB agar plates containing the appropriate antibiotics (see 2.4.1 Cultivation of *E. coli* strains) and incubated at 37 °C overnight.

2.2.10 CloneJET PCR Cloning Kit

The CloneJET PCR Cloning Kit from Thermo Fisher Scientific Inc. was used to clone amplified PCR products directly into the linearized cloning vector pJET1.2. The big advantage of this method is that no phosphorylation step of the PCR product is necessary prior cloning. The procedure was performed following the manufacturers' protocol. A standard ligation mixture is shown in Table 19. The ligation mixture was incubated at RT (22 °C) for 20 min. Then, the ligation mixture was inactivated at 65 °C for 10 min, desalted and subsequently used for transformation.

Table 19 Standard ligation mixture of pJET1.2 cloning kit

2 x Reaction buffer	10 µL
purified PCR product (75 ng)	x µL
pJET1.2/blunt Cloning Vector (50 ng)	1 µL
T4 DNA Ligase	1 µL
ddH_2O	x µL
	20 µL

2.2.11 Sequencing

Sequencing was conducted to determine the correct sequence of the amplified DNA fragments. For that reason, 10 µL of the DNA fragment to be sequenced were supplemented with 4 µL (5 µM) of the appropriate primer and sent for sequencing to LGC Genomics GmbH (Berlin, Germany).

2.3 Conjugation

The transfer of plasmid DNA into *R. eutropha* H16 cells was performed via conjugation. Two different methods were applied.

2.3.1 Conjugation with the donor strain *E. coli* S17-1

Single colonies of *E. coli* S17-1 harboring the plasmid DNA (donor) and wild-type *R. eutropha* H16 (acceptor) were picked to inoculate overnight cultures (ONCs): *R. eutropha* H16 was grown in 5 mL TSB media at 28 °C for 20 h and the *E. coli* S17-1 strains harboring the plasmids were grown in 5 mL LB media, supplemented with the appropriate antibiotics, at 37 °C for approximately 20 h. Afterwards, the cells were harvested by centrifugation (3220 x g, 20 min at 4 °C; Eppendorf centrifuge 5810 R) and the cell pellets were resuspended in 0.1 mL NaCl (0.9 %). Subsequently, 100 µL of both, donor and acceptor, suspensions were trickled on NB media and incubated at 28 °C for 20 h. Then, the cells were resuspended with 3 mL NaCl (0.9 %) and 100 µL were plated out on TSB plates containing 0.6 % fructose and the appropriate antibiotics. The plates were incubated for about 48 h at 28 °C till cell growth was visible. In the following, single colonies were re-streaked for purification purposes prior further use.

2.3.2 Conjugation with the helper plasmid pRK2013

At times, the desired plasmid DNA could only be transformed into *E. coli* Top10 cells, but not into *E. coli* S17-1 cells. For this reason, the *E. coli* strain HB101 harboring the mobilization helper plasmid pRK2013 was used for the plasmid transfer by triparental mating [67]. Single colonies of *E. coli* Top10 harboring the plasmids (donor), *E. coli* HB101 [pRK2013] and wild-type *R. eutropha* H16 were picked to inoculate ONCs: the *E. coli* strains were both grown in 3 mL LB media containing kanamycin [40 µg mL^{-1}] and *R. eutropha* H16 was grown as described above. The mating process was performed following the previous description, but with the exception of mixing three strains together instead of two.

2.4 Media, cultivation and harvesting

2.4.1 Cultivation of *E. coli* strains

E. coli strains were cultivated in lysogeny broth (LB) medium (Carl Roth GmbH CO. KG; Heidelberg, Germany) or 2 x TY media at 37 °C. The composition for 2 x TY media is as follows: 10 [g L^{-1}] yeast extract, 16 [g L^{-1}] peptone and 5 [g L^{-1}] NaCl. For petri dishes, 20 [g L^{-1}] agar-agar (Carl Roth GmbH) were added to liquid media before autoclaving. After autoclaving, the media was supplemented with either kanamycin [40 µg mL^{-1}], chloramphenicol [25 µg mL^{-1}] or ampicillin [100 µg mL^{-1}]. All antibiotics were obtained from Carl Roth GmbH & Co KG, Karlsruhe, Germany.

2.4.2 Cultivation of *Ralstonia eutropha* H16

The wild-type *R. eutropha* H16 strain was grown in tryptic soy broth (TSB; BD Diagnostic Systems; Heidelberg, Germany) or nutrient broth (NB) at 28 °C. After conjugation, *R. eutropha* H16 transconjugants were grown at 28 °C on TSB agar plates supplemented with 0.6 % fructose, gentamycin [20 µg mL^{-1}] and either kanamycin [200 µg mL^{-1}] or chloramphenicol [50 µg mL^{-1}]. For the cultivation of *R. eutropha* H16 transconjugants harboring cm^r plasmids in liquid media, the concentration of chloramphenicol was increased to 75 [µg mL^{-1}]. The ingredients of NB media are 5 [g L^{-1}] peptone and 3 [g L^{-1}] beef extract.

2.4.3 Fermentation conditions for secretion assays

Fermentations for the examination of secretion productivity had to be free from dextrose and fructose as it would disturb the activity assays for CelA (see 2.12 Reducing sugar assay) and Lev (see 2.13 Levanase activity assay). Therefore, *R. eutropha* H16 transconjugants carrying secretion plasmids were cultivated in LB media supplemented with 1 % glycerol, gentamycin [20 µg mL^{-1}] and either kanamycin [200 µg mL^{-1}] or chloramphenicol [75 µg mL^{-1}]. Single colonies of *R. eutropha* H16 transconjugants were used to inoculate 3 mL of LB media in 15 mL centrifuge tubes (Greiner Bio-One; Kremsmünster, Austria) and grown overnight at 28 °C in a rotor shaker. For the main culture, 20 mL of LB media containing the appropriate supplementation was inoculated to an OD_{600} of 0.2 and grown at 28 °C and 130 rpm. After 15 h, the fermentations were

harvested by centrifugation at 3220 x g at 4 °C for 30 min. For the determination of the secretion efficiency, the cell-free supernatant was yielded and stored at 4 °C until use.

2.5 Isolation of periplasmatic fraction

Isolation of the periplasma was prepared according to a method described by Bernhard et al. [13]. One mL of *R. eutropha* H16 cells was harvested at 16.1 x g for 5 min at 4 °C. Following a washing step with 100 µL 10 mM Tris-HCl, pH 7.5 (16.1 x g, 4°C), the cells were resuspended in 50 µL of 10 mM Tris-HCl pH 7.8 containing 0.5 M sucrose and incubated for 10 min at 30 °C in the presence of 1 mM EDTA. The incubation was continued at RT for 30 min with the subsequent addition of lysozyme (10 mg g^{-1} [wet weight] of cells). Afterwards the mixture was centrifuged at full speed for 20 min at 4 °C and the periplasmatic fraction was isolated by harvesting the supernatant.

2.6 Measurement of protein concentration

Protein concentrations were determined using the method of Bradford [70] via the Bio-Rad protein assay (Bio-Rad Laboratories Inc.; Hercules, USA). For quantification of the protein amount in cell-free supernatant, the microassay procedure for microtiter plates was applied. 160 µL of the protein sample (culture supernatant) or blank (LB media) were added to 40 µL protein assay dye reagent concentrate (Bio-Rad Laboratories Inc.). After incubation for 30 min at RT, 150 µL of the mixture were measured at 595 nm in platereader FLUOstar Omega (BMG Labtech GmBH; Ortenberg, Germany). For generating the calibration curve, different dilutions of bovine serum albumin (BSA) in LB media were used: 0.2 [µg mL^{-1}], 0.5 [µg mL^{-1}], 1 [µg mL^{-1}], 2.5 [µg mL^{-1}], 5 [µg mL^{-1}], 10 [µg mL^{-1}], 15 [µg mL^{-1}], 30 [µg mL^{-1}], 75 [µg mL^{-1}]. The determination of the protein concentrations were assayed in triplicates and calculated according to the equation from the BSA calibration curve (see 7.3).

2.7 Methanol/ Chloroform protein precipitation

To be suitable for proteomic analysis, protein samples should be free from salts and other interfering agents, such as detergents, lipids and nucleic acids and need to have an

appropriate protein concentration. Precipitation with methanol and chloroform has been reported to have the greatest yields of protein recovery [71, 72]. The method is divided in two parts: First, one mL of the supernatant from *R. eutropha* H16 transconjugants was mixed with 570 µL methanol and the mixture was vortexed thoroughly. 190 µL of chloroform were then added and the samples were vortexed and centrifuged at full speed for 5 min in a table centrifuge. During this step, an initial phase separation occurred and the mixture is separated into hydrophobic and hydrophilic layers. Proteins possess both hydrophobic and hydrophilic layers and therefore, will precipitate at the interface between the two phases. After centrifugation, the top aqueous layer, containing salts, detergents, reducing agents and nucleic acids, was removed and the protein is precipitated and pelleted by the addition of 300 µL of methanol and centrifugated at full speed and 4 °C for 30 min. The supernatant was removed and the protein pellet was then air-dried and dissolved in 20 µL of 1 x final sample buffer (FSB). The composition of 2 x FSB buffer is described in Table 20.

Table 20 Composition of 2 x FSB buffer

0.5 M Tris-HCl (pH 6.8)	7.5 mL
10 % SDS	3 mL
β-mercaptoethanol	3 mL
Glycerol	6 mL
Bromophenol Blue	0.0012 g
ddH_2O	10.5 mL
	30 mL

2.8 Sodium dodecyl sulphate-polyacrylamide gel electrophoresis

The SDS-PAGE (sodium dodecyl sulfate polyacrylamide gel electrophoresis) was carried out to analyse the proteins in either the whole-cell lysates or the supernatants of *R. eutropha* H16 transconjugants. Thereby, proteins were separated according to their size in a self-made 12 % polyacrylamide gel containing SDS. After pouring the resolving gel, it was covered with butanol to smooth the gel surface and polymerised for approximately 1 h. Then, the stacking gel was poured onto the resolving gel, polymerised and stored at 4 °C until use. The volumes for the resolving and stacking gel are calculated for pouring 5 gels (Table 21).

Table 21 Composition of resolving and stacking gels for SDS-PAGE
Volumes are calculated for pouring 5 gels each

	Resolving gel (12 %)	**Stacking gel (4 %)**
30 % Acrylamide/Bis solution (Bio-Rad Laboratories Inc.)	12.8 mL	3 mL
Resolving gel buffer stock[1]	8 mL	-
Stacking gel buffer stock[2]	-	2.5 mL
10 % Ammonium persulfate (APS)	100 µL	40 µL
Tretramethylethylenediamine (TEMED)	40 µL	20 µL
Bromophenol Blue	-	20 µL
H_2O	11.2 mL	12 mL

[1] resolving gel buffer: 0.5 M Tris, 0.4 % SDS, pH 8.8

[2] stacking gel buffer: 0,5 M Tris, 0.4 % SDS, pH 6.8

The supernatants of the fermentation samples were first precipitated with methanol and chloroform (see 2.7 Methanol/ Chloroform protein precipitation). Five µL of the precipitated protein samples, corresponding to the protein amount found in 250 µL of culture supernatant, were loaded onto the gel. When the SDS-PAGE samples were prepared to be whole cell lysates, 1 mL of the culture broth was harvested and spun down. The supernatant was discarded and the cell pellet was resuspended in potassium phosphate buffer (pH 7.4, 0.1 M). The samples were OD_{600} normalised according to the following formula:

$$OD_{600}\ x\ 33.3 = \ \mu l\ of\ buffer$$

5.5 µL of the *R. eutropha* H16 samples were used for further SDS-PAGE sample preparation. Prior to loading onto the gel, the cells were prepared according to the description in Table 22 and disrupted by heating the reaction mixture to 99 °C for 10 min.

Table 22 Sample preparation for SDS-gel.

	***R. eutropha* H16**
Resuspended cells	5.5 µL
FSB Buffer 4x	2.5 µL
NaOH (0.1 M)	1 µL
SDS (20 %)	1 µL
	10 µL

Five µL of the standard PageRuler™ Prestained Protein Ladder (Thermo Fisher Scientific Inc.) were used to determine the size of the proteins (Figure 4).

For the electrophoresis, the chamber was filled with 1 x running buffer (25 mM Tris, 192 mM glycine, 0.1 % SDS) and the gel was run at 200 V for 10 min followed by 110 V for about 1 h using the SE 250 Mighty Small II electrophoresis unit (Hoefer Inc.; Massachusetts, USA) and the PowerPac™ Basic Power Supply (Bio-Rad Laboratories Inc.; Hercules, USA).

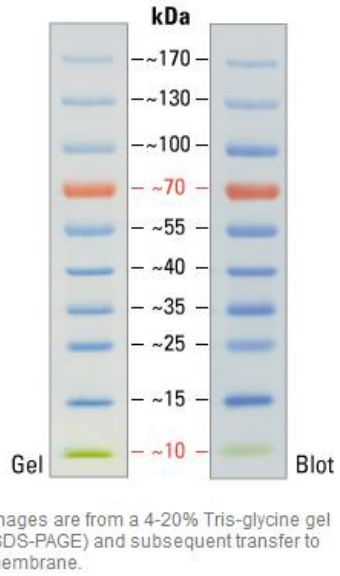

Figure 4 PageRulerTM Prestained Protein Ladder (Thermo Fisher Scientific Inc.)

The gel was then either stained with Coomassie Brilliant Blue solution (0.25 % Brilliant Blue G 250, 10 % acetic acid, 50 % ethanol) for 20 min followed by discolouration with acetic acid (10 %) overnight or further used for western blotting.

2.9 Western Blot

hGH can be detected via immunodetection methods. The SDS-PAGE, which separated the proteins in the culture supernatant were transferred onto a 0.2 µm nitrocellulose membrane (Roti® - NC, Carl Roth GmbH) via blotting with the TE22 mini tank transfer unit (Amersham Biosciences, GE Healthcare; Little Chalfont, UK). The transfer tank was filled with 1 x transfer buffer (12 mM Tris, 96 mM glycine, 10 % methanol) and blotting was performed at maximal 500 V for 1 h with the power supply PowerEase500 (Life Technologies; California, USA). To see if the protein transfer was successful, the membrane was stained with an aqueous Ponceau S solution (0.5 % Ponceau S, 1 % acetic acid). Destaining was performed with H_2O. For immunodetection, the membrane first had to be blocked with 5 % milk in 1 x tris buffered saline with TritonX-100 (TBST; 50 mM tris (pH 7.4), 150 mM NaCl, 0.1 % TritonX-100) for 1 h at RT. The membrane was rinsed twice with 1 x TBST, before being incubated with the primary antibody overnight at 4 °C and intermittent shaking. After the incubation with the primary antibody [GH (T-20):

sc10365], the membrane was washed 3 times with 1 x TBST for 5 min at moderate shaking. Then, the membrane was incubated with secondary antibody [donkey anti-Goat IgG coupled with alkaline phosphatase: sc-3852 or selfmade 2nd antibody] for 1 h at RT and moderate shaking. The membrane was washed again and then detected with either BCIP®/NBT (Sigma-Aldrich; Missouri, USA) or SignalFire™ Elite ECL Reagent (Cell Signaling Technology Inc., Massachusetts, USA). For the second detection method, Reagent A and Reagent B were mixed in a 1:1 ratio before use. The chemiluminescent signal was then captured with the G:Box Bioimaging System (Syngene, Cambridge, UK).

2.10 Enzyme linked immunosorbent assay

The Enzyme linked immunosorbent assay (ELISA) was applied to indirectly detect the amount of secreted hGH by *R. eutropha* H16 transconjugants harboring hGH secretion plasmids. The primary antibody [GH (T-20): sc-10365], which binds specifically to hGH and is then bound by an enzyme-bound secondary antibody, was diluted 1:300 in TBST/TMP. The secondary antibody [donkey anti-Goat IgG coupled with alkaline phosphatase: sc-3852] is used for the optical detection by colour change and was diluted 1:5000 in TBST/TMP. After centrifugation of the fermentation samples, 50 µL of the cell-free culture supernatants were transferred to special flat-bottomed 96-well ELISA microtiter plates (medium binding, Greiner Bio-One GmbH), which possess an increased binding efficiency for proteins, and incubated for 3 h. Afterwards, the sample solutions were removed from the microtiter plates by pipette. Following a washing step with 100 µL of 1 x Tris buffered saline (TBS) for each well, the plates were then blocked for 15 min with 50 µL blocking solution (milk and protein powder in tris buffered saline (TBS/TMP): 50 mM Tris adjusted to pH 7.4 using HCl, 150 mM NaCl, 40 [g L^{-1}] milk powder, 10 [g L^{-1}] protein powder) and then washed again with 100 µL 1 x TBS. Then, 50 µL of the primary antibody solution were pipetted into each well and incubated for 1 h at RT. After removal of the first antibody solution, the plates were once washed with TBST/TMP and twice washed with TBS/TMP. Afterwards, 200 µL of the secondary antibody were transferred into each well and incubated for 45 min at RT. After removal of the second antibody solution, the plates were once washed with TBST/TMP, once with TBS/TMP and once with 1 x TBS. The staining was done using 50 µL of BCIP®/NBT solution (Sigma-Aldrich; Missouri, USA). As a substrate of alkaline phosphatase, BCIP (5-bromo-4-

chloro-3-indolyl) is hydrolysed and following two intermediate steps, the purple coloured formazan is formed.

2.11 Congo red clearing zone assay

The Congo red clearing zone assay was conducted to screen *R. eutropha* H16 transconjugants for CelA activity and secretion efficiency. Congo red can be used as an indicator for β-D-glucanase activity as it shows a strong interaction with polysaccharides containing contiguous β-(1→4)–linked D-gluco-pyranosyl units, but does not bind into fragment smaller than cellohexaose [73, 74]. Single colonies of *R. eutropha* H16 transconjugants were transferred on TSB agar plates containing 0.6 % Carboxymethylcellulose (CMC) and incubated overnight at 28°C. The following day, the cells were washed off with NaCl (0.9 %) and the plates were then stained with an aqueous solution of Congo red (0.2 % in distilled H_2O) for 30 min with intermittent shaking. Finally, the plates were repeatedly washed with 0.9 % NaCl and the enzymatic activity was visible by a discolouration to yellow. The NaCl solution eluted the dye in the clearing zone, where the cellulose has been degraded into simple sugars by CelA. For the determination of the activity of secreted CelA, 100 µL of cell-free supernatant were filled in holes stamped into agar containing 0.6 % CMC and incubated overnight at 37°C. The staining process was conducted the same way as described above. Additionally, in order to enhance the contrast between the halo and the background, the plates were treated with 0.1 M HCl leading to a colour change from red to purple.

2.12 Reducing sugar assay

For quantitative comparison of the secretion efficiency of *R. eutropha* H16 cells harboring CelA secretion plasmids, a highly sensitive reducing-sugar assay was applied. The assay is based on the formation of osazones from reducing sugars and *para*-hydrobenzoic acid hydrazide (pHBAH) [75]. The screening was performed in a 96-well mirotiterplate format. A stock solution was prepared containing 6.35 g pHBAH (Sigma H9882) and 5 mL HCl (37 %) per 100 mL. The working solution was prepared freshly for each measurement by diluting the stock 1:5 v/v with 0,625 M NaOH. For the substrate conversion, 150 µL of the substrate solution (1.75 % CMC in 50 mM Citrate, 50 mM NaPi, 50 mM Borate, pH 7.0)

were transferred to a 96-well plate. 30 µL of the enzyme sample (culture supernatant) were then added to each well. The plates were sealed and incubated at 50 °C for 30 min and 150 rpm. For the subsequent reducing-sugar assay, 50 µL of the substrate conversion reaction or in case of standards, dilution of glucose were pipetted into 150 µL of pre-chilled pHBAH-working solution in a 96-well plate suitable for thermocyclers. The plates were incubated at 95 °C for 5 min and then cooled to 4 °C in a GeneAmp® PCR System 2700 thermocycler. 150 µL of the assay samples were transferred to a new polystyrol microplate and the absorbance was measured at 430 nm in platereader FLUOstar Omega. Calibration was done using glucose concentrations ranging from 0.01 to 1.0 [mg mL^{-1}] dissolved in LB media. The determination of the glucose concentrations were assayed in triplicates and calculated according to the equation from the pHBAH glucose calibration curve (see 7.4).

2.13 Levanase activity assay

The levanase activity assay was conducted to measure the secretion efficiency of *R. eutropha* H16 transconjugants carrying Lev secretion plasmids. The activity of Lev in the supernatant was examined by measuring the liberation of glucose following incubation with the sucrose. Therefore, the Glucose UV Hexokinase method was applied, which is based on the reactions shown in Figure 5. For the substrate conversion, 50 µL sucrose solution [50 mg mL^{-1}] were transferred to a 96-well v-bottom microtiterplate. Then, 50 µL of the enzyme sample (culture supernatant) or blank (LB media) were added to each well and incubated at 50 °C for 90 min at 150 rpm. For the detection of glucose, 190 µL of Glucose-UV reagent (DIPROmed GmbH; Wegelsdorf, Austria) were pipetted into each well of an UV-microtiterplate and 10 µL of the enzyme reaction sample or in case of standards, dilution of glucose, were added to it. After 10 min incubation in the dark, NADH was measured at 340 nm in platereader FLUOstar Omega. Calibration was done using glucose concentrations from 0.01 to 1.0 [mg mL^{-1}] dissolved in LB media. The determination of the glucose concentrations were assayed in triplicates and calculated according to the equation from the glucose-UV calibration curve (see 7.5).

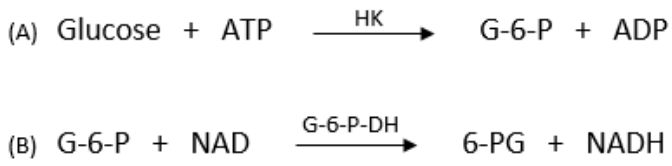

Figure 5 Glucose UV Hexokinase method
Glucose is phosphorylated by adenosine-5'-triphosphate (ATP), in a reaction catalysed by the hexokinase (HK). The glucose-6-phosphate (G-6-P) formed is oxidized to 6-phospho-gluconate (6-PG) by glucose-6-phosphate dehydrogenase (G-6-P-DH). In this same reaction an equimolar amount of Nicotinamide Adenine Dinucleotide (NAD) is reduced to NADH, with a resulting increase in absorbance at 340 nm.

2.14 Construction of pCRep-P_{tac}-eGFP-reverse

The plasmid pKRep-P_{tac}-eGFP was used as a starting vector for the construction of pCRep-P_{tac}-eGFP-reverse (Figure 6). At first, the selection marker kanamycin (*kan*^{r}) was exchanged with the chloramphenicol resistance gene (*cm*^{r}). Therefore, *cm*^{r} was amplified out of pJET_cmR (# 216 of the internal plasmid list by the research group of Petra Köfinger) with the primers CMRfwd_XhoI_NotI (# 533) and Rev-cmR-SpeI (# 338). Due to the sequence of the forward primer, an additional *Xho*I restriction site was introduced, which is necessary for the expression cassette to be turned around. Then, the amplified *cm*^{r} cassette was purified and both the plasmid pKRep-P_{tac}-eGFP and the PCR product *cm*^{r} fragment were cut with *Not*I and *Spe*I. Prior ligation, *cm*^{r} was dephosphorylated and the ligation reaction was transformed into *E. coli* Top10. Subsequently, pCRep-XhoI was isolated and used for further development of pCRep-P_{tac}-eGFP-reverse. pCRep-XhoI consists of the replication origin *Rep*, mobilisation region *mob*, partitioning region *par* and the selection marker *cm*^{r}, but does not contain an expression cassette.

The plasmid pKRep-XhoI was constructed in the same way. *Kan*^{r} was amplified out of pKRep-P_{tac}-eGFP with the primers KANfwd_XhoI_NotI (# 534) and Rev-kanR-SpeI (# 69). After purification, the PCR fragment *kan*^{r} was digested with *Not*I and *Spe*I and ligated into the backbone of pKRep-P_{tac}-eGFP, also cut with *Not*I and *Spe*I. This cloning step was necessary to introduce the *Xho*I restriction site in a template with the *kan*^{r} resistance, which will be needed in later cloning steps.

The next step in the construction of the plasmid pCRep-P_{tac}-eGFP-reverse is the incorporation of the reverse expression cassette. Therefore, a fragment (P_{tac}-eGFP-rrnB) consisting of the *tac* promoter (P_{tac}), the gene of interest *eGFP* and the terminator *rrnB* was amplified out of pKRep-P_{tac}-eGFP with the primers PTac_XhoI (# 536) and rrnB_NotI

(# 535). After purification, the PCR product P_{tac}-eGFP-rrnB and the pCRep-XhoI were digested with *Xho*I and *Not*I and following ligation and transformation into *E. coli* Top10, pKRep-P_{tac}-eGFP-reverse was isolated.

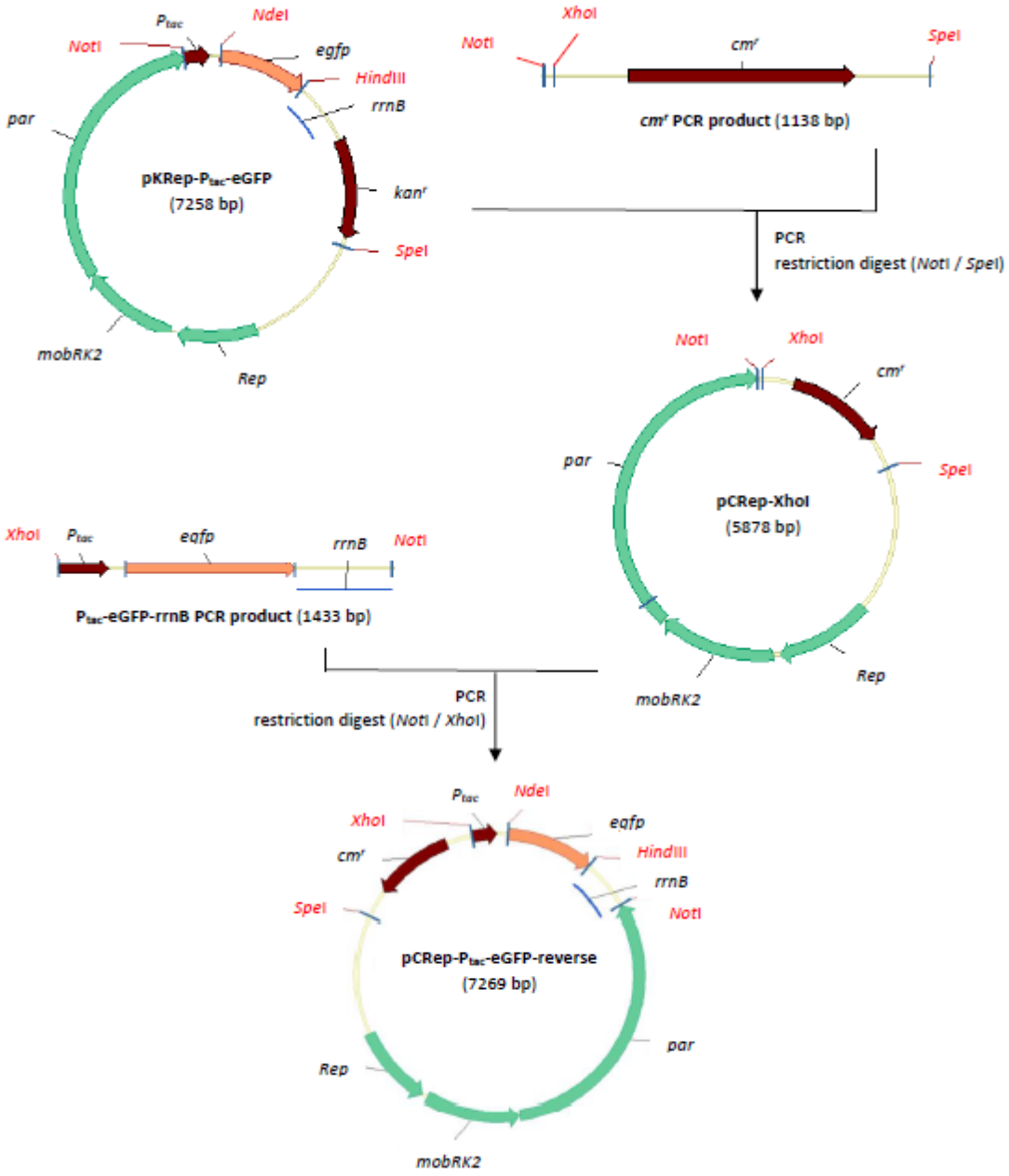

Figure 6 Construction of pCRep-P_{tac}-eGFP-reverse
Following amplification of cm^r of pJET1.2_cmr with primers CMRfwd_XhoI_NotI (# 533) and Rev-cmR-SpeI (# 338), the PCR product and the starting vector pKRep-P_{tac}-eGFP were digested with *Not*I and *Spe*I. Following ligation and transformation into *E. coli* Top10, pCRep-XhoI was isolated. A fragment consisting of P_{tac}, eGFP and rrnB was amplified of pKRep-P_{tac}-eGFP with primers Ptac_XhoI (# 536) and rrnBrev_NotI (# 535) and cloned into the backbone of pCRep-XhoI via the restriction sites *Not*I and *Xho*I. Following ligation and transformation into *E. coli* Top10, pCRep-P_{tac}-eGFP-reverse was isolated.

2.15 Construction of pCRep-P_{tac}-hGHΔS, pCRep-P_{tac}-celAoCΔS and pCRep-P_{tac}-levΔS

As the next step, the 3 reporter genes without their original signal sequence (ΔS) had to be cloned into the backbone of pCRep-P_{tac}-eGFP-reverse (Figure 7). *hGHΔS* was amplified of pPic9-hGH (# 1629 - IMBT's culture collection) with primers hGH_fwd_NdeI (# 539) and hGH_rev_HindIII (# 540) and *celAoCΔS* was amplified of pMS470_celAoCdS_NtHis [59] with primers celAoCdS_fwd_NdeI (# 537) and celAoCdS_rev_HindIII (# 538). *LevΔS* was already cloned into the pKRep-P_{tac} backbone vector with the restriction sites *Nde*I and *Hind*III during previous work by Steffen Gruber using primers lev_fwd_NdeI (# 541) and lev_rev_HindIII (# 542). After purification of the PCR products, the reporter genes *hGHΔS* and *celAoCΔS* were directly cloned into the linearized cloning vector pJET1.2 and the subsequently isolated plasmids pJET_hGHΔS and pJET_celAoCΔS were sent to sequencing to verify the sequence of the amplified reporter genes. Following sequence confirmation, pJET_hGHΔS, pJET_celAoCΔS, pKRep-P_{tac}-levΔS and pCRep-P_{tac}-eGFP-reverse were digested with *Nde*I and *Hind*III and the reporter genes *hGHΔS*, *celAoCΔS* and *levΔS* were ligated into the backbone of pCRep-P_{tac}-eGFP-reverse. Following transformation into *E. coli* Top10, pCRep-P_{tac}-hGHΔS, pCRep-P_{tac}-celAoCΔS and pCRep-P_{tac}-levΔS were isolated.

2.16 Construction of pCRSF1010-P_{tac}-hGHΔS, pCRSF1010-P_{tac}-celAoCΔS and pCRSF1010-P_{tac}-levΔS

First results showed that the mobilisation region *mobRK2* seemed to be instable and therefore, had to be exchanged with the *RSF1010* origin and mobilisation region (Figure ***7***). *RSF1010* was cut out of pKRSF1010-P_{tac}-eGFP with *Not*I and *Spe*I and ligated into the backbones of pCRep-P_{tac}-hGHΔS, pCRep-P_{tac}-celAoCΔS and pCRep-P_{tac}-levΔS, also digested with *Not*I and *Spe*I. Following transformation into *E. coli* Top10, pCRSF1010-P_{tac}-hGHΔS, pCRSF1010-P_{tac}-celAoCΔS and pCRSF1010-P_{tac}-levΔS were isolated.

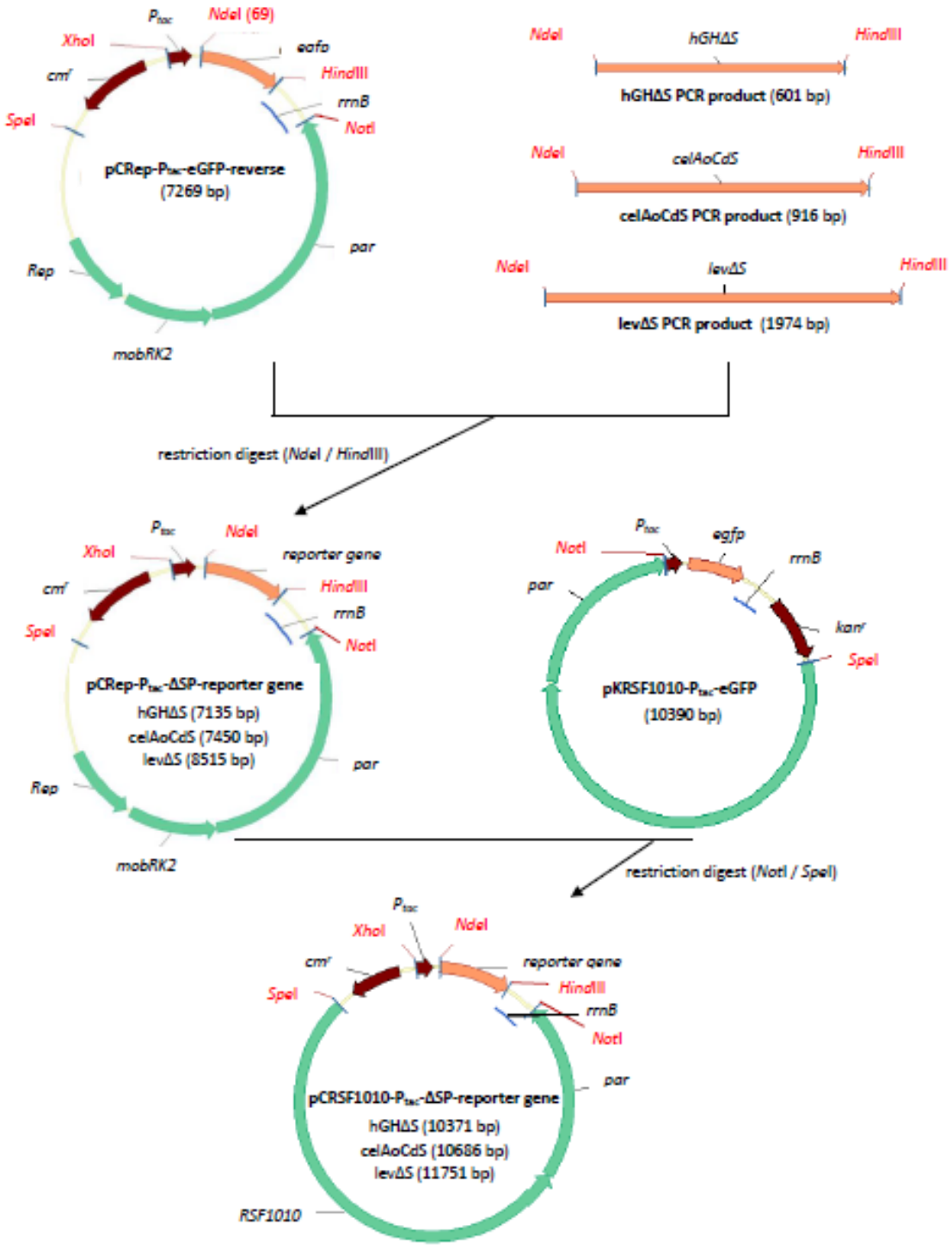

Figure 7 Construction of the basic secretion plasmids: pCRep-P_{tac}-hGHΔS, pCRep-P_{tac}-celAoCΔS, pCRep-P_{tac}-levΔS, pCRSF1010-P_{tac}-hGHΔS, pCRSF1010-P_{tac}-celAoCΔS and pCRSF1010-P_{tac}-levΔS

In the following, eGFP in pCRep-P_{tac}-eGFP-reverse was exchanged with the 3 reporter genes *hGH*, *celAoC* and *lev*. Therefore, the reporter genes had to be amplified without their original signal sequence. *hGHΔS* was amplified with primers hGH_fwd_NdeI (# 539) and hGH_rev_HindIII (# 540). *celAoCΔS* was amplified with primers celAoCdS_fwd_NdeI (#537) and celAoCdS_rev_HindIII (# 538). *levΔS* was already cloned into the pKRep-P_{tac} backbone vector with the restriction sites *Nde*I *and Hind*III during previous work by Steffen Gruber using primers lev_fwd_NdeI (# 541) and lev_rev_HindIII (# 542). The reporter genes were then ligated into the backbone of pCRep-P_{tac}-eGFP-reverse by the restriction sites *Nde*I and *Hind*III. Following transformation into *E. coli* Top10, pCRep-P_{tac}-hGHΔS, pCRep-P_{tac}-celAoCdS and pCRep-P_{tac}-levΔS were isolated. First observation during conjugation revealed that the *ori* and *mob* region had to be exchanged. Therefore, *RSF1010* was cut out of pKRSF1010-P_{tac}-eGFP and cloned into the backbones of pCRep-P_{tac}-hGHΔS, pCRep-P_{tac}-celAoCΔS and pCRep-P_{tac}-levΔS by the restriction sites *Not*I and *Spe*I. Following transformation into *E. coli* Top10, pCRSF1010-P_{tac}-hGHΔS, pCRSF1010-P_{tac}-celAoCΔS and pCRSF1010-P_{tac}-levΔS were isolated.

2.17 Construction of pKRep-P_{tac}-SP-hGH, pKRep-P_{tac}-SP-celA, pKREp-P_{tac}-SP-lev, pKRSF1010-P_{tac}-SP-hGH, pKRSF1010-P_{tac}-SP-celA and pKRSF1010-P_{tac}-SP-lev

The next step was the construction of the secretion vector (Figure 8). Therefore, each signal sequence had to be amplified of genomic DNA from *R. solanacearum* (# 623 – IMBT's culture collection) or *R. eutropha* H16 (#1 – IMBT's culture collection) with the forward (SP-Sec-fwd; # 544, 546, 548, 550, 552, 554, 556, 558, 560, 562, 564, 566, 568, 570, 572, 574, 576, 578, 580, 582, 584) and the reverse primers (SP-Sec-rev-NdeI; # 545, 547, 549, 551, 553, 555, 557, 559, 561, 563, 565, 567, 569, 571, 573, 575, 577, 579, 581, 583, 585) for each signal peptide. At the same time, *kan*^{r} was amplified of pKRep-XhoI with primers Rev-kanR-SpeI (# 69) and signal_oe_rev (# 543). All forward primers of each signal sequence contained a 20 bp sequence complementary to the sequence of primer signal_oe_rev (# 543). Following purification of the PCR products, the signal sequences were fused to the *kan*^{r} PCR product via overlap extension PCR with the primers Rev-kanR-SpeI (# 69) and SP-Sec-rev-NdeI (# 544, 546, 548, 550, 552, 554, 556, 558, 560, 562, 564, 566, 568, 570, 572, 574, 576, 578, 580, 582, 584), which introduce the restriction sites *Nde*I and *Spe*I to the cloning fragments (SP-*kan*^{r}). After purification, the products of the overlap extension PCR were directly ligated into pJET1.2 and sent for sequencing. Following confirmation of the sequence, the plasmids pJET1.2_SP's containing the cloning fragments of the signal peptides were cut with *Nde*I and *Spe*I and cloned into the backbones of the basic vectors pCRep-P_{tac}-hGHΔS, pCRep-P_{tac}-celAoCΔS, pCREp-P_{tac}-levΔS, pKRSF1010-P_{tac}-hGHΔS, pKRSF1010-P_{tac}-celAoCΔS and pKRSF1010-P_{tac}-levΔS, which all were also digested with *Nde*I and *Spe*I. Figure 8 only shows the construction of the final used secretion vectors based on the *RSF1010* origin. The secretion plasmids based on the *Rep* origin and mobilization region were constructed in the same way.

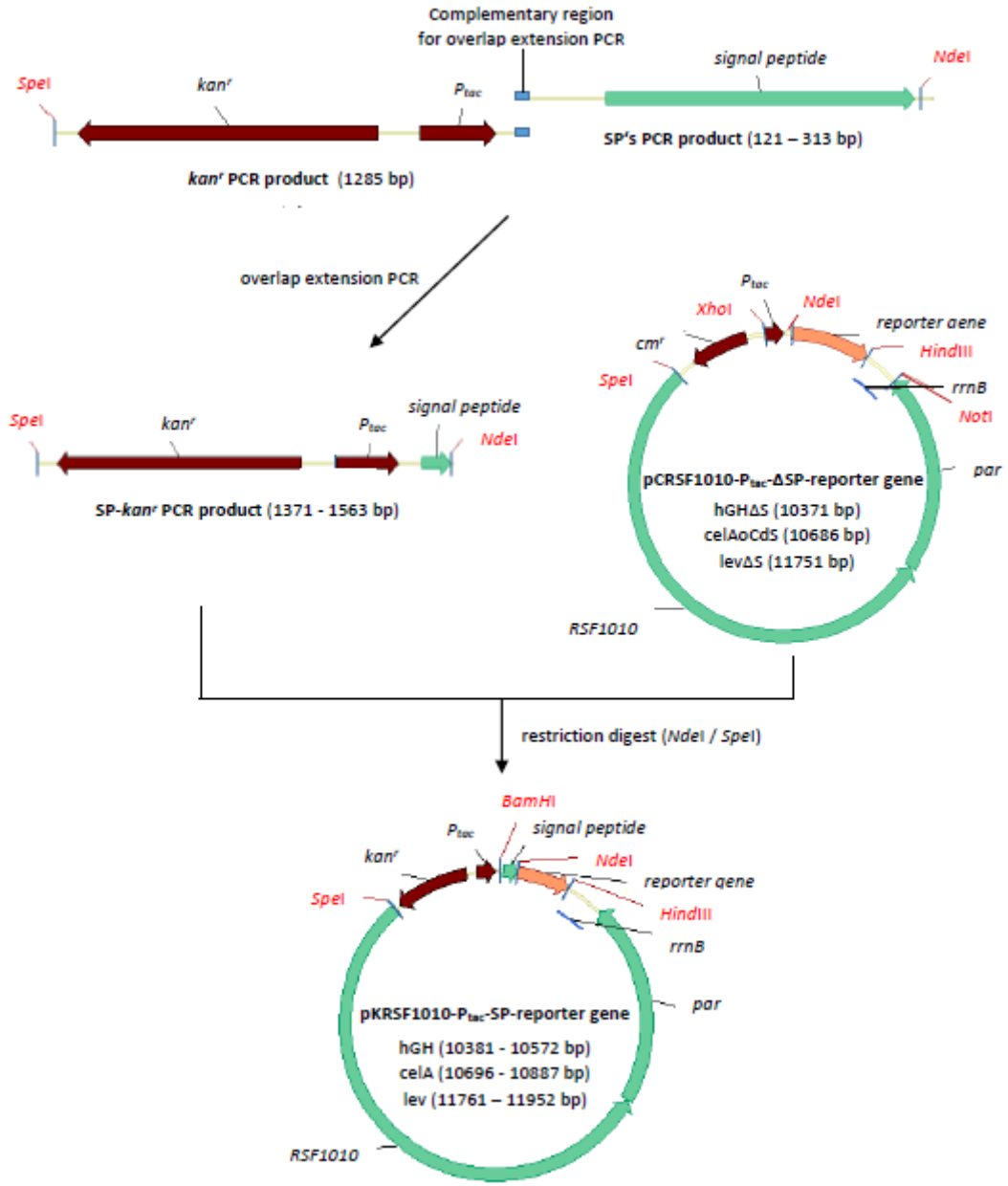

Figure 8 Construction of the secretion plasmids pKRSF1010-P_{tac}-SP-hGH, pKRSF1010-P_{tac}-SP-celA and pKRSF1010-P_{tac}-SP-lev

The signal sequences were amplified of genomic DNA from *R. solanacearum* and *R. eutropha* H16. At the same time, *kan*^{r} was amplified of pKRep-XhoI with primers Rev-kanR-SpeI (# 69) and signal_oe_rev (# 543). The forward primers of each signal sequence contained a 20 bp sequence complementary to the sequence of primer signal_oe_rev (# 543) and after purification of the PCR products, the cloning fragments SP's-KAN were amplified via overlap extension PCR. Following ligation into pJET1.2 and confirmation of the sequence, the cloning fragments SP's-KAN were cloned into pCRSF1010-P_{tac}-hGHΔS, pCRSF1010-P_{tac}-celAoCΔS and pCRSF1010-P_{tac}-levΔS via the restriction sites *Nde*I and *Spe*I.

3 Results

3.1 Construction of a basic vector for secretion in *Ralstonia eutropha* H16

At the beginning, the basic vector was constructed on the basis of the plasmid pKRep-P_{tac}-eGFP by Steffen Gruber [10]. To enhance the cloning efficiency, various modifications on the plasmid had to be performed. The selection marker was exchanged to the chloramphenicol resistance marker (*cm*^{r}) and the backbone vector was turned around allowing a resistance marker exchange while constructing the secretion plasmids. Finally, eGFP was exchanged with one of the three model proteins (hGH, CelA or Lev) for the investigation of recombinant secretory production.

3.1.1 Exchange of resistance marker

First the selection marker *kan*^{r} was exchanged with *cm*^{r}. The *cm*^{r} (1138 bp) cassette was amplified as described in the material and methods section (see 2.2.2.1 General set up for gene amplification). Following purification, the PCR product as well as the plasmid pKRep-P_{tac}-eGFP were digested with *Not*I and *Spe*I. To obtain the desired fragments and to determine the accurate size of the DNA fragments, a preparative gel was run. Afterwards, the concentrations of the purified DNA solutions were measured using Nanodrop and following ligation the ligation mixtures were transformed into *E. coli* Top10. Single colonies were then streaked out for plasmid isolation and a restriction digest was carried out using *Spe*I and *Xho*I, which was previously introduced by the primers. Due to the results of the restriction digest (Figure 9), the cloning of *cm*^{r} into the vector backbone (pCRep-XhoI) was successful as two fragments in the size of 4755 bp and 1099 bp can be observed after a *Xho*I and *Spe*I digest. Additionally, *kan*^{r} with the additional *Xho*I site was added to the vector backbone as described above. Figure 9 also shows the successful cloning of pKRep-XhoI as two fragments in the size of 4755 bp and 994 bp are shown in lane 2 after a restriction digest with *Xho*I and *Spe*I.

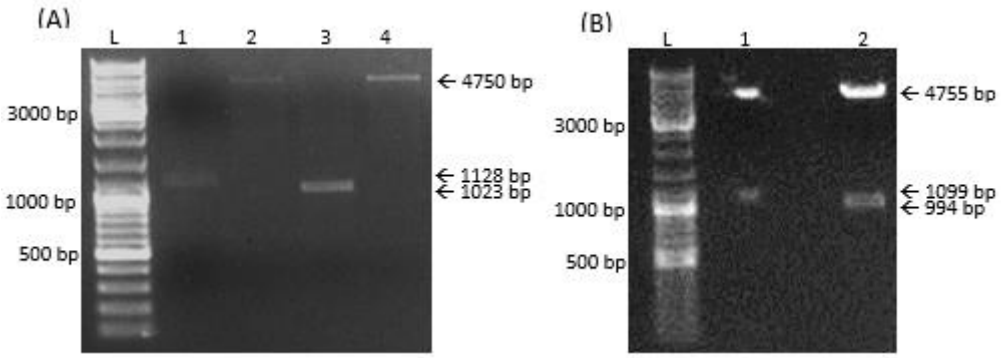

Figure 9 Agarose gel of (A) DNA fragments for the exchange of the resistance marker after digestion with *Not*I and *Spe*I and (B) restriction digest of ligation products with *Xho*I and *Spe*I
(A1) *cm*^{r} (1128 bp) **(A2,4)** pKRep-P_{tac}-eGFP (4750 bp) and **(A3)** *kan*^{r} (1023 bp); **(B1)** pCRep-XhoI (4755 bp and 1099 bp) and **(B2)** pKRep-XhoI (4755 bp and 994 bp); **L.:** Gene Ruler™ DNA Ladder Mix (500 ng)

3.1.2 Construction of turnaround backbone vector

Following the resistance marker exchange, the vector backbone could now be turned around because of the additional restriction site *Xho*I, which was introduced with the forward primer for the *cm*^{r} fragment (see Figure 6 Construction of pCRep-Ptac-eGFP-reverse). A 1420 bp fragment (P_{tac}-eGFP-rrnB) containing the P_{tac}, *egfp* and the terminator region *rrnB* was ampflified and after purification, the PCR product as well as the plasmid pCRep-P_{tac}-eGFP were digested with *Not*I and *Xho*I. Following gel electrophoresis, purification, determination of the DNA concentrations and ligation, the reaction mix was transformed into *E. coli* Top10. Single colonies were streaked out for plasmid isolation and a restriction digest was performed using *Nde*I and *Spe*I. The results of the restriction digest (Figure 10) show that the reversal of the vector backbone was successful since the digestion with *Nde*I and *Spe*I shows two fragments in the size of 5886 bp and 1383 bp in lane 1 and lane 4.

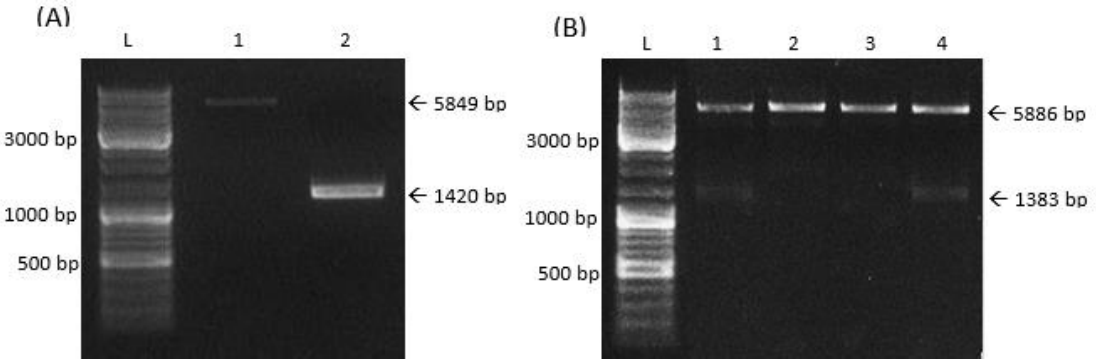

Figure 10 Agarose gel of (A) restriction digest of pCrep-XhoI and P_{tac}-eGFP-rrnB with *Not*I and *Xho*I and (B) restriction digest of pCRep-P_{rac}-eGFP-reverse with *Nde*I and *Spe*I
(A1) backbone of pCrep-XhoI (5849 bp) and **(A2)** PCR product P_{tac}-eGFP-rrnB (1420 bp); **(B1-4)** pCRep-P_{rac}-eGFP-reverse (5886 bp and 1383 bp); **L.:** Gene Ruler™ DNA Ladder Mix (500 ng)

3.1.3 Construction of pCRep-P_{tac}-hGHΔS, pCRep-P_{tac}-celAoCΔS and pCRep-P_{tac}-levΔS

Due to the results of the restriction digest (Figure 10), clone 4 of pCRep-P_{tac}-eGFP-reverse was used for the subsequent cloning of the secretion plasmids. The next step to be implemented was the exchange of the gene of interest. The reporter genes *hGHΔS* and *celAoCΔS* were amplified via PCR (see 2.2.2.1 General set up for gene amplification) and blunt-end ligated into the vector pJET1.2. The forward primers used for the amplification of the reporter genes introduced a *Nde*I restriction site to the 5'- end of the genes, whereas the reverse primers introduced a *Hind*III restriction site to the 3'- end of *hGHΔS* and *celAoCΔS*. During previous work by Steffen Gruber, the reporter gene *levΔS* was already cloned into pKRep-P_{tac} backbone vector with the restriction sites *Nde*I and *Hind*III. Following confirmation of the sequence accuracy, the plasmids harboring the genes of interest, as well as the plasmid pCRep-P_{tac}-eGFP-reverse were cut with *Nde*I and *Hind*III. According to the fragment size of the reporter genes, the ligations were set up using the following molar ratios (Table 23).

Table 23 Molar ratios for the ligation reactions during the cloning of the reporter genes into the backbone of pCRep-P_{tac}-eGFP-reverse

	Backbone	Insert	Molar ratio
pCRep-P_{tac}-hGHΔS	60 ng (6759 bp)	20 ng (587 bp)	1 : 4
pCRep-P_{tac}-celAoCΔS	60 ng (6759 bp)	26 ng (902 bp)	1 : 3
pCRep-P_{tac} –LevΔS	40 ng (6759 bp)	24 ng (1967 bp)	1 : 2.5

After transformation, single colonies were streaked out for plasmid isolation and a restriction digest using *Nde*I and *Hind*III was conducted. Figure 11 shows the results of the restriction digest on the examples (A) pJET1.2_celAoCΔS, pJET1.2_hGHΔS, (B) pCRep-P_{tac}-celAoCΔS and (C) pCRep-P_{tac}-levΔS. Figure 11 A shows the expected restriction pattern of pJET1.2_celAoCΔS cut with *Nde*I and *Hind*III as three bands in the size of 2717 bp, 902 bp and 260 bp can be observed. The band at 2717 bp represents the backbone of the pJET1.2 vector and the band at 902 bp corresponds to the *celAoCΔS* fragment. The band at approximately 260 bp in picture A is the result of the second *Hind*III restriction site in the backbone of pJET1.2. Figure 11 A also shows the successful

construction of pJET1.2_hGHΔS as three fragments in the size of 2717 bp, 587 bp and 260 bp can be observed following restriction digest with *Nde*I and *Hind*III. The bands in the size of 2717 bp and 260 bp correspond to the same fragments as mentioned above. The band in the size of 587 bp represents *hGHΔS.* In lane 5 and 6, an additional faded band at about 850 bp can be seen, which resembles the fragment *hGHΔS* including the part of the pJET1.2 backbone till the *Hind*III site, as *Nde*I had not cut completely. Figure 11 B shows the successful construction of pCRep-P_{tac}-celAoCΔS as two fragments in the size of 6548 bp and 902 bp can be observed after digestion with *Nde*I and *Hind*III. Figure 11 C shows the results of the restriction digest of pCRep-P_{tac}-levΔS with *Nde*I and *Hind*III. The desired restriction pattern are two fragments in the size of 6548 bp and 1967 bp. Following restriction, the agarose gel showed a slightly different insert size in lane 1 compared to the insert size of lane 2 or 3. Since the plasmid showing the correct restriction pattern could not yet be identified, plasmids 1 and 2 were sent for sequencing. Sequencing results showed that plasmid 2 had the correct sequence, whereas the sequencing results plasmid 1 showed an insertion element incorporated after the P_{tac}. Furthermore, the beginning part of the *lev* gene was missing leading to a slightly shorter insert size following digestion with *Nde*I and *Hind*III. The construction of pCRep-P_{tac}-hGHΔS was also successful as the restriction digest with *Nde*I and *Hind*III displayed the expected fragments in the size of 587 bp and 6548 bp (data not shown). In the following, the *Rep* origin had to be exchanged by the *RSF1010* origin, see therefore the material and method section (2.16 Construction of pCRSF1010-P_{tac}-hGHΔS, pCRSF1010-P_{tac}-celAoCΔS and pCRSF1010-P_{tac}-levΔS).

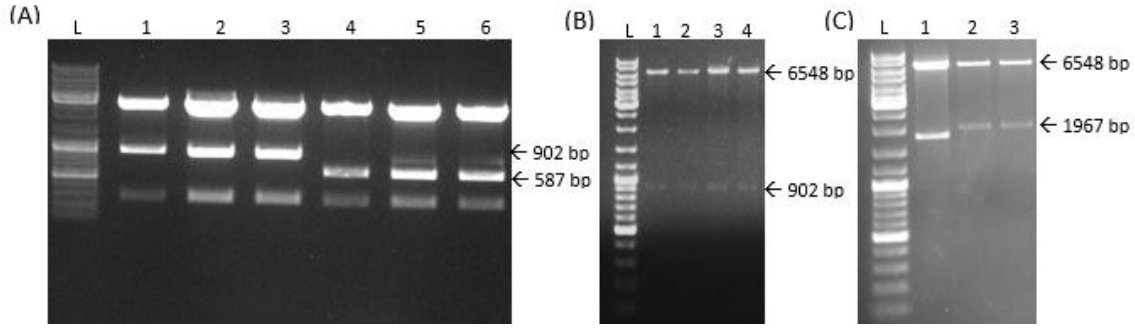

Figure 11 Agarose gel showing the successful insertion of the reporter genes into the basic plasmids for secretion following restriction digest with *Nde*I and *Hind*III
(A1-3) pJET1.2_celAoCΔS (2717 bp + 902 bp + 260 bp) and **(A4-6)** pJET1.2_hGHΔS (2717 bp + 587 bp + 260 bp; **(B1-4)** pCRep-P_{tac}-celAoCΔS (6548 bp + 902 bp); and **(C1-3)** pCRep-P_{tac}-levΔS (6548 bp + 1967 bp); **L.:** Gene Ruler™ DNA Ladder Mix (500 ng)

3.1.4 Construction of the basic plasmids pCRSF1010-P_{tac}-hGHΔS, pCRSF1010-P_{tac}-celAoCΔS and pCRSF1010-P_{tac}-levΔS

As a result of difficulties during the transfer of the secretion plasmids into *R. eutropha* H16 (see 3.3 Conjugation of secretion plasmids into *Ralstonia eutropha* H16), the origin of replication and the mob region of the basic secretion vectors were exchanged with the *RSF1010* origin including the *mob* region using the restriction enzymes *Not*I and *Spe*I (see 2.16 Construction of pCRSF1010-P_{tac}-hGHΔS, pCRSF1010-P_{tac}-celAoCΔS and pCRSF1010-P_{tac}-levΔS). The successful exchange of the origin of replication for all secretion plasmids was verified with restriction digest using *Spe*I and *Hind*III (Figure 12). Lane 2 to 5 revealed the expected restriction pattern of pCRSF1010-P_{tac}-celAoCΔS following digestion with *Spe*I and *Hind*III as two fragments in the size of 8399 bp and 2287 bp can be observed. In lane 1, pCRep-P_{tac}-celAoCΔS cut with *Spe*I and *Hind*III was loaded as a control to compare the size of the insert. The same size of the insert confirmed the successful construction of pCRSF1010-P_{tac}-celAoCΔS. The construction of pCRSF1010-P_{tac}-levΔS (lane 7 to 10) could also be confirmed as the restriction digest with *Spe*I and *Hind*III also displayed the expected restriction pattern as two fragments in the size of 8399 bp and 3352 bp can be seen. Lane 12 to 15 showed the expected fragments in the size of 8399 bp and 1972 bp of the restriction digest of pCRSF1010-P_{tac}-hGHΔS with *Spe*I and *Hind*III. In lane 11, the control pCRep-P_{tac}-hGHΔS cut with *Spe*I and *Hind*III showed the same insert size (1972 bp) and the backbone of 5163 bp. The same insert size of pCRSF1010-P_{tac}-hGHΔS and pCRSF1010-P_{tac}-hGHΔS confirmed the successful construction of pCRSF1010-P_{tac}-hGHΔS

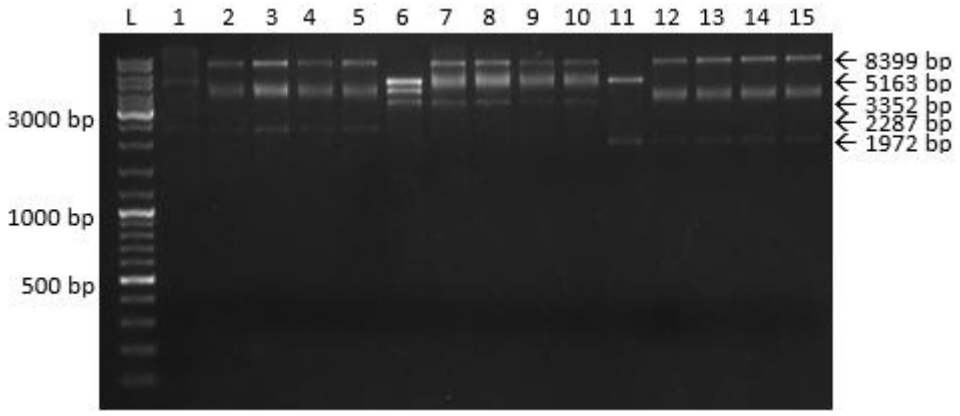

Figure 12 Agarose gel of the basic secretion plasmids based on the *RSF1010* origin after restriction digest with *Spe*I and *Hind*III

(1) pCRep-P_{tac}-celAoCΔS (5163 bp and 2287 bp), **(2-5)** pCRSF1010-P_{tac}-celAoCΔS (8399 bp and 2287 bp), **(6)** pCRep-P_{tac}-levΔS (5163 bp and 3352 bp), **(7-10)** pCRSF1010-P_{tac}-levΔS (8399 bp and 3352 bp), **(11)** pCRep-P_{tac}-hGHΔS (5163 bp and 1972 bp), **(12-15)** pCRSF1010-P_{tac}-hGHΔS (8399 bp and 1972 bp); **L.:** Gene Ruler™ DNA Ladder Mix (500 ng)

3.2 Construction of secretion plasmids for the use in *Ralstonia eutropha* H16

After completion of the basic secretion plasmids, the essential part for secretion, the signal sequences, had to be cloned into the backbone vectors. In the beginning, only five signal peptides were tested as a first proof of principle. The five signal peptides chosen were previously reported as strong secretion signals for identified exoproteins in *R. solanacearum* [19] and the primers were designed according to the sequence of *R. solanacearum* GMI1000. Following first experiments to proof secretion productivity, primers for 15 other signal peptides out of *R. solanacearum* and 1 other signal peptide out of *R. eutropha* H16 were ordered.

3.2.1 Prediction of signal sequences

The discrimination between Sec and Tat signal peptides and the prediction of the cleavage site was performed computationally using the online tool PRED-TAT from the computational genetics research group of the University of Thessaly [63]. The method is based on Hidden Markov Models (HMMs) and possesses a modular architecture suitable for both Sec- and Tat- specific signal peptides [66]. Based on the results of the prediction, ten signal peptides for the Sec-dependent pathway, ten signal peptides for the Tat pathway from *R. solanacearum* and another Tat signal sequence from *R. eutropha* H16 were chosen for the investigation of the secretory pathway in *R. eutropha* H16 (Table 2). Figure 13 shows an example of the prediction results for Sec (A) and Tat (B) signal sequences and Table 24 lists the cleavage sites and the reliability score of each signal sequence. The various sizes of the signal peptides are listed in Table 2. The primers were then designed to amplify the signal sequences including the complete cleavage site out of genomic DNA from *R. solanacearum* or *R. eutropha* H16 (i.e. ALA-YD for pehB: the last amino acid of the amplified signal peptide would be aspartic acid). Furthermore, the reverse primers were designed to introduce a *Nde*I site to the 3'- end of the signal sequence to enable the cloning via restriction digestion.

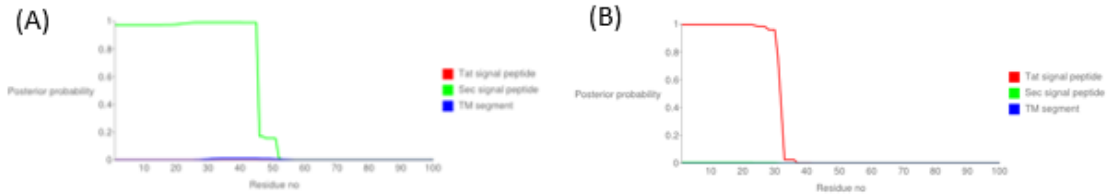

Figure 13 Prediction of signal sequences by PRED-TAT

(A) Prediction of the Sec signal sequence aac and **(B)** prediction of the tat signal sequence NosL

Table 24 Results from the prediction of the signal sequences by PRED-TAT

Signal peptide	Cleavage site	Reliability score	*Signal peptide*	Cleavage site	Reliability score
SP's for sec-dependent pathway			*SP's for tat pathway*		
PehB	ALA-YD	0.946	*NosL*	DAA-AP	0.989
Pme	ALA-VT	0.923	*F504_2199*	ASA-QA	0.994
Egl	AAA-TD	0.995	*F504_2437*	ASR-AT	0.996
cbhA	VHA-EA	0.989	*rlpB*	LRG-NN	0.989
Tek	ESG-AS	0.961	*F504_2793*	AQA-ET	0.944
Aac	AHG-SR	0.955	*amiC*	AFG-AN	0.998
TreA	ACA-DV	0.981	*nasF*	AWA-AG	1.000
PqaA	ALA-RA	0.992	*iorB2*	GDA-AD	0.999
F504_4738	AHG-QD	0.994	*ReH16 NosZ*	AAA-AV	0.998
F504_2783	AHA-QS	1.000	*pehC*	ATA-AT	0.984
			Rsc NosZ	SAA-AT	0.967

3.2.2 Amplification of the signal sequences

Due to the high GC content of *R. solanacearum* and *R. eutropha* H16, the signal peptides were amplified with the addition of GC Enhancer (New Englands Biolab Inc.) and the PCR reaction was set up as described in material and methods (see 2.2.2.1 General set up for gene amplification). Genomic DNA from *R. solanacearum* (# 623 – IMBT's culture collection) and *R. eutropha* H16 (#1 – IMBT's culture collection) served as template DNA. To determine the correct fragment sizes and to purify the PCR reactions from possible unspecific DNA fragments, a 2 % preparative agarose gel was run. In order to enlarge the size of the cloning fragments and to enable the resistance marker exchange, the signal peptides were fused to the *kan*^{r} via overlap extension PCR (see Figure 8 Construction of the secretion plasmids pKRSF1010-P_{tac}-SP-hGH, pKRSF1010-P_{tac}-SP-celA and pKRSF1010-

P_{tac}-SP-lev). Figure 14 shows (A) a selection of signal peptides amplified out of genomic DNA from *R. solanacearum* as well as (B) a selection of the extended cloning fragments (SP's-KAN) containing the signal peptides and the *kan*^{r} after overlap extension PCR. The bright bands seen on both gel pictures represent the desired DNA fragments, which were purified and used for continuing steps. The slight bands as seen in lane 1, 3 and 4 of (A) represent unspecific DNA amplification.

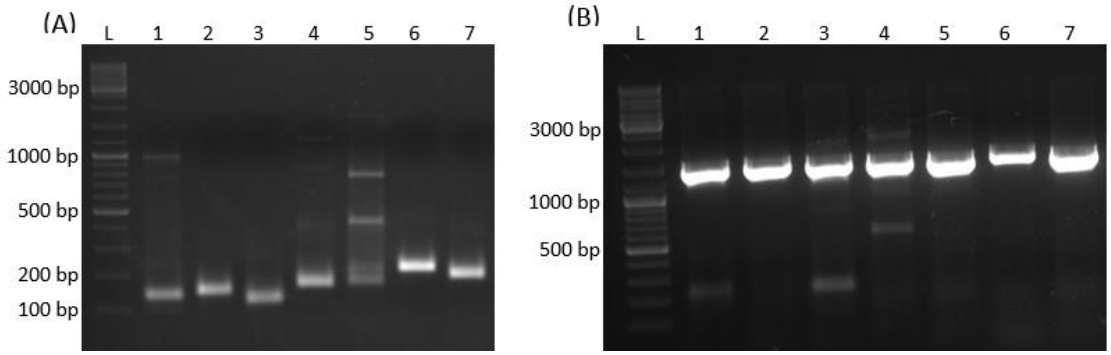

Figure 14 Agarose gel of (A) amplified signal sequences and **(B) amplified overlap extension products (A1)** NosL (166 bp), **(A2)** F504_2437 (178 bp), **(A3)** F504_2793 (154 bp), **(A4)** nasF (196 bp), **(A5)** iorB2 (199 bp), **(A6)** pehC (214 bp), **(A7)** Rsc NosZ (196 bp) and **(B1)** NosLKAN (1416 bp), **(B2)** F501_2199KAN (1437 bp), **(B3)** F504_2437KAN (1428 bp), **(B4)** RlpBKAN (1413 bp), **(B5)** F504_2793KAN (1404 bp), **(B6)** amiCKAN (1467 bp), **(B7)** nasFKAN (1446 bp); **L.:** Gene Ruler^{TM} DNA Ladder Mix (500 ng)

For verification of the correct sequences, the products of the overlap extension PCR were blunt-end ligated into the pJET1.2 vector. After transformation into *E. coli* Top10, single colonies were streaked out for plasmid isolation and restriction digested with *Nde*I and *Spe*I. Positive clones were sent to sequencing to determine the correct sequence of the signal sequences.

The sequencing results of the first five signal peptides showed a higher similarity to the newly sequenced strain *R. solanacearum* FQY-4 instead of *R. solanacearum* GMI1000 [76]. The signal sequences *pheB*, *cbhA* and *tek* appear to have a 100 % identity to *R. solanacearum* FQY-4, whereas the signal sequences *pme* and *egl* were revealed to be hybrid signal peptides due to base pair exchanges caused by the primer binding sequences, which were designed after the sequence of *R. solanacearum* GMI1000. The amino acid sequences for the signal peptides can found in the appendix (see 7.2 Amino acid sequences of signal peptides), where the positions of the amino acid exchanges are marked in yellow. For the following signal sequences, the primers were designed according to the sequence of *R. solancearum* FQY-4.

The sequencing results of the following 16 signal sequences are listed in Table 25. The signal sequences *F504_2199*, *iorB2*, *pehB*, *NosZ*, *Aac* and *F504_4738* display base pair exchanges, which might lead to amino acid exchanges. However, the repetition for the genomic amplification of the signal peptides showed the same results, which points to genomic reason being the reason for base pair exchanges and not to mutations because of amplification errors. The amino acid sequences of all signal peptides can be found in the appendix (see 7.2 Amino acid sequences of signal peptides). The positions of the amino acid exchanges are marked in yellow. The nucleotide sequences of all signal sequences can be found in the IMBT's strain collection.

Table 25 Sequencing results of signal peptides

Number	Signal sequence	Sequencing results
Signal sequences for sec-dependent pathway		
S1	pehB	100 % identity to *R. solanacearum* FQY-4
S2	Pme	Compared to *R. solanacearum* FQY-4 there are 2 bp exchanges, which lead to the exchange of the aa Met to Thr and Leu to Pro. One bp exchange is caused by the primer sequence.
S3	Egl	Compared to *R. solanacearum* FQY-4 there are 4 bp exchanges, but no aa exchange
S4	cbhA	100 % identity to *R. solanacearum* FQY-4
S5	Tek	100 % identity to *R. solanacearum* FQY-4
S6	Aac	Compared to *R. solanacearum* FQY-4 there is 1 bp exchange, which leads to the exchange of the aa Ala to Thr
S7	treA	100 % identity to *R. solanacearum* FQY-4
S8	PqaA	100 % identity to *R. solanacearum* FQY-4
S9	F504_4738	Compared to *R. solanacearum* FQY-4 there are 2 bp exchanges, whereas only 1 leads to an exchange of the aa Ser to Asn
S10	F504_2783	100 % identity to *R. solanacearum* FQY-4
Signal sequences for tat pathway		
T1	NosL	100 % identity to *R. solanacearum* FQY-4
T2	F504_2199	Compared to *R. solanacearum* FQY-4 there are 3 bp exchanges, whereas 2 lead to an exchange of the aa Ala to Val and Ser to Asn
T3	F504_2437	100 % identity to *R. solanacearum* FQY-4
T4	RlpB	100 % identity to *R. solanacearum* FQY-4
T5	F504_2793	100 % identity to *R. solanacearum* FQY-4
T6	amiC	100 % identity to *R. solanacearum* FQY-4
T7	nasF	100 % identity to *R. solanacearum* FQY-4
T8	iorB2	Compared to *R. solanacearum* FQY-4 there is 1 bp exchange, but no aa exchange

T9	ReH16 NosZ	100 % identity to *R. eutropha* H16
T10	pehC	Compared to *R. solanacearum* FQY-4 there is 1 bp exchange, which leads to the exchange of the aa Thr to Ala
T12	Rsc NosZ	Compared to *R. solanacearum* FQY-4 there are 4 bp exchanges, whereas 2 lead to the aa exchange from Pro to Gln and from Pro to Ser

3.2.3 Construction of the secretion plasmids pKRep-P_{tac}-SP-hGH, pKRep-P_{tac}-SP-celA and pKRep-P_{tac}-SP-lev

Even though sequencing results revealed that *egl* and *pme* were hybrid signal sequences and that *F504_2199*, *iorB2*, *pehB*, *NosZ*, *Aac* and *F504_4738* were not identical to the published sequence of *R. solanacearum* FQY-4 in NCBI, the fragments were cloned into the secretion plasmids. The basic secretion vectors were digested with *Nde*I and *Spe*I, thereby cutting out the *cm*^{r}, and the pJET1.2 plasmids containing the signal sequences and the *kan*^{r} fragment were digested with the same restriction enzymes. Following agarose gel electrophoresis, the desired fragments were purified and used for ligation. After transformation, single colonies were streaked out for plasmid isolation and a control restriction digest with *BamH*I and *Hind*III was performed (data not shown). The results of the restriction digest showed that the construction of following plasmids (Table 26) was successful and the secretion plasmids showing the correct restriction pattern were sent for sequencing. Following sequencing, the successful construction of pCRep-P_{tac}-pme-hGH, pCRep-P_{tac}-egl-hGH, pCRep-P_{tac}-cbhAme-hGH, pCRep-P_{tac}-pme-celA, pCRep-P_{tac}-egl-celA, pCRep-P_{tac}-pme-lev, pCRep-P_{tac}-egl-lev could be confirmed and the following plasmids were then transferred into *R. eutropha* H16 via conjugation.

Table 26 Overview of successful construction of secretion plasmids

Signal sequence	pCRep-P_{tac}-Hgh	pCRep-P_{tac}-celA	pCRep-P_{tac}-lev
pehB	-	-	-
Pme	✓	✓	✓
Egl	✓	✓	✓
Cbha	✓	-	-
Tek	-	-	-

3.2.4 Construction of the secretion plasmids pKRSF1010-P_{tac}-SP-hGH, pKRSF1010-P_{tac}-SP-celA and pKRSF1010-P_{tac}-SP-lev

Due to the high mutation rate of the *mob* region because of the *Rep* origin, the final secretion plasmids were based on the *RSF1010* origin. The incorporation of the signal sequences into the backbone of pCRSF1010-P_{tac}-hGHΔS, pCRSF1010-P_{tac}-celAoCΔS or pCRSF1010-P_{tac}-levΔS was conducted as described above using the restriction enzymes *Nde*I and *Spe*I. After ligation and transformation, single colonies were first screened via Colony PCR and following plasmid isolation, positive ones were then restriction digested with *Bam*HI and *Hind*III (data not shown). For final affirmation, plasmids showing the correct restriction pattern were sent for sequencing to confirm the completion of the designed secretion plasmids. An overview of all constructs is listed in Table 27**.** ✓ marks the complete constructs, whereas ✘ marks the constructs, also showing the correct restriction pattern, but sequencing results revealed either insertion elements or mutations within the reporter gene or the signal sequences.

Table 27 Overview of completed secretion plasmids for constitutive expression

pKRSF1010-Ptac-SP	-hGH	-celA	-lev	*pKRSF1010-P_{tac}-SP*	-hGH	-celA	-lev
SP's for Sec dependent secretory pathway				***SP's for Tat dependent secretory pathway***			
pehB	✘	✘	-	*NosL*	✘	✓	✓
Pme	✓	✓	✓	*F504_2199*	✘	-	✓
Egl	✓	✓	✓	*F504_2437*	✓	✓	✘
cbhA	✓	✓	-	*RlpB*	✓	✓	✓
Tek	✘	-	✓	*F504_2793*	✘	✓	-
Aac	✓	✓	✘	*amiC*	✓	✓	✓
treA	✓	✓	✘	*nasF*	✓	✓	✓
pqaA	✘	-	✓	*iorB2*	✓	✓	✓
F504_4738	✓	✓	✓	*ReH16 NosZ*	✘	✓	✘
F504_2783	✘	-	✓	*pehC*	✘	-	✘
				Rsc NosZ	✓	✓	✓

✓ marks the successful construction of the following secretion plasmids

✘ marks the secretion plasmids that showed the correct restriction pattern, but where sequencing results revealed mutations within the signal sequences or the reporter genes.

3.3 Conjugation of secretion plasmids into *Ralstonia eutropha* H16

3.3.1 Conjugation of secretion plasmids based on *Rep* origin into *Ralstonia eutropha* H16

Following sequencing, the confirmed secretion plasmids were transformed into *E. coli* S17-1, which can act as a donor strain during conjugative transfer of plasmid DNA into *R. eutropha* H16. The conjugation of pKRep-P_{tac}-egl-hGH into *R. eutropha* H16 worked as expected and after 48 h incubation at 28 °C, many *R. eutropha* H16 transconjugants could be obtained on TSB plates containing 0.6 % fructose and the appropriate antibiotics. However, during the transfer of the secretion plasmids pKRep-P_{tac}-pme-hGH and pKRep-P_{tac}-cbhA-hGH problems, such as irregular growth or no growth were observed and therefore, single colonies of *E. coli* S17-1 harboring the particular secretion plasmids were streaked out for plasmid isolation. The plasmids pKRep-P_{tac}-pme-hGH, pKRep-P_{tac}-cbhA-hGH and pKRep-P_{tac}-egl-hGH were then sent for sequencing. Sequencing results revealed random mutations, like for example repeats within the *mob* region of pKRep-P_{tac}-pme-hGH. Figure 15 shows an excerpt of the obtained sequence results of the mob region in pKRep-P_{tac}-egl-hGH and pKRep-P_{tac}-pme-hGH. The sequence of pKRep-P_{tac}-egl-hGH is the correct one, whereas in pKRep-P_{tac}-pme-hGH repeats (GCCCG) were incorporated into the *mob* region. Because of the instability of the *Rep* origin and mobilisation region, the secretion plasmids were re-cloned on the basis of the *RSF1010* origin (see 2.16 Construction of pCRSF1010-P_{tac}-hGHΔS, pCRSF1010-P_{tac}-celAoCΔS and pCRSF1010-P_{tac}-levΔS).

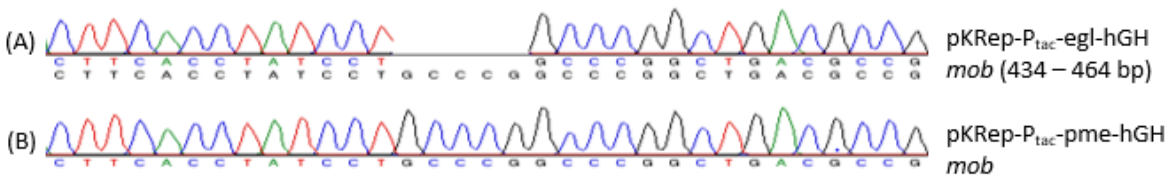

Figure 15 Sequencing results of the *mob* region in pKRep-P_{tac}-egl-hGH and pKRep-P_{tac}-pme-hGH
(A) shows part of the correct sequence of *mob* in pKRep-P_{tac}-egl-hGH (434 – 461 bp within the *mob* region), whereas in **(B)** pKRep-P_{tac}-pme-hGH repeats (GCCCG) were incorporated at 446 bp within the *mob* region.

3.3.2 Conjugation of secretion plasmids based on the *RSF1010* origin into *Ralstonia eutropha* H16

Another problem occurred during the transfer of all except three CelA secretion plasmids and some Lev secretion plasmids into *R. eutropha* H16. The particular plasmids could not be transformed into *E. coli* S17-1 and therefore were transferred into *R. eutropha* H16 via triparental mating with the help of the *E. coli* HB101 harboring the helper plasmid pRK2013. The unsuccessful transformation of *E. coli* S17-1 with CelA and Lev secretion plasmids might be due to the constitutive expression and simultaneous secretion of the proteins, which could lead to the toxic accumulation of CelA or Lev in the periplasm. For a more detailed explanation, see the discussion section (4.2 Secretion of CelA by *Ralstonia eutropha* H16). Table 28 lists the method used for each individual secretion plasmid.

Table 28 Conjugative plasmid transfer method for all secretion plasmids

pKRSF1010-P_{tac}-SP-	-hGH	-celA	-lev
Sec- specific signal sequences			
pehB	-	-	-
Pme	*E. coli* S17-1	*E. coli* S17-1	*E. coli* S17-1
Egl	*E. coli* S17-1	*E. coli* S17-1	*E. coli* S17-1
cbhA	*E. coli* S17-1	pRK2013	-
Tek	-	-	pRK2013
Aac	*E. coli* S17-1	pRK2013	-
treA	*E. coli* S17-1	pRK2013	
pqaA	-	-	*E. coli* S17-1
F504_4738	*E. coli* S17-1	pRK2013	*E. coli* S17-1
F504_2783	-	-	pRK2013
Tat- specific signal sequences			
NosL	-	*E. coli* S17-1	*E. coli* S17-1
F504_2199	-	-	*E. coli* S17-1
F504_2437	*E. coli* S17-1	pRK2013	-
RlpB	*E. coli* S17-1	pRK2013	pRK2013
F504_2793	-	pRK2013	-
amiC	*E. coli* S17-1	pRK2013	pRK2013
nasF	*E. coli* S17-1	pRK2013	*E. coli* S17-1
iorB2	*E. coli* S17-1	pRK2013	*E. coli* S17-1
ReH16 NosZ	-	pRK2013	-
pehC	-	-	-
Rsc NosZ	*E. coli* S17-1	pRK2013	pRK2013

3.4 Screening of *Ralstonia eutropha* H16 transconjugants

3.4.1 Screening of *Ralstonia eutropha* H16 transconjugants harboring hGH secretion plasmids: pKRSF1010-P_{tac}-SP-hGH

Following conjugation into *R. eutropha* H16, transconjugants were first selected for their resistance to kanamycin. The second screening of *R. eutropha* H16 transconjugants carrying the desired hGH secretion plasmids was done by conducting a Colony PCR with the forward primers of each signal sequence (SP-Sec-fwd; # 546, 548, 552, 558, 560, 562, 564, 566, 570, 574, 576, 578, 584, 583, 585) and the reverse primer hGH_rev_HindIII (# 540). The transfer of the hGH secretion plasmids using either the conjugative method through *E. coli* S17-1 was successful as bands in the size of 685 – 781 bp could be observed for all hGH secretion constructs. Figure 16 displays an example of the performed Colony PCR.

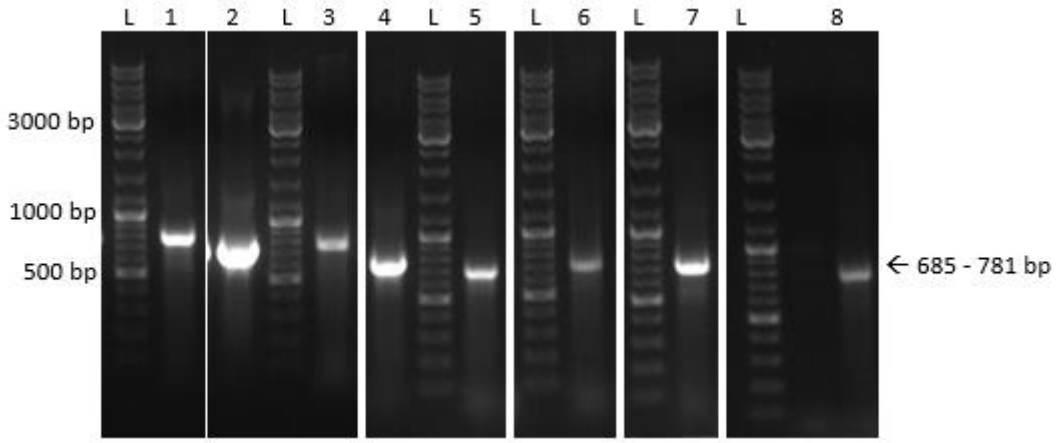

Figure 16 Agarose gel of Colony PCR of *R. eutropha* H16 transconjugants carrying hGH secretion plasmids
(1) pKRSF1010-P_{tac}-RscNosZ-hGH transconjugant 1 **(2)** pKRSF1010-P_{tac}-nasF-hGH transconjugant 4, **(3)** pKRSF1010-P_{tac}-treA-hGH transconjugant 1, **(4)** pKRSF1010-P_{tac}-ReH16NosZ-hGH transconjugant 4, **(5)** pKRSF1010-P_{tac}-pme-hGH transconjugant 4, **(6)** pKRSF1010-P_{tac}-F504_4738-hGH transconjugant 1, **(7)** pKRSF1010-P_{tac}-amiC-hGH transconjugant 1, **(8)** pKRSF1010-P_{tac}-iorB2-hGH transconjugant 1, **L.:** Gene Ruler™ DNA Ladder Mix (500 ng)

3.4.2 Screening of *Ralstonia eutropha* H16 transconjugants harboring CelA secretion plasmids: pKRSF1010-P_{tac}-SP-celA

R. eutropha H16 transconjugants harboring the CelA secretion plasmids should be able to express CelA and therefore, the successful transfer of the secretion plasmids into *R. eutropha* H16 could be screened on the basis of their cellulase activity. After conjugation, single colonies were streaked out on TSB agar plates containing 0.6 % CMC and grown overnight at 37 °C. The next morning, the colonies were washed off and the

plates were stained with Congo red (see 2.2.21 Congo red clearing zone assay). After multiple washing steps, yellow halos, indicating cellulase activity, could be detected as seen in Figure 17. A difference in the size of the halo could be observed, indicating that some signal sequences might secrete more CelA into the environment than others. The biggest halos can be observed in *R. eutropha* H16 transconjugants harboring CelA secretion plasmids with the following signal sequences: *amiC, cbhA, aac, F504_2793* and *NosZ* from *R. solanacearum,* as well as, *NosZ* from *R. eutropha* H16. In comparison, *R. eutropha* H16 transconjugants carrying CelA secretion plasmids with other signal sequences, such as *RlpB, egl, iorB2* and *pme* displayed very small halos. For every construct, 4 transconjugants were streaked out and tested for their CelA activity. Altogether, similar activity levels could be observed for all 4 transconjugants of each CelA secretion construct. However, transconjugant 1 of *R. eutropha* H16 [pKRSF1010-P_{tac}-NosL-celA] (#57 in Figure 17) did not display any cellulase activity and was replaced by transconjugant 5 for the following experiments. A clear preference for one of the secretion pathways could not yet be detected, as both signal sequences specific for the Sec- pathway (*cbhA* and *aac*) and for the Tat- pathway (*amiC*, *F504_2793*, *NosZ* from *R. eutropha* H16 and *R. solanacearum*) displayed bigger halos. Furthermore, signal peptides from *R. solanacearum* and *R. eutropha* H16 seem to be applicable to achieve successful recombinant protein secretion.

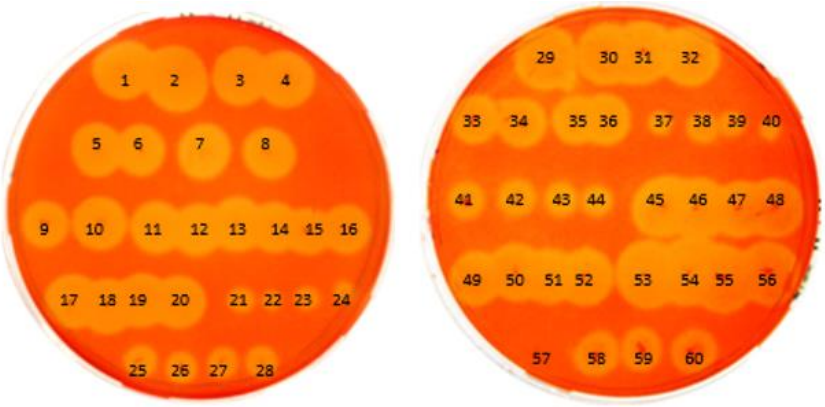

Figure 17 Congo red plate assay with *R. eutropha* H16 transconjugants harboring CelA secretion plasmids (1-4) *R.e.*H16 [pKRSF1010-P_{tac}-amiC-celA] transconjugants 1-4, **(5-8)** *R.e.*H16 [pKRSF1010-P_{tac}-RscNosZ-celA] transconjugants 1-4, **(9-12)** *R.e.*H16 [pKRSF1010-P_{tac}-F504_4738-celA] transconjugants 1-4, **(13-16)** *R.e.*H16 [pKRSF1010-P_{tac}-nasF-celA] transconjugants 1-4, **(17-20)** *R.e.*H16 [pKRSF1010-P_{tac}-F504_2437-celA] transconjugants 1-4, **(21-24)** *R.e.*H16 [pKRSF1010-P_{tac}-rlpB-celA] transconjugants 1-4, **(25-28)** *R.e.*H16 [pKRSF1010-P_{tac}-egl-celA] transconjugants 1-4, **(29-32)** *R.e.*H16 [pKRSF1010-P_{tac}-cbhA-celA] transconjugants 1-4, **(33-36)** *R.e.*H16 [pKRSF1010-P_{tac}-treA-celA] transconjugants 1-4, **(37-40)** *R.e.*H16 [pKRSF1010-P_{tac}-iorB2-celA] transconjugants 1-4, **(41-44)** *R.e.*H16 [pKRSF1010-P_{tac}-pme-celA] transconjugants 1-4, **(45-48)** *R.e.*H16 [pKRSF1010-P_{tac}-aac-celA] transconjugants 1-4, **(49-52)** *R.e.*H16 [pKRSF1010-P_{tac}-ReH16-celA] transconjugants 1-4, **(53-56)** *R.e.*H16 [pKRSF1010-P_{tac}-F504_2793-celA] transconjugants 1-4, **(57[1]-60)** *R.e.*H16 [pKRSF1010-P_{tac}-NosL-celA] transconjugants 1-4

[1] for the following assays transconjugant 5 was used and renamed "transconjugant 1"

3.4.3 Screening of *Ralstonia eutropha* H16 transconjugants harboring Lev secretion plasmids: pKRSF1010-P_{tac}-SP-lev

Following conjugation into *R. eutropha* H16, transconjugants were first selected for their resistance to kanamycin. The second screening of *R. eutropha* H16 transconjugants carrying the desired Lev secretion plasmids was done by conducting a Colony PCR with the forward primers of each signal sequence (SP-Sec-fwd; # 546, 548, 552, 558, 560, 562, 564, 566, 570, 574, 576, 578, 584, 583, 585) and the reverse primer Lev_rev_HindIII (# 542). The transfer of the Lev secretion plasmids using either the conjugative method through *E. coli* S17-1 or *E. coli* HB101 [pRK2013] was successful as bands in the size of 2058 – 2154 bp could be observed for all Lev secretion constructs in all *R. eutropha* H16 transconjugants. Figure 18 displays an example of the performed Colony PCR.

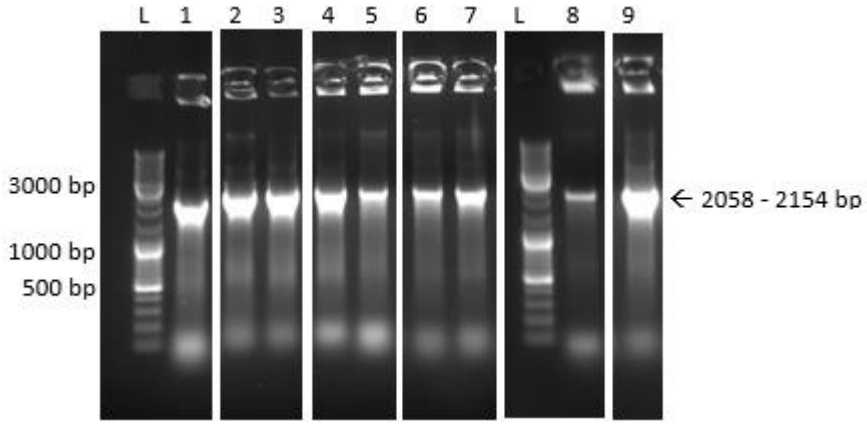

Figure 18 Agarose gel of Colony PCR of *R. eutropha* H16 transconjugants carrying Lev secretion plasmids
(1) pKRSF1010-P_{tac}-amiC-lev transconjugant 1, **(2)** pKRSF1010-P_{tac}-nasF-lev transconjugant 4, **(3)** pKRSF1010-P_{tac}-RscNosZ-lev transconjugant 1, **(4)** pKRSF1010-P_{tac}-pme-lev transconjugant 4, **(5)** pKRSF1010-P_{tac}-RlpB-lev transconjugant 1, (6) pKRSF1010-P_{tac}-tek-lev transconjugant 4, **(7)** pKRSF1010-P_{tac}-F504_2199-lev transconjugant 1, **(8)** pKRSF1010-P_{tac}-F504_2783-lev transconjugant 1, **(9)** pKRSF1010-P_{tac}-F504_4738-lev transconjugant 1, **L.:** Gene Ruler™ DNA Ladder Mix (500 ng)

3.5 Investigation of hGH secretion by *Ralstonia eutropha* H16

For the examination of the hGH secretion efficiency, 4 single colonies of *R. eutropha* H16 transconjugants harboring hGH secretion plasmids were used to inoculate 3 mL of LB media containing 0.6 % fructose and the appropriate antibiotics. The preculture was incubated overnight at 28 °C. The next day, the main culture, 20 mL of LB media with 0.6 % fructose and the appropriate antibiotics, were inoculated to an OD_{600} of 0.2 and further incubated at 28 °C and 130 rpm. Following 15 h of incubation, the OD_{600} was measured for each *R. eutropha* H16 transconjugant and the fermentation broth was then

centrifuged for 20 min at 3220 x g and 4 °C to harvest the cells. Figure 19 displays the results of the OD_{600} measurement, which revealed fluctuating growth behaviour within *R. eutropha* H16 carrying identical constructs. *R. eutropha* H16 [pKRSF1010-P_{tac}-Δ49] (empty vector control) was used as a reference for expected growth and as a negative control for the following assays.

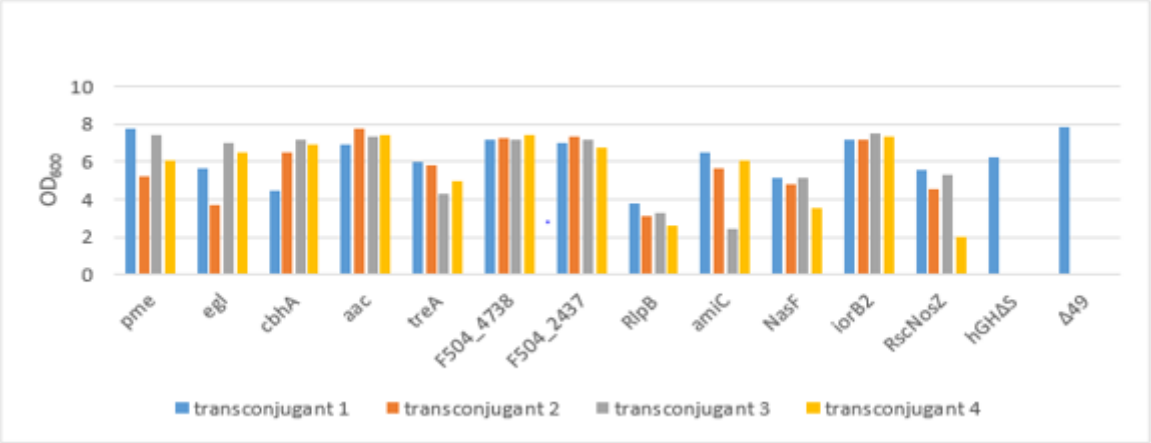

Figure 19 OD_{600} values of *R. eutropha* H16 transconjugants carrying either hGH secretion plasmids (pKRSF1010-P_{tac}-SP-hGH)[1] or the negative control plasmids (pKRSF1010-P_{tac}-hGHΔS and pKRSF1010-P_{tac}-Δ49)
Precultures of *R. eutropha* H16 transconjugants were used to inoculate LB media supplemented with 1 % glycerol and the appropriate antibiotics to an OD_{600} of 0.2 and incubated for 15 h at 28 °C and 130 rpm.
[1] pKRSF1010-P_{tac}-SP-hGH describes the general hGH secretion plasmid. Exchanging "SP" with the individual signal peptides names the different hGH secretion plasmids.

Following centrifugation, the cell-free supernatants were harvested and their protein concentrations were measured in triplicates using the Bradford protein assay (see 2.6 Measurement of protein concentration). The results of the measurement are shown in Figure 20. The measured protein concentrations in the cell-free supernatants vary significantly, ranging from 8.4 [µg mL^{-1}] for pKRSF1010-P_{tac}-RlpB-hGH to 83.9 [µg mL^{-1}] protein for pKRSF1010-P_{tac}-egl-hGH. Furthermore, *R. eutropha* H16 transconjugants carrying the same hGH secretion constructs were expected to secrete the same amounts of protein into the extracellular medium. However, the four *R. eutropha* H16 transconjugants carrying either pKRSF1010-P_{tac}-egl-hGH, pKRSF1010-P_{tac}-cbhA-hGH, pKRSF1010-P_{tac}-aac-hGH, pKRSF1010-P_{tac}-amiC-hGH, pKRSF1010-P_{tac}-nasF-hGH or pKRSF1010-P_{tac}-RscNosZ-hGH displayed a wide range of measured protein concentrations in 1 mL cell-free supernatant (e.g. 19.6 – 46.9 µg mL^{-1} for *R. eutropha* H16 [pKRSF1010-P_{tac}-nasF-hGH]).

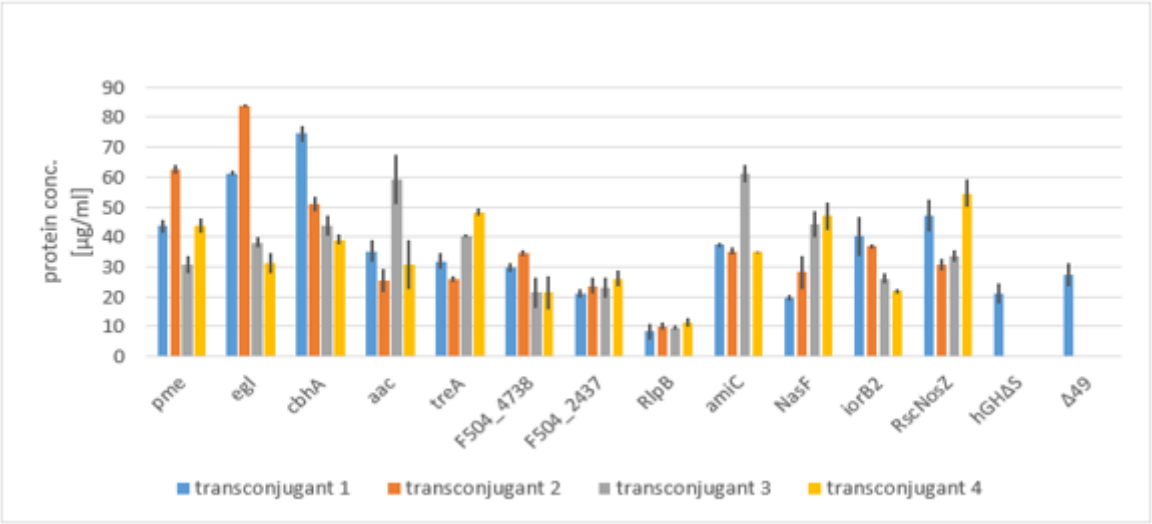

Figure 20 Protein concentrations in the supernatant of *R. eutropha* H16 transconjugants carrying either hGH secretion plasmids (pKRSF1010-P_{tac}-SP-hGH)[1] or the negative control plasmids (pKRSF1010-P_{tac}-hGHΔS and pKRSF1010-P_{tac}-Δ49)

[1] pKRSF1010-P_{tac}-SP-hGH describes the general hGH secretion plasmid. Exchanging "SP" with the individual signal peptides names the different hGH secretion plasmids.

To detect the hGH levels of the cell-free supernatant, an ELISA (see 2.10 Enzyme linked immunosorbent assay) was performed in triplicates. Following detection with BCIP®/NBT, a purple colour was to be expected, if hGH was present in the cell-free supernatant. However, the results of the ELISA were inconclusive as identical samples, supernatants from *R. eutropha* H16 transconjugants, as well as, the positive control, *Pichia pastoris* GS115:pPic+hGH (# 3460 – IMBT's culture collection), showed great variety in their discolouration (data not shown).

Due to the insufficient results of the ELISA assay, two western blots were carried out to verify the presence of hGH in the cell-free supernatant of *R. eutropha* H16 transconjugants. The first western blot was performed using the primary antibody [GH (T-20)] and the secondary antibody [anti-goat IgG coupled with alkaline phosphatase]. Following the detection reaction with BCIP®/NBT, a purple band at the expected size of 22 kDa could not be seen (data not shown). The second western blot was performed using a different secondary antibody [selfmade 2nd antibody], which was coupled with horseradish peroxidase. After the subsequent detection with a chemiluminiscent (SignalFire™ Elite Reagent), a signal could only be detected in the positive control sample (*P. pastoris* GS115:pPic+hGH), but not in the cell-free supernatant samples of *R. eutropha* H16 transconjugants (data not shown).

3.6 Investigation of CelA secretion by *Ralstonia eutropha* H16

For the examination of the CelA secretion efficiency, 4 single colonies of *R. eutropha* H16 transconjugants harboring CelA secretion plasmids were used to inoculate 3 mL of LB media supplemented with 0.6 % fructose and the appropriate antibiotics, following overnight incubation at 28 °C. The next day, the main culture, 20 mL of LB media with 0.6 % fructose and the appropriate antibiotics, were inoculated to an OD_{600} of 0.2 and incubated at 28 °C and 130 rpm. Following 15 h of incubation, the OD_{600} was measured for each *R. eutropha* H16 transconjugant and the fermentation broth was then centrifuged for 20 min at 3220 x g and 4 °C to obtain cell-free supernatant. To confirm the results of the secretion assays, the fermentations were repeated twice, once with all 4 transconjugants of each construct and once with only the first transconjugant of each construct. Figure 21 - Figure 23 show the results of the OD_{600} measurement of each fermentation round. Compared to the empty vector control, *R. eutropha* H16 [pKRSF1010-P_{tac}-Δ49], all except *R. eutropha* H16 [pKRSF1010-P_{tac}-NosL-celA], showed the same growth behaviour after 15 h incubation. In the first fermentation round, transconjugants 2 and 4 of *R. eutropha* H16 [pKRSF1010-tac-F504_2437-celA] also showed a slower growth, but in the second fermentation round, their OD_{600} represented regular growth behaviour.

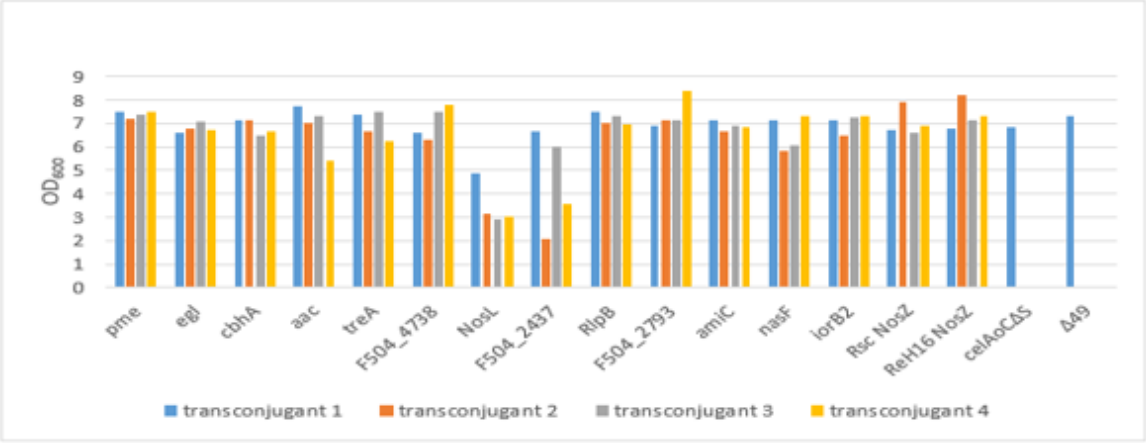

Figure 21 OD_{600} values of the first fermentation round of *R. eutropha* H16 transconjugants carrying either CelA secretion plasmids (pKRSF1010-P_{tac}-SP-celA)[1] or the negative control plasmids (pKRSF1010-P_{tac}-celAoCΔS and pKRSF1010-P_{tac}-Δ49)

Precultures of *R. eutropha* H16 transconjugants were used to inoculate LB media supplemented with 1 % glycerol and the appropriate antibiotics to an OD_{600} of 0.2 and incubated for 15 h at 28 °C and 130 rpm.

[1] pKRSF1010-P_{tac}-SP-celA describes the general CelA secretion plasmid. Exchanging "SP" with the individual signal peptides names the different CelA secretion plasmids.

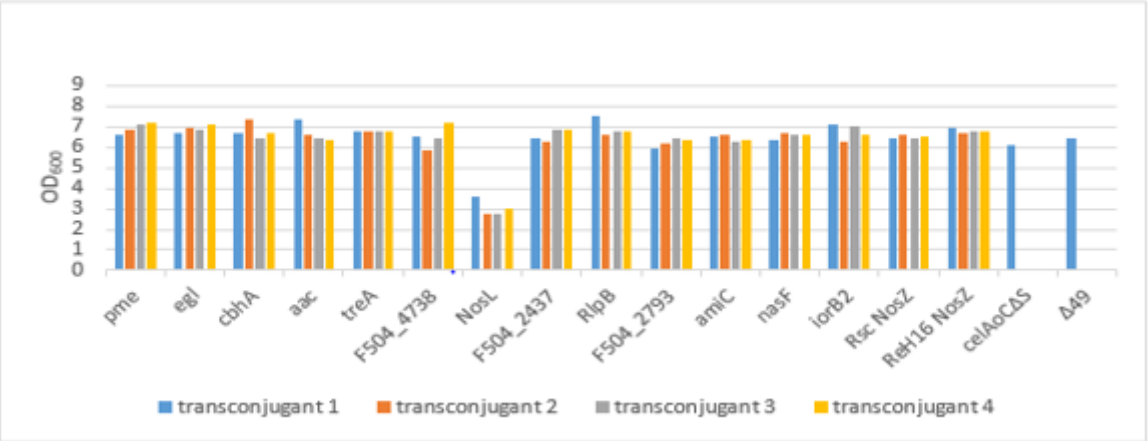

Figure 22 OD_{600} values of the second fermentation round of *R. eutropha* H16 transconjugants carrying either CelA secretion plasmids (pKRSF1010-P_{tac}-SP-celA)[1] or the negative control plasmids (pKRSF1010-P_{tac}-celAoCΔS and pKRSF1010-P_{tac}-Δ49)

Precultures of *R. eutropha* H16 transconjugants were used to inoculate LB media supplemented with 1 % glycerol and the appropriate antibiotics to an OD_{600} of 0.2 and incubated for 15 h at 28 °C and 130 rpm.

[1] pKRSF1010-P_{tac}-SP-celA describes the general CelA secretion plasmid. Exchanging "SP" with the individual signal peptides names the different CelA secretion plasmids.

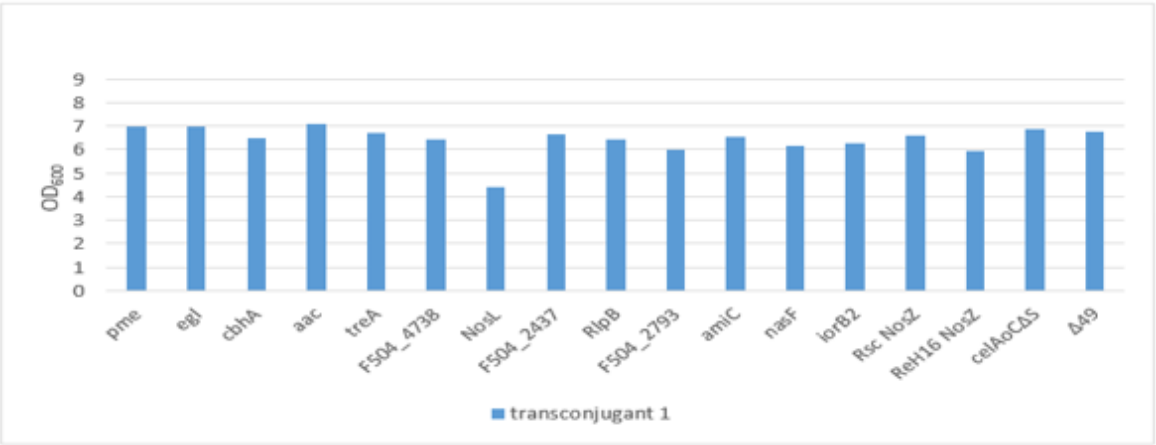

Figure 23 OD_{600} values of the third fermentation round of *R. eutropha* H16 transconjugants carrying either CelA secretion plasmids (pKRSF1010-P_{tac}-SP-celA)[1] or the negative control plasmids (pKRSF1010-P_{tac}-celAoCΔS and pKRSF1010-P_{tac}-Δ49)

Precultures of *R. eutropha* H16 transconjugants were used to inoculate LB media supplemented with 1 % glycerol and the appropriate antibiotics to an OD_{600} of 0.2 and incubated for 15 h at 28 °C and 130 rpm.

[1] pKRSF1010-P_{tac}-SP-celA describes the general CelA secretion plasmid. Exchanging "SP" with the individual signal peptides names the different CelA secretion plasmids.

Due to the lower OD_{600} values of *R. eutropha* H16 [pKRSF1010-P_{tac}-NosL-celA] in all fermentation rounds, the appearances of the cells were examined for irregularities, such as e.g. insufficient segmentation, under the microscope. However compared to the empty vector control, *R. eutropha* H16 transconjugants harboring CelA secretion plasmids showed no abnormal shape and Figure 24 shows a selection of the augmented pictures.

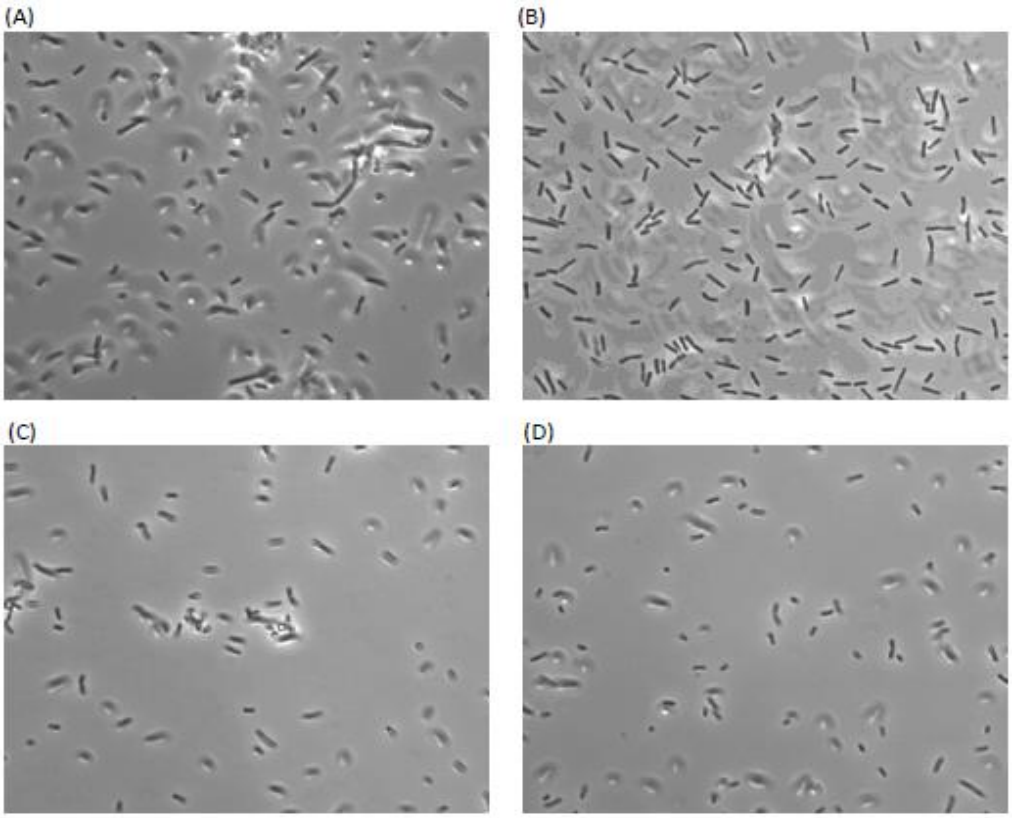

Figure 24 1000 x magnification of *R. eutropha* H16 transconjugants viewed by transmitted light
(A) *R. eutropha* H16 [pKRSF1010-P_{tac}-Δ49]; **(B)** *R. eutropha* H16 [pKRSF1010-P_{tac}-NosL-celA] transconjugant 2; **(C)** *R. eutropha* H16 [pKRSF1010-P_{tac}-F504_2793-celA] transconjugant 2, and **(D)** *R. eutropha* H16 [pKRSF1010-P_{tac}-egl-celA] transconjugant 4

Following centrifugation, the cell-free supernatants were harvested and the protein concentrations were measured in triplicates using the Bradford protein method (see 2.6 Measurement of protein concentration). The results of the protein concentration measurement can be seen in Figure 25 - Figure *27* and do not reveal any significant increase of the total protein concentrations in the supernatant of *R. eutropha* H16 transconjugants carrying CelA secretion plasmids, compared to the negative controls, pKRSF1010-P_{tac}-celAoCΔS and pKRSF1010-P_{tac}-Δ49.

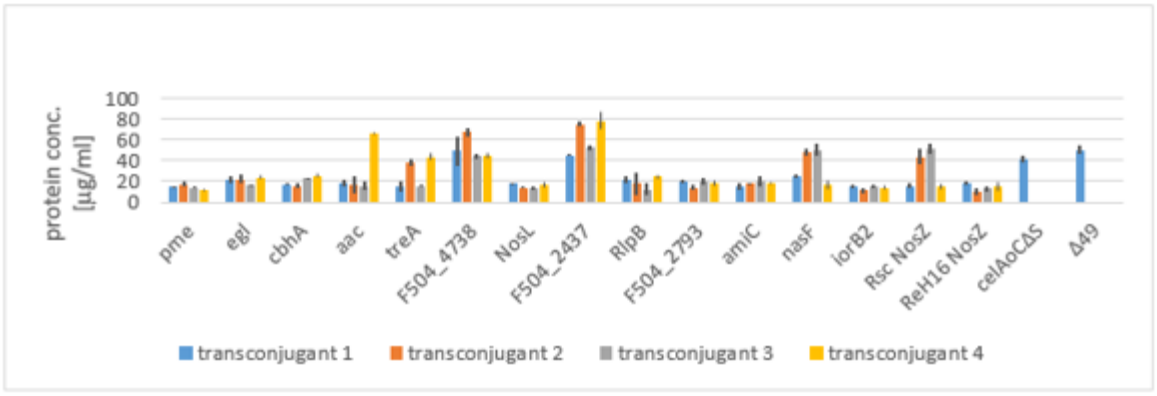

Figure 25 Protein concentrations in the supernatant from the first fermentation round of *R. eutropha* H16 transconjugants carrying either CelA secretion plasmids (pKRSF1010-P_{tac}-SP-celA)[1] or the negative control plasmids (pKRSF1010-P_{tac}-celAoCΔS and pKRSF1010-P_{tac}-Δ49)

[1] pKRSF1010-P_{tac}-SP-celA describes the general CelA secretion plasmid. Exchanging "SP" with the individual signal peptides names the different CelA secretion plasmids.

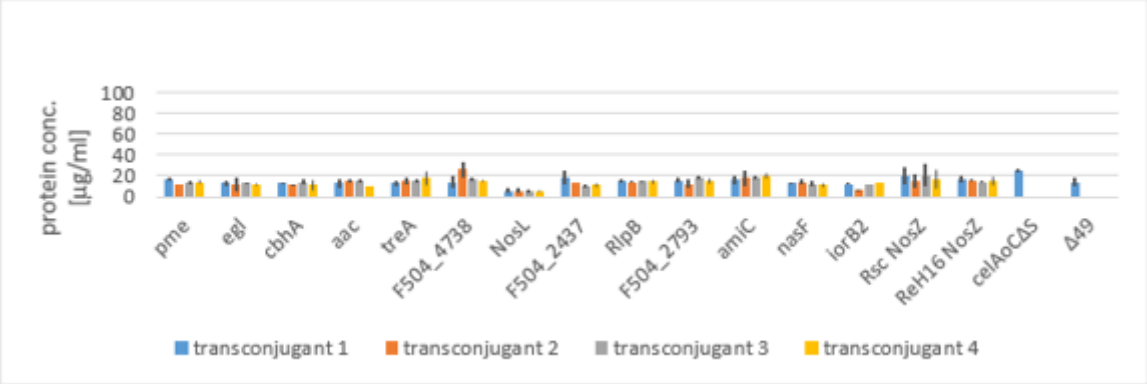

Figure 26 Protein concentrations in the supernatant from the second fermentation round of *R. eutropha* H16 transconjugants carrying either CelA secretion plasmids (pKRSF1010-P_{tac}-SP-celA)[1] or the negative control plasmids (pKRSF1010-P_{tac}-celAoCΔS and pKRSF1010-P_{tac}-Δ49)

[1] pKRSF1010-P_{tac}-SP-celA describes the general CelA secretion plasmid. Exchanging "SP" with the individual signal peptides names the different CelA secretion plasmids.

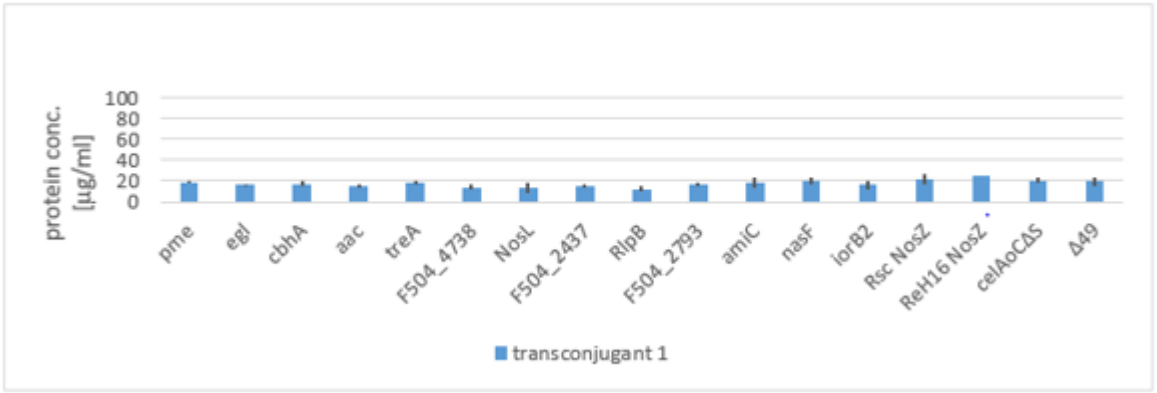

Figure 27 Protein concentrations from the third fermentation round of the cell-free supernatant of *R. eutropha* H16 transconjugants carrying either CelA secretion plasmids (pKRSF1010-P_{tac}-SP-celA)[1] or the negative control plasmids (pKRSF1010-P_{tac}-celAoCΔS and pKRSF1010-P_{tac}-Δ49)

[1] pKRSF1010-P_{tac}-SP-celA describes the general CelA secretion plasmid. Exchanging "SP" with the individual signal peptides names the different CelA secretion plasmids.

The existence of CelA in the cell-free supernatant of *R. eutropha* H16 transconjugants was detected via a qualitative and a quantitative activity assay. Both assays were based on the degradation of CMC following enzyme incubation. Figure 28 shows the results of the qualitative Congo red assay (see 2.11 Congo red clearing zone assay) and the brighter halos indicate CelA activity. The different sizes of the halo revealed the diverse levels of activity and thereby, the individual efficiencies of the signal sequences. CelA activity can be detected in the supernatant of the following *R. eutropha* H16 transconjugants: [pKRSF1010-P_{tac}-cbhA-celA], [pKRSF1010-P_{tac}-aac-celA], [pKRSF1010-P_{tac}-treA-celA], [pKRSF1010-P_{tac}-F504_4738-celA], [pKRSF1010-P_{tac}-F504_2437-celA], [pKRSF1010-P_{tac}-F504_2793-celA], [pKRSF1010-P_{tac}-amiC-celA], [pKRSF1010-P_{tac}-nasF-celA], [pKRSF1010-P_{tac}-RscNosZ-celA] and [pKRSF1010-P_{tac}-ReH16NosZ-celA]. Holes 6 and 21 were filled with the positive control, 1.2 µg purified CelACcHis. To exclude the possibility of functional CelA secretion due to cell lysis, holes 5 and 18 were filled with *R. eutropha* H16 [pKRSF1010-P_{tac}-celAoCΔS], while holes 10 and 20 were filled with supernatants of *R. eutropha* H16 transconjugants harboring the empty vector control (pKRSF1010-P_{tac}-Δ49). Since *R. eutropha* H16 [pKRSF1010-P_{tac}-celAoCΔS] displayed only very small halos, it can be stated that the determinated CelA activities of the above mentioned transconjugants are due to a functional secretion mechanism and not because of cell lysis.

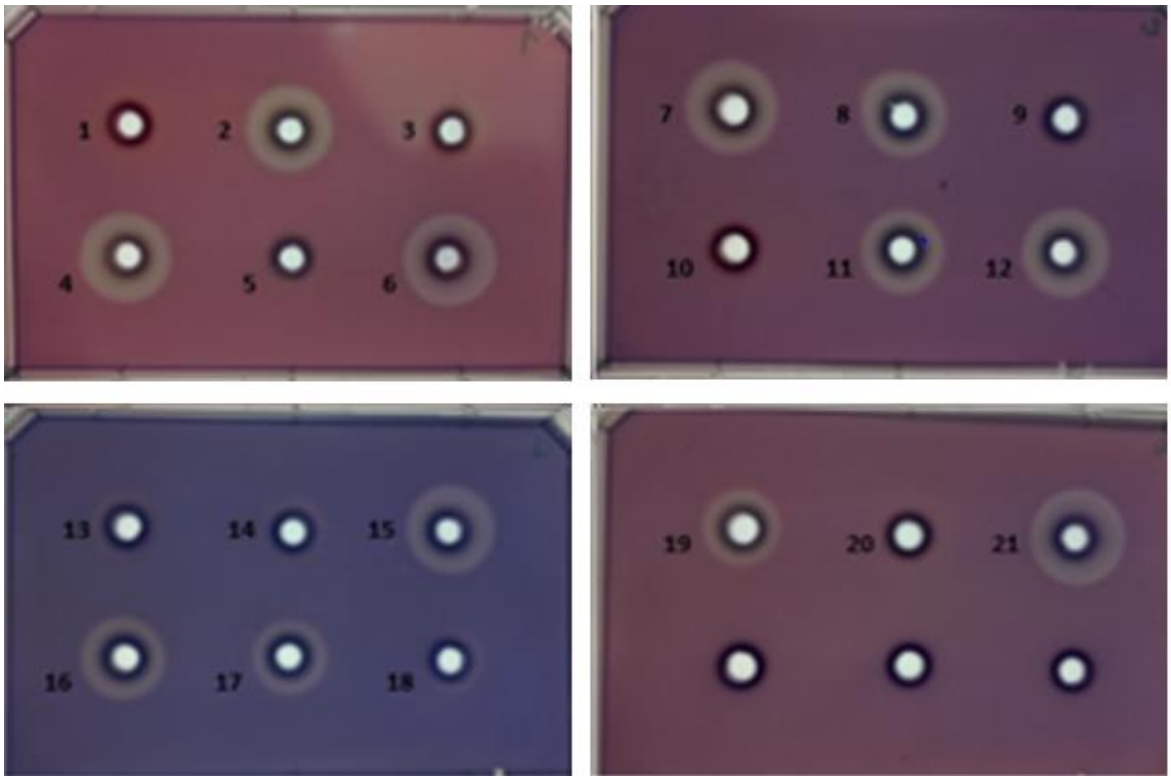

Figure 28 Congo red assay using cell-free supernatant of *R. eutropha* H16 transconjugants harboring the following CelA secretion plasmids of the third fermentation round: (1) pKRSF1010-P_{tac}-NosL-celA, **(2)** pKRSF1010-P_{tac}-F504_2437-celA, **(3)** pKRSF1010-P_{tac}-RlpB-celA, **(4)** pKRSF1010-P_{tac}-F504_2793-celA, **(7)** pKRSF1010-P_{tac}-amiC-celA, **(8)** pKRSF1010-P_{tac}-nasF-celA, **(9)** pKRSF1010-P_{tac}-iorB2-celA, **(11)** pKRSF1010-P_{tac}-RscNosZ-celA, **(12)** pKRSF1010-P_{tac}-ReH16NosZ-celA, **(13)** pKRSF1010-P_{tac}-pme-celA, **(14)** pKRSF1010-P_{tac}-egl-celA, **(15)** pKRSF1010-P_{tac}-cbhA-celA, **(16)** pKRSF1010-P_{tac}-aac-celA, **(17)** pKRSF1010-P_{tac}-treA-celA, **(19)** pKRSF1010-P_{tac}-F504_4738-celA. The negative control plasmids are **(5), (18)** pCRSF1010-P_{tac}-celAoCΔS and **(10), (20)** pKRSF1010-P_{tac}-Δ49. The positive control is **(6), (21)** 1.2 µg purified celACcHis. The plates were treated with 0.1 M HCl leading to a colour change from red to purple.

Quantitative comparison of the CelA secretion efficiency of the individual signal sequences was accomplished applying the pHBAH assay (see 2.12 Reducing sugar assay). 150 µL of an aqueous CMC solution (1.75 %) were incubated for 5 min with 30 µL cell-free supernatant from *R. eutropha* H16 transconjugants and subsequently, the liberated reducing sugars, calibrated on the basis of glucose, were detected photometrically. Figure 29 - Figure 31 show the results, in the form of liberated glucose [mg mL^{-1}], of the pHBAH assay with the samples of *R. eutropha* H16 transconjugants. The supernatant of the following *R. eutropha* H16 transconjugants, [pKRSF1010-P_{tac}-F504_2793-celA], [pKRSF1010-P_{tac}-F504_2437-celA], [pKRSF1010-P_{tac}-amiC-celA], [pKRSF1010-P_{tac}-cbhA-celA], [pKRSF1010-P_{tac}-aac-celA], [pKRSF1010-P_{tac}-RscNosZ-celA], [pKRSF1010-P_{tac}-ReH16NosZ-celA], [pKRSF1010-P_{tac}-nasF-celA], [pKRSF1010-P_{tac}-treA-celA], and [pKRSF1010-P_{tac}-F504_4738-celA], listed from highest to lowest activity, were able to hydrolyze CMC. Altogether three fermentation rounds were executed under the same

conditions, reproducing results could be achieved in all cases, except for *R. eutropha* H16 [pKRSF1010-P_{tac}-NosL-celA] transconjugants 2 and 4 and *R. eutropha* H16 [pKRSF1010-P_{tac}-aac-celA] transconjugant 4, which revealed significant higher CelA activities in the first round of fermentation. In the second round, the pHBAH assay was also carried out with the positive control, CelACcHis and 0.036 µg CelACcHis were able to liberate 0.484 [mg mL^{-1}] glucose, while 0.018 µg CelACcHis were able to release 0.325 [mg mL^{-1}] glucose. Slightly lower glucose concentrations, 0.253 [mg mL^{-1}] and 0.222 [mg mL^{-1}], could be measured after incubation of CMC with *R. eutropha* H16 [pKRSF1010-P_{tac}-F504_2793-celA] and *R. eutropha* H16 [pKRSF1010-P_{tac}-amiC-celA]. During the first round of fermentation glucose concentrations of 0.514 [mg mL^{-1}] or 0.343 [mg mL^{-1}] could be measured in the enzyme reaction mix of [pKRSF1010-P_{tac}-F504_2437-celA] or [pKRSF1010-P_{tac}-aac-celA].

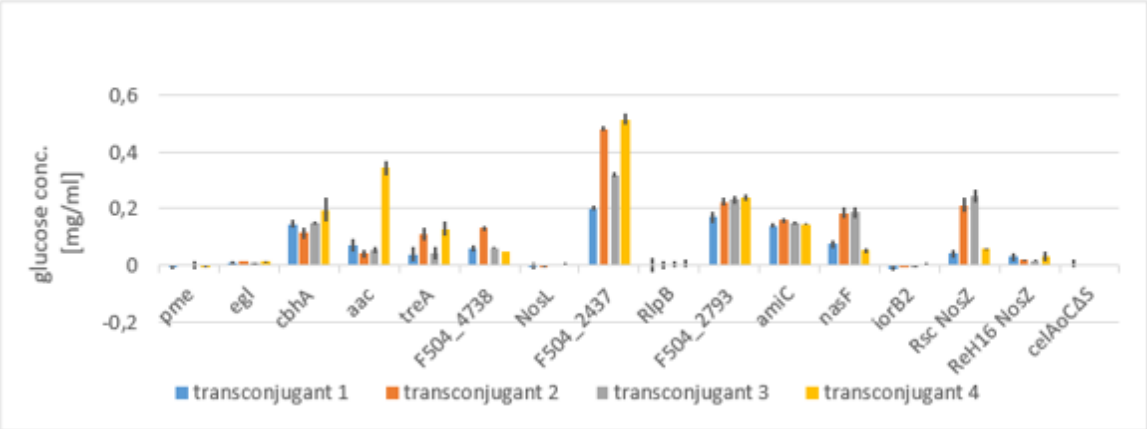

Figure 29 Results from the pHBAH assay of the first fermentation round: the concentration of glucose in the enzyme reaction sample is measured following incubation of CMC with the cell-free supernatant of *R. eutropha* H16 transconjugants carrying either CelA secretion plasmids (pKRSF1010-P_{tac}-SP-celA)[1] or the negative control plasmid (pKRSF1010-P_{tac}-celAoCΔS).

[1] pKRSF1010-P_{tac}-SP-celA describes the general CelA secretion plasmid. Exchanging "SP" with the individual signal peptides names the different CelA secretion plasmids.

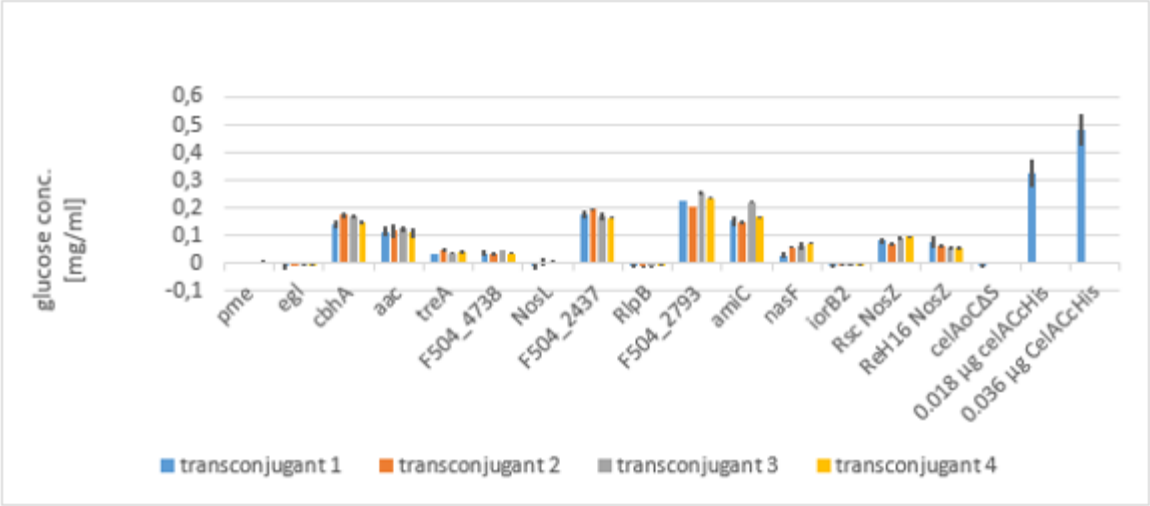

Figure 30 Results from the pHBAH assay of the second fermentation round: the concentration of glucose in the enzyme reaction sample is measured following incubation of CMC with the cell-free supernatant of *R. eutropha* H16 transconjugants carrying either CelA secretion plasmids (pKRSF1010-P_{tac}-SP-celA)[1] or the negative control plasmid (pKRSF1010-P_{tac}-celAoCΔS).
[1] pKRSF1010-P_{tac}-SP-celA describes the general CelA secretion plasmid. Exchanging "SP" with the individual signal peptides names the different CelA secretion plasmids.

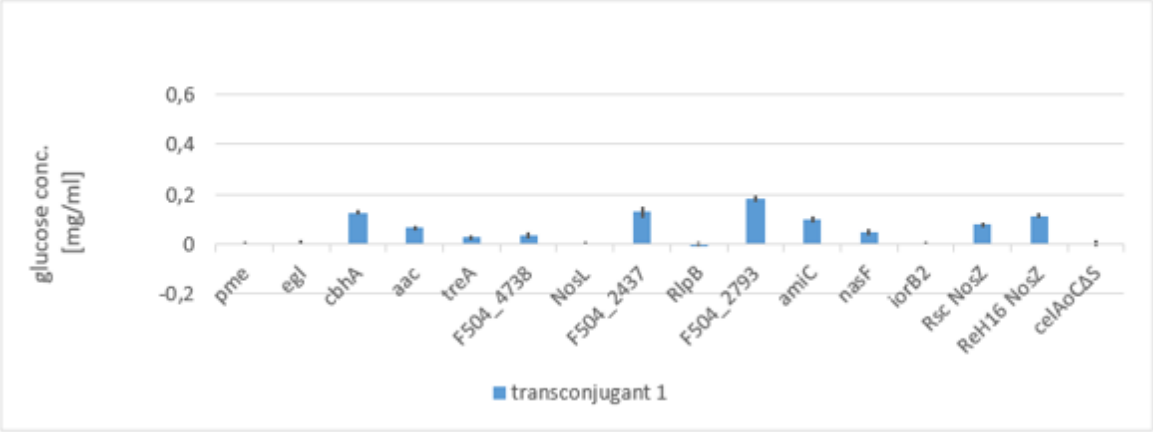

Figure 31 Results from the pHBAH assay of the third fermentation round: the concentration of glucose in the enzyme reaction sample is measured following incubation of CMC with the cell-free supernatant of *R. eutropha* H16 transconjugants carrying either CelA secretion plasmids (pKRSF1010-P_{tac}-SP-celA)[1] or the negative control plasmid (pKRSF1010-P_{tac}-celAoCΔS).
[1] pKRSF1010-P_{tac}-SP-celA describes the general CelA secretion plasmid. Exchanging "SP" with the individual signal peptides names the different CelA secretion plasmids.

In two-step secretion systems, the secretion efficiency depends on the secretion rate across the IM into the periplasma and on the secretion rate of the OM. To see if high amounts of active CelA were accumulated in the middle of both membranes, the periplasmic fraction was isolated by rupturing the OM with lysozyme (see 2.5 Isolation of periplasmatic fraction). The CelA activity of the periplasmic fraction was then determined via the Congo red assay (see 2.11 Congo red clearing zone assay). Figure 32 shows the

results of the Congo red assay with the periplasmic fraction of the different *R. eutropha* H16 transconjugants. CelA activity could be detected in the periplasm of the following *R. eutropha* H16 transconjugants: [pKRSF1010-P_{tac}-cbhA-celA], [pKRSF1010-P_{tac}-aac-celA], [pKRSF1010-P_{tac}-treA-celA], [pKRSF1010-P_{tac}-F504_4738-celA], [pKRSF1010-P_{tac}-F504_2437-celA], [pKRSF1010-P_{tac}-F504_2793-celA], [pKRSF1010-P_{tac}-amiC-celA], [pKRSF1010-P_{tac}-nasF-celA], [pKRSF1010-P_{tac}-RscNosZ-celA] and [pKRSF1010-P_{tac}-ReH16NosZ-celA]. Holes 5 and 18, as well as 10 and 20 were filled with the periplasmic fraction of the negative controls *R. eutropha* H16 [pKRSF1010-P_{tac}-celAoCΔS] and [pKRSF1010-P_{tac}-Δ49], respectively, whereas hole 6 and hole 21 were filled with the positive control, 1.2 µg purified CelACcHis.

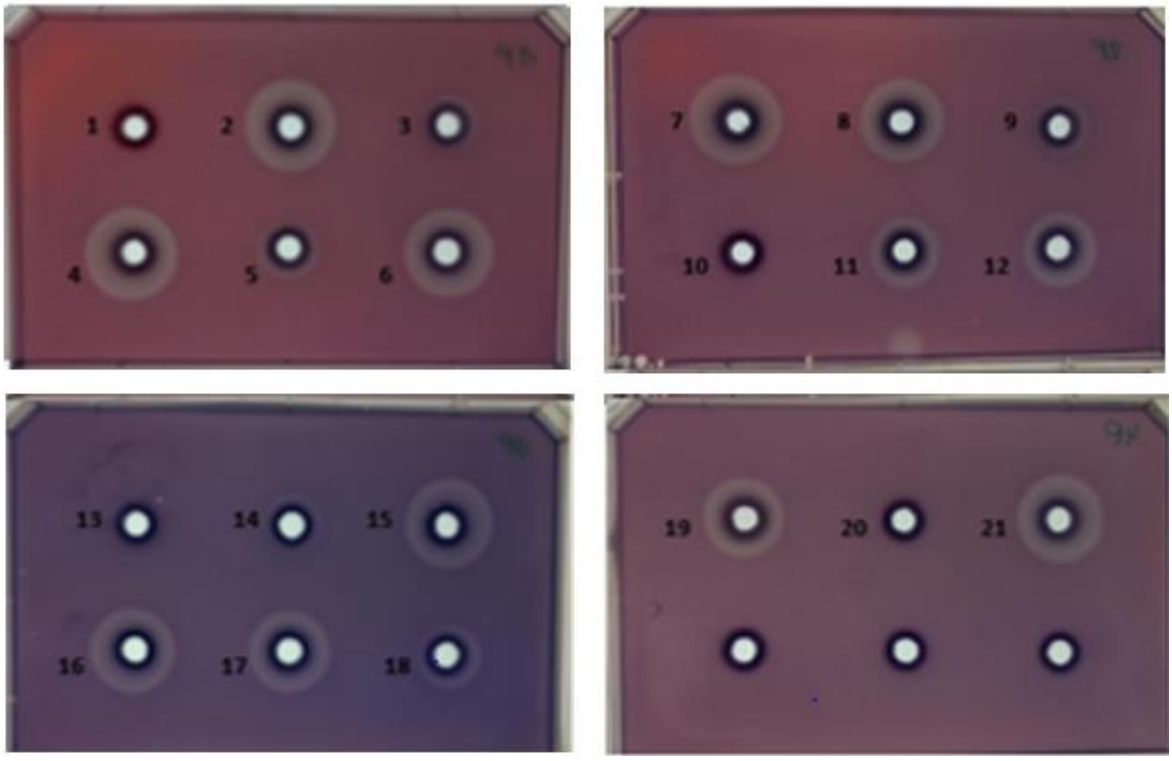

Figure 32 Congo red assay of the periplasmic fraction of *R. eutropha* H16 transconjugants harboring the following CelA secretion plasmids of the third fermentation round: (1) pKRSF1010-P_{tac}-NosL-celA, **(2)** pKRSF1010-P_{tac}-F504_2437-celA, **(3)** pKRSF1010-P_{tac}-RlpB-celA, **(4)** pKRSF1010-P_{tac}-F504_2793-celA, **(7)** pKRSF1010-P_{tac}-amiC-celA, **(8)** pKRSF1010-P_{tac}-nasF-celA, **(9)** pKRSF1010-P_{tac}-iorB2-celA, **(11)** pKRSF1010-P_{tac}-RscNosZ-celA, **(12)** pKRSF1010-P_{tac}-ReH16NosZ-celA, **(13)** pKRSF1010-P_{tac}-pme-celA, **(14)** pKRSF1010-P_{tac}-egl-celA, **(15)** pKRSF1010-P_{tac}-cbhA-celA, **(16)** pKRSF1010-P_{tac}-aac-celA, **(17)** pKRSF1010-P_{tac}-treA-celA, **(19)** pKRSF1010-P_{tac}-F504_4738-celA. The negative control plasmids are **(5), (18)** pCRSF1010-Ptac-celAoCΔS and **(10), (20)** pKRSF1010-P_{tac}-Δ49. The positive control is **(6), (21)** 1.2 µg purified celACcHis. The plates were treated with 0.1 M HCl leading to a colour change from red to purple.

Furthermore, a SDS-PAGE was conducted to demonstrate the expression of CelA in *R. eutropha* H16 transconjugant cells at the protein level. *R. eutropha* H16 cells of 1 mL fermentation broth were harvested by centrifugation and prepared according to the

protocol (see 2.8 Sodium dodecyl sulphate-polyacrylamide gel electrophoresis). Upon protein separation via electrophoresis, bands in the expected size of 33 kDa, corresponding to CelA could not be detected in any *R. eutropha* H16 transconjugants (Figure 33). Lanes 1 to 10 represent the proteins of the whole-cell lysates of *R. eutropha* H16 transconjugants carrying CelA secretion plasmids, while slots 11 and 12 were loaded with the whole-cell lysates of *R. eutropha* H16 [pKRSF1010-celAoCΔS] and the empty vector control, *R. eutropha* H16 [pKRSF1010-Δ49], respectively. All lanes show the exact same protein pattern suggesting that CelA cannot be detected in the cells of *R. eutropha* H16 transconjugants. Two possible reasons might be that either CelA is not present in the cells due to being secreted or that while active, the amount of expressed CelA is not very high and therefore, cannot be detected at the protein level.

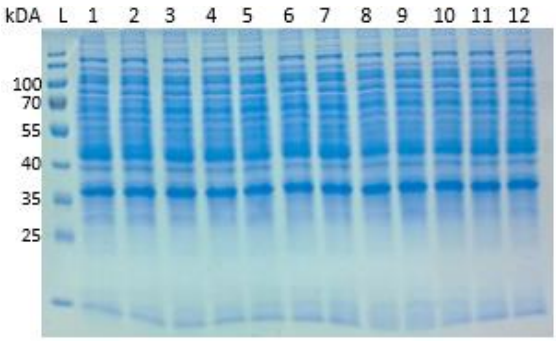

L PageRuler™ Prestained Protein Ladder
1. *R.e.*H16 [pKRSF1010-P_{tac}-amiC-celA] transconjugant 2
2. *R.e.*H16 [pKRSF1010-P_{tac}-aac -celA] transconjugant 1
3. *R.e.*H16 [pKRSF1010-P_{tac}-aac-celA] transconjugant 4
4. *R.e.*H16 [pKRSF1010-P_{tac}-RscNosZ-celA] transconjugant 1
5. *R.e.*H16 [pKRSF1010-P_{tac}-treA-celA] transconjugant 1
6. *R.e.*H16 [pKRSF1010-P_{tac}-F504_2793 -celA] transconjugant 1
7. *R.e.*H16 [pKRSF1010-P_{tac}-F504_2793-celA] transconjugant 3
8. *R.e.*H16 [pKRSF1010-P_{tac}-F504_4738-celA] transconjugant 1
9. *R.e.*H16 [pKRSF1010-P_{tac}-egl-celA] transconjugant 1
10.*R.e.*H16 [pKRSF1010-P_{tac}-F504_2437-celA] transconjugant 1
11.*R.e.*H16 [pKRSF1010-P_{tac}-celAoCΔs]
12.*R.e.*H16 [pKRSF1010-P_{tac}-Δ49]

Figure 33 SDS-PAGE of whole-cell lysates from *R. eutropha* H16 transconjugants

In summary, Table 29 compares the measured secretion efficiencies of all assays. Altogether, similar results could be achieved for all signal peptides and the determined signal peptide hits (e.g. CbhA, Aac, F504_2437, F504_2793, AmiC) consistently show high levels of CelA activity in the extracellular medium. *R. eutropha* H16 transconjugants carrying the CelA secretion plasmids with the signal peptides TreA and F504_4738 displayed higher CelA activity levels in the Congo red assay with the whole cells and the periplasmic fraction than with the cell-free supernatant, suggesting that the second step of the secretion limited the overall yield of extracellular CelA. Furthermore, no preference for the native origin of the signal peptide can be observed as both NosZ signal peptides (from *R. eutropha* H16 and *R. solanacearum*) show similar CelA activity levels in the cell-free supernatant of *R. eutropha* H16 transconjugants.

Table 29 Overview of the individual CelA activity levels measured for each signal peptide of *R. eutropha* H16 transconjugants

	Congo red assay whole cells	Congo red assay cell-free supernatant	pHBAH assay cell-free supernatant	Congo red assay periplasmic fraction
Sec- specific signal sequences				
Pme	+	-/+	-	-
Egl	+	-/+	-	-
cbhA	+++	+++	+++	+++
Aac	+++	++	+++	+++
treA	++	+	+	++
F504_4738	++	+	+	++
Tat- specific signal sequences				
NosL	++	-	-	-
F504_2437	++	+++	+++	+++
RlpB	+	-	-	-/+
F504_2793	+++	+++	++++	+++
amiC	+++	+++	+++	+++
nasF	++	++	++	++
iorB2	+	-	-	-/+
ReH16 NosZ[1]	++	+++	++	++
Rsc NosZ[2]	++	++	++	++

[1] *ReH16 NosZ* stands for the *NosZ* signal sequence derived from *R. eutropha* H16
[2] *Rsc NosZ* stands for the *NosZ* signal sequence derived from *R. solanacearum*

3.7 Investigation of Lev secretion by *Ralstonia eutropha* H16

For the examination of the Lev secretion efficiency, two fermentation rounds were carried out. Therefore, 4 single colonies of *R. eutropha* H16 transconjugants harboring Lev secretion plasmids were used to inoculate 3 mL of LB media containing 0.6 % fructose and the appropriate antibiotics and the preculture was incubated overnight at 28 °C. The next day, the main culture, 20 mL of LB media with 0.6 % fructose and the appropriate antibiotics, were inoculated to an OD_{600} of 0.2 and incubated at 28 °C and 130 rpm. Following 15 h of incubation, the OD_{600} was measured for each *R. eutropha* H16 transconjugant and the fermentation broth was then centrifuged for 20 min at 3220 x g at 4 °C. Figure 34 and Figure 35 show OD_{600} values of the first and the second fermentation rounds, respectively. Due to limited equipment availability, not all Lev secretion constructs could be fermented in the first round. Compared to the growth of *R. eutropha* H16 [pKRSF1010-P_{tac}-Δ49], R. *eutropha* H16 transconjugants harboring Lev secretion plasmids showed generally lower OD_{600} values and an irregular growth behaviour within transconjugants carrying identical constructs.

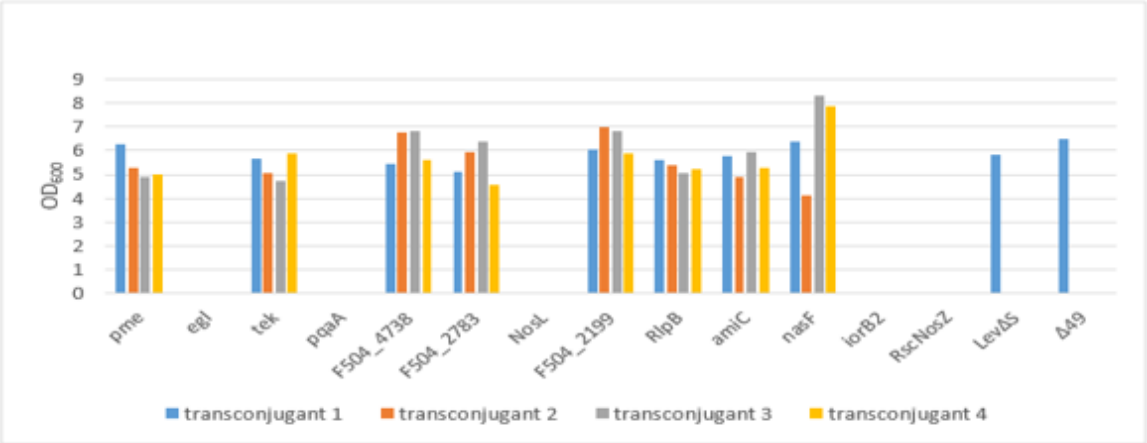

Figure 34 OD_{600} values of the first fermentation round of *R. eutropha* H16 transconjugants carrying either Lev secretion plasmids (pKRSF1010-P_{tac}-SP-lev)[1] or the negative control plasmids (pKRSF1010-P_{tac}-levΔ and pKRSF1010-P_{tac}-Δ49)

Precultures of *R. eutropha* H16 transconjugants were used to inoculate LB media supplemented with 1 % glycerol and the appropriate antibiotics to an OD_{600} of 0.2 and incubated for 15 h at 28 °C and 130 rpm.

[1] pKRSF1010-P_{tac}-SP-lev describes the general Lev secretion plasmid. Exchanging "SP" with the individual signal peptides names the different Lev secretion plasmids.

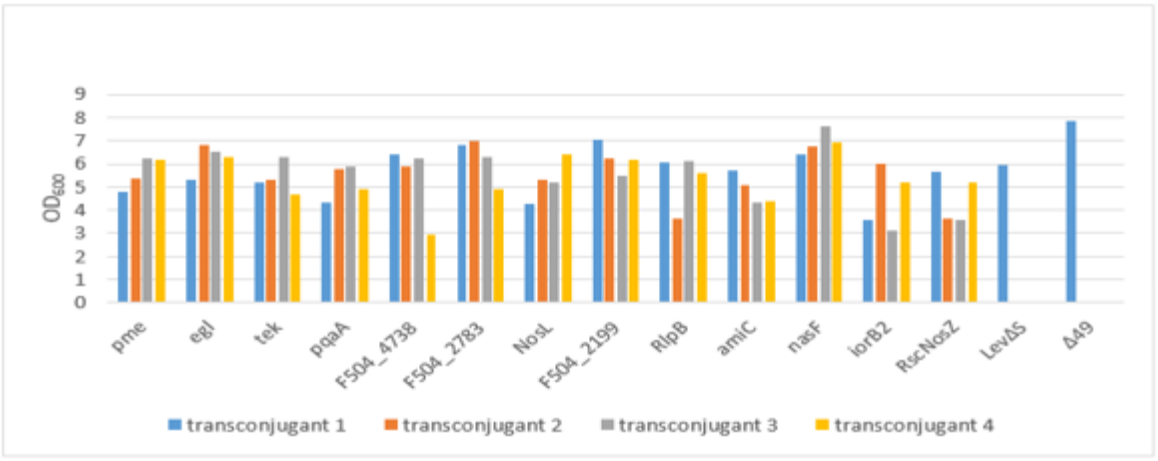

Figure 35 OD_{600} values of the second fermentation round of *R. eutropha* H16 transconjugants carrying either Lev secretion plasmids (pKRSF1010-P_{tac}-SP-lev)[1] or the negative control plasmids (pKRSF1010-P_{tac}-levΔ and pKRSF1010-P_{tac}-Δ49)

Precultures of *R. eutropha* H16 transconjugants were used to inoculate LB media supplemented with 1 % glycerol and the appropriate antibiotics to an OD_{600} of 0.2 and incubated for 15 h at 28 °C and 130 rpm.

[1] pKRSF1010-P_{tac}-SP-lev describes the general Lev secretion plasmid. Exchanging "SP" with the individual signal peptides names the different Lev secretion plasmids.

Following centrifugation, the cell-free supernatants were harvested and the protein concentrations were measured in triplicates using the Bradford method (see 2.6 Measurement of protein concentration). The results of the Bradford protein assay can be seen in Figure 36 - Figure 37 and showed great variety of the protein concentrations, ranging from 9.8 µg mL^{-1} for pKRSF1010-P_{tac}-NosL-lev to 80.6 µg mL^{-1} for pKRSF1010-P_{tac}-F504_2783-lev. Furthermore, *R. eutropha* H16 transconjugants carrying the same Lev

secretion constructs were expected to secrete the same amounts of protein concentrations into the extracellular medium. However, the four *R. eutropha* H16 transconjugants carrying either pKRSF1010-P_{tac}-tek-lev, pKRSF1010-P_{tac}-F504_4738-lev, pKRSF1010-P_{tac}-F504_2783-lev, pKRSF1010-P_{tac}-amiC-lev or pKRSF1010-P_{tac}-nasF-lev displayed a wide range of measured protein concentrations in 1 mL cell-free supernatant (e.g. from 20.3 – 58.0 µg mL^{-1} for *R. eutropha* H16 [pKRSF1010-P_{tac}-nasF-lev] in the first fermentation round).

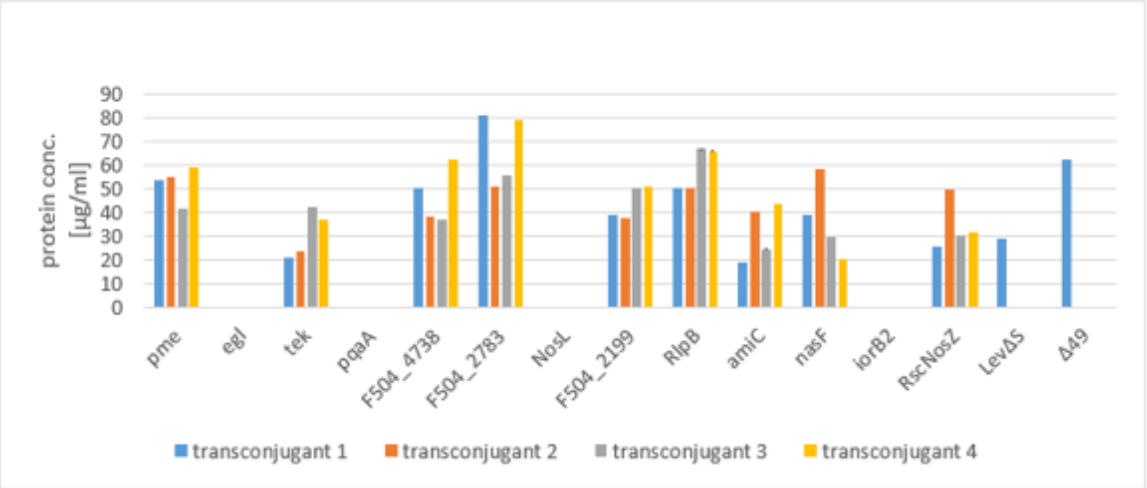

Figure 36 Protein concentrations in the supernatant from the first fermentation round of *R. eutropha* H16 transconjugants carrying either Lev secretion plasmids (pKRSF1010-P_{tac}-SP-lev)[1] or the negative control plasmids (pKRSF1010-P_{tac}-levΔ and pKRSF1010-P_{tac}-Δ49)

[1] pKRSF1010-P_{tac}-SP-lev describes the general Lev secretion plasmid. Exchanging "SP" with the individual signal peptides names the different Lev secretion plasmids.

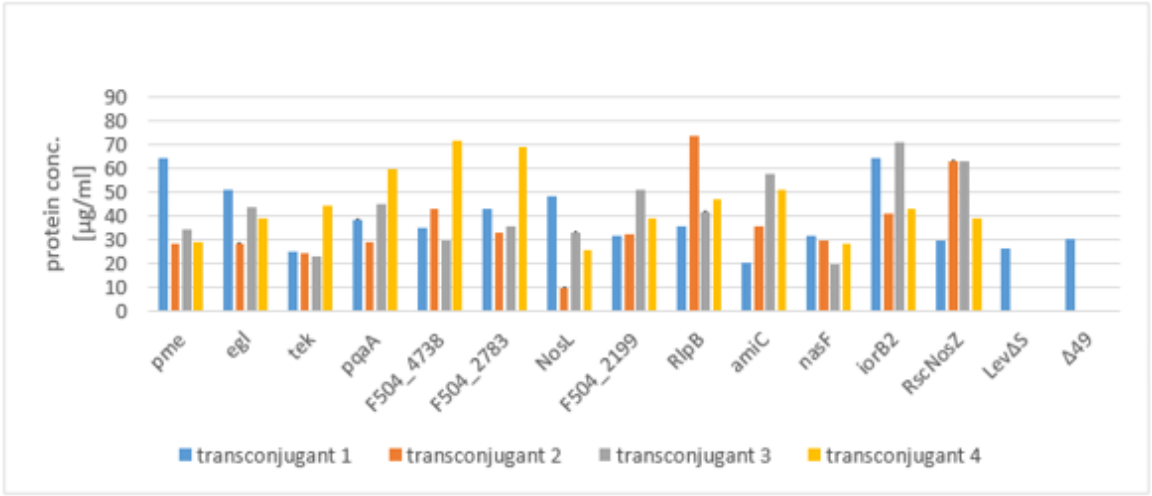

Figure 37 Protein concentrations in the supernatant from the second fermentation round of *R. eutropha* H16 transconjugants carrying either Lev secretion plasmids (pKRSF1010-P_{tac}-SP-lev)[1] or the negative control plasmids (pKRSF1010-P_{tac}-levΔ and pKRSF1010-P_{tac}-Δ49)

[1] pKRSF1010-P_{tac}-SP-lev describes the general Lev secretion plasmid. Exchanging "SP" with the individual signal peptides names the different Lev secretion plasmids.

To detect the existence of Lev in cell-free supernatant of *R. eutropha* H16 transconjugants, the levanase activity assay was applied (see 2.13 Levanase activity assay). Therefore, 50 µL of an aqueous sucrose solution were incubated at 50 °C for 90 min with 50 µL of the supernatant of *R. eutropha* H16 fermentation samples and the liberated glucose molecules [mg mL^{-1}] were detected subsequently. The results of the first and the second fermentation round are displayed in Figure 38 and Figure 39, respectively. Lev activity can be detected in the supernatant of the following *R. eutropha* H16 transconjugants: [pKRSF1010-P_{tac}-F504_2783-lev], [pKRSF1010-P_{tac}-NosL-lev], [pKRSF1010-P_{tac}-F504_2199-lev], [pKRSF1010-P_{tac}-amiC-lev], [pKRSF1010-P_{tac}-RscNosZ-lev] and [pKRSF1010-P_{tac}-RlpB-lev], but compared to the positive control, the supernatant of *P. pastoris* CBS 7435 mutS *aox1*::Lev-*HIS4*, the activity is very low. The levanase activity assay was then repeated using larger volumes of supernatant (100 µL and 150 µL), as well as prolonged incubation times, but no significant difference in the activity could be detected after applying other reaction conditions (data not shown).

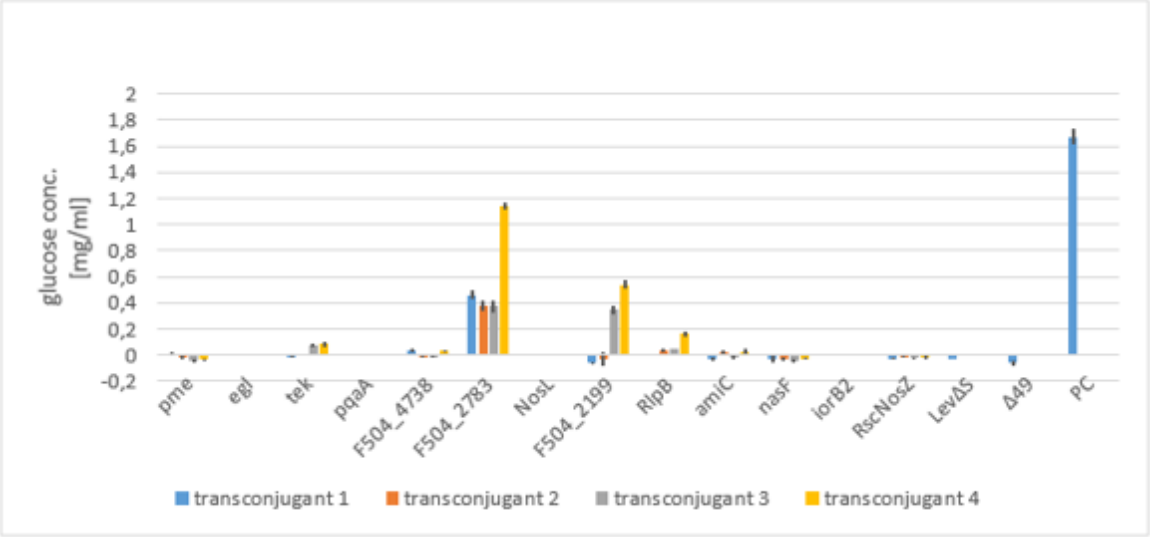

Figure 38 Results from the glucose-UV-assay of the first fermentation round: the concentration of glucose in the enzyme reaction sample is measured following incubation of sucrose with the cell-free supernatant of *R. eutropha* H16 transconjugants carrying either Lev secretion plasmids (pKRSF1010-P_{tac}-SP-lev)[1] or the negative control plasmids (pKRSF1010-P_{tac}-levΔS and pKRSF1010-P_{tac}-Δ49). The positive control (PC) is the supernatant of *P. pastoris* CBS 7435 mutS *aox1*::Lev-*HIS4*

[1] pKRSF1010-P_{tac}-SP-lev describes the general Lev secretion plasmid. Exchanging "SP" with the individual signal peptides names the different Lev secretion plasmids.

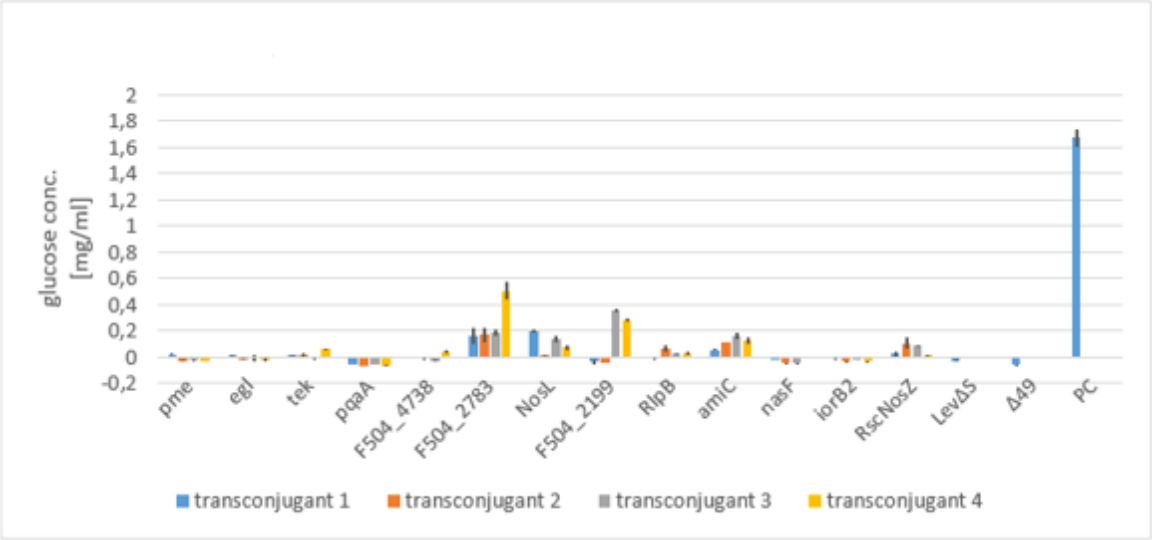

Figure 39 Results from the glucose-UV-assay of the second fermentation round: the concentration of glucose in the enzyme reaction sample is measured following incubation of sucrose with the cell-free supernatant of *R. eutropha* H16 transconjugants carrying either Lev secretion plasmids (pKRSF1010-P_{tac}-SP-lev)[1] or the negative control plasmids (pKRSF1010-P_{tac}-levΔS and pKRSF1010-P_{tac}-Δ49). The positive control (PC) is the supernatant of *P. pastoris* CBS 7435 mutS *aox1::*Lev-*HIS4*

[1] pKRSF1010-P_{tac}-SP-lev describes the general Lev secretion plasmid. Exchanging "SP" with the individual signal peptides names the different Lev secretion plasmids.

Furthermore, a SDS-PAGE was performed to verify the existence of Lev in the cell-free supernatant of *R. eutropha* H16 transconjugants at the protein level. The proteins in the supernatant were precipitated using methanol and chloroform (see 2.7 Methanol/ Chloroform protein precipitation) and dissolved in 1 x FSB-buffer. Sample volumes corresponding to the protein amount found in 250 µL cell-free supernatant were loaded onto the gel. Following electrophoresis, bands in the expected size of 73.32 kDa, corresponding to Lev, could not be detected in any sample of *R. eutropha* H16 transconjugants (Figure 40). Slot 1 to 12 were loaded with protein samples of *R. eutropha* H16 transconjugants harboring Lev secretion plasmids, whereas lane 13 and 14 revealed the proteins in the supernatants of *R. eutropha* H16 [pKRSF1010-P_{tac}-levΔS] and the *R. eutropha* H16 transconjugant carrying the empty vector control (pKRSF1010-P_{tac}-Δ49), respectively. As all the lanes show exactly the same protein pattern, it can be stated that it was not possible to detect Lev at the protein level in the cell-free supernatants.

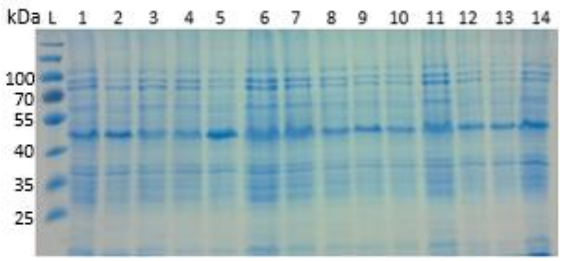

L PageRuler™ Prestained Protein Ladder
1. *R.e.*H16 [pKRSF1010-P_{tac}-NosL-lev] transconjugant 1
2. *R.e.*H16 [pKRSF1010- P_{tac}-F504_2199-lev] transconjugant 4
3. *R.e.*H16 [pKRSF1010- P_{tac}-RlpB-lev] transconjugant 2
4. *R.e.*H16 [pKRSF1010- P_{tac}-amiC-lev] transconjugant 6
5. *R.e.*H16 [pKRSF1010- P_{tac}-nasF-lev] transconjugant 1
6. *R.e.*H16 [pKRSF1010- P_{tac}-iorB2-lev] transconjugant 3
7. *R.e.*H16 [pKRSF1010- P_{tac}-RscNosZ-lev] transconjugant 3
8. *R.e.*H16 [pKRSF1010- P_{tac}-pme-lev] transconjugant 1
9. *R.e.*H16 [pKRSF1010- P_{tac}-egl-lev] transconjugant 3
10. *R.e.*H16 [pKRSF1010- P_{tac}-tek-lev] transconjugant 4
11. *R.e.*H16 [pKRSF1010- P_{tac}-F504_4738-lev] transconjugant 4
12. *R.e.*H16 [pKRSF1010- P_{tac}-F504_2783-lev] transconjugant 1
13. *R.e.*H16 [pKSRF1010-P_{tac}-levΔS]
14. *R.e.*H16 [pKRSF1010- P_{tac}-Δ49]

Figure 40 SDS-PAGE of precipitated proteins from the supernatant of *R. eutropha* H16 transconjugants

4 Discussion

The recombinant production of pharmaceutical and industrial proteins has increased greatly over the last 40 years and many expression hosts have been intensively studied. Whenever possible, the secretory production of the desired proteins is the preferred strategy due to the many advantages the secretory system has compared to the intracellular protein expression system. The simplified purification of the protein of interest, as well as, the lower probility of protein degradation caused by proteases in the cells describe just a few of the highlights of the secretory protein production system [21, 22]. Compared to Gram-positive bacteria, the recombinant protein secretion in Gram-negative bacteria is more difficult as the protein has to be translocated across the inner and the outer membranes. In Gram-negative bacteria the recombinant translocation of the desired proteins depends on natural occurring secretion pathways, which have been genetically modified [26]. The simplest modification to achieve the secretion of a foreign protein, is the fusion of a signal sequence to the 5'- end of the gene of interest [25]. Following the intracellular transcription and translation of the protein, the signal peptide is recognized and the preprotein is exported across the inner membrane via either the Sec- or the Tat- translocase. In recent years, *R. eutropha* H16 has sparked increasing attention as an alternative expression host to *E. coli* and several studies focused on the development of plasmid or integration based expression systems for the production of heterologous proteins [7, 8, 10]. However, the secretory production of recombinant proteins has not been examined yet, and thus, the goal of this master thesis was the secretion of the recombinant proteins hGH, CelA and Lev by *R. eutropha* H16. Therefore, 21 secretion peptides, predicted from identified exoproteins of *R. solanacearum* and *R. eutropha* H16 were fused to the 5'-terminal end of the reporter genes.

4.1 Secretion of hGH by *Ralstonia eutropha* H16

The human growth hormone was chosen as a reporter protein for the investigation of secretion by *R. eutropha* H16 because of its eukaryotic origin, its small size of 22 kDa and because it has no need for posttranslational modifications. Furthermore, hGH was one of the first products industrially produced by biotechnological approaches and its secretion has been studied extensively in *E. coli*, *P. pastoris* and *S. cerevisiae* [77, 78, 79]. The best

yields could be achieved by the methylotrophic yeast, *P. pastoris*, where 49 [µg mL^{-1}] hGH could be secreted into the extracellular medium, which makes up 40 % of the total protein amount found in the culture medium supernatant [78]. In *E. coli*, periplasmic yields of 10 – 15 [µg mL^{-1} A_{600}^{-1}] hGH have been reported after fusion of hGH to the OmpA signal peptide [77, 80]. Furthermore, the periplasmatic environment of *E. coli* was proven to be appropriate for proper processing and folding of hGH [77]. In addition to the periplasmic expression of hGH, Hsiung et al. reported yields of [4.5 µg mL^{-1} A_{550}^{-1}] in the culture supernatant after coexpression of hGH and bacteriocin release protein (BRP) in *E. coli*. By coexpressing BRP, hGH could be isolated without rupturing the *E. coli* cells and thereby the steps of the purification could be reduced [81].

Following plasmid construction, the hGH secretion plasmids were transferred into *R. eutropha* H16 via conjugation. The conjugation of pKRep-P_{tac}-egl-hGH into *R. eutropha* H16 worked as expected, and a large number of transconjugants, showing uniform growth appearance, appeared on the agar plates after conjugation. On the other hand, the transfer of pKRep-P_{tac}-pme-hGH and pKRep-P_{tac}-cbhA-hGH led to unsatisfying conjugation results. Following the mating process of *E. coli* S17-1 harboring the desired plasmids, and wild-type *R. eutropha* H16, rarely any transconjugants grew on the agar plates and the few that actually did grow, displayed unbalanced growth, which was indicated by the various sizes of the transconjugants. To resolve the cause of the irregular growth of the *R. eutropha* H16 transconjugants, the plasmids pKRep-P_{tac}-pme-hGH and pKRep-P_{tac}-egl-hGH were sent to sequencing with primers binding in the *mob* region and the sequences of both plasmids were compared. The sequencing results of pKRep-P_{tac}-egl-hGH (normal growth behaviour of corresponding *R. eutropha* H16 transconjugants) did not display any alterations to the published sequence, whereas the sequencing results of pKRep-P_{tac}-egl-hGH exposed mutations, in the form of repeats, in the *mob* region, which was therefore revealed to be the cause of irregular growth behaviour in *R. eutropha* H16. Upon gathering of the newly discovered information, as well as, similar observations made by the other members of the research group of Petra Köfinger, the secretion plasmids were recloned on the basis of the more stable *RSF1010* derivative expression vector.

Of all 21 signal sequences that were investigated for their hGH secretion potential, it first seemed possible to successfully construct all except two hGH secretion plasmids

(pKRSF1010-P_{tac}-F504_2199-hGH and pKRSF1010-P_{tac}-pehC-hGH). However, upon the subsequent sequencing, the number of signal sequences successfully inserted into the hGH secretion plasmids, was reduced to the following twelve: *pme, egl, cbhA, aac, treA, F504_4738, F504_2437, RlpB, amiC, nasF, iorB2*, and *RscNosZ*. The sequencing results of the hGH secretion constructs containing the other seven signal sequences *(pehB, tek, PqaA, F504_2783, NosL, F504_2793*, and *ReH16NosZ*) repeatedly revealed mutations in hGH, such as the incorporation of an extra thymine in the 5'- end of the reporter gene, or the exchange of a cytosine into a thymine at nucleotide position 94. The additional thymine in hGH would have caused a shift in the reading frame of hGH resulting in a completely different translation from the original sequence. Furthermore, the exchange of a cytosine into a thymine would have resulted in the incorporation of a stop codon in the middle of the hGH sequence and therefore, the above mentioned hGH secretion plasmids could not be used in the following experiments to analyse the secretion efficiency of *R. eutropha* H16. It is believed that the mutations in the above mentioned hGH secretion constructs, as well as, the unsuccessful ligation of hGH secretion plasmids containing *F504_2199* and *pehC*, might be because of the extra cellular burden on *E. coli* Top10 cells when put under constitutive expression conditions along with subsequent initiation of strong secretion. Hence, stress responses are induced which might lead to an inhibition of growth or to higher mutation rate [82]. As a consequence, it was decided to examine the secretion of hGH under constitutive expression conditions only for the twelve successfully constructed hGH secretion plasmids and the inspection of the remaining signal peptides will be considered when protein expression can be tightly regulated, e.g. by the induction of IPTG. Thereby, the stress put on the cells by constitutive expression can be eliminated and hopefully, the mutation rate can be decreased significantly.

Following plasmid construction, the hGH secretion plasmids were transferred into *R. eutropha* H16 via conjugation and cultivated for secretion assays. The growth behaviour of the *R. eutropha* H16 transconjugants carrying hGH secretion plasmids however, varied greatly. While the OD_{600} values of *R. eutropha* H16 transconjugants carrying either pKRSF1010-P_{tac}-iorB2-hGH, pKRSF1010-P_{tac}-F504_2437-hGH, pKRSF1010-F504_4738-hGH, pKRSF1010-P_{tac}-aac-hGH, or pKRSF1010-P_{tac}-cbhA-hGH were in accordance to the growth of the empty vector control, *R. eutropha H16* transconjugants

harboring pKRSF1010-P_{tac}-RlpB-hGH, pKRSF1010-P_{tac}-nasF-hGH, or pKRSF1010-P_{tac}-RscNosZ-hGH revealed significantly lower OD_{600} values. The lower OD_{600} values suggest that the constitutive expression and secretion of hGH has a negative impact on *R. eutropha* H16 leading to the inhibition of growth (cell lysis/ death). Growth inhibition could also be caused by high expression and secretion levels leading to the toxic accumulation of hGH in either the cytoplasm or the periplasm. However, none of the particular signal peptides (RlpB, nasF and RscNosZ) has been reported to be particular strong signal peptides and therefore, further tests would be necessary to resolve the issue.

Three assays were then executed to determine the total protein amount and the hGH presence in the cell-free supernatant of *R. eutropha* H16. The results of the Bradford protein assay are poor, and a significantly wide range of varying protein concentration could be detected. In regards to the growth behaviour, no correlation could be witnessed as the supernatant of transconjugants with either lower or higher OD_{600} values displayed both either lower or higher concentrations of total proteins.

The first assay applied to detect hGH, was the enzyme linked immunosorbent assay (ELISA). ELISA is a very sensitive method to specifically detect desired proteins. Using a secondary antibody benefits the procedure in a way so that the reaction can be amplified by binding multiple copies of the secondary antibody to the primary antibody. The results of the conducted ELISA's, however, remained to be inconclusive and discoloration corresponding just to the presence of hGH could not be detected in 50 µL of cell-free supernatant of *R. eutropha* H16 transconjugants. Unfortunately, at this point it cannot be said whether the amount of hGH found in only 50 µL is too low to be detectable or if hGH was processed incorrectly and therefore, the C-terminal epitope mapping of the primary antibody might not available. To increase the amount of possible hGH, another immunodetection method was applied and protein samples corresponding to the amount of protein found in 250 µL culture supernatant (5 x increase to protein amount applied in ELISA) were loaded on a SDS-PAGE and further transferred onto a western blot membrane. The western blot was conducted twice, with two distinct secondary antibodies. However, both western blots did not reveal any detectable hGH in the cell-free supernatants of *R. eutropha* H16.

Summarizing, the successful secretory production of hGH by *R. eutropha* H16 could not be confirmed. However it cannot be said, whether it was just because hGH was not secreted at all or at low concentrations or also because of incorrect processing. If the problem with detection was because of low concentration of hGH, the expression level could be increased by the application of a stronger promoter, such as P_{T5} or P_{j5} [10]. Furthermore, the expression level could be raised under regulated expression conditions. To find out, if incorrect processing could be the cause of the detection problems, the protein could be analysed via sequence analysis or peptide mapping, respectively [77]. However, therefore the amount of expressed hGH also has to be higher allowing the isolation of the hGH protein.

4.2 Secretion of CelA by *Ralstonia eutropha* H16

Cellulase A isolated from *S. cellulosum* has a molecular weight of ~33 kDa. It was chosen as a reporter protein for the investigation of secretion by *R. eutropha* H16 because of its prokaryotic origin, its median size of 33 kDa, and because of the availability of sensitive activity assays based on the hydrolyzation of CMC, as well as, the high specific activity of CelAoC. The purified CelAoC exhibited a specific activity of either 296 [U mg^{-1}] or 245 [U mg^{-1}], depending on the position of the added 6 x His-tag [61]. Additionally, during the course of my project laboratory, the intracellular expression of CelA in *R. eutropha* H16 has been successfully achieved by P_{tac} acting as a constitutive promoter.

The CelA secretion plasmids based on *Rep* origin were used as a first proof of functional recombinant protein secretion. Following plasmid construction, pKRep-P_{tac}-pme-celA and pKRep-P_{tac}-egl-celA were transferred into *R. eutropha* H16 and a Congo red assay with the cell-free supernatant of *R. eutropha* H16 transconjugants was carried out and yellow halos, indicating CelA activity in the extracellular fraction, could be observed (data not shown). Thereby, the principle function of secretion in *R. eutropha* H16 could be proven and primers for further signal sequences were ordered.

Of all 21 signal sequences that were investigated for their CelA secretion potential, 15 signal sequences could be cloned into the CelA secretion plasmids based on the *RSF1010* origin: *pme, egl, cbhA, aac, treA, F504_4738*, *NosL, F504_2437, RlpB, F504_2793, amiC, nasF, iorB2, RscNosZ*, and *ReH16NosZ*. The cloning of the remaining 5 signal sequences

(*F405_2199, pehC, pehB, tek, PqaA*, and *F504_2783*) could not be achieved repeatedly and the unsuccessful construction of the particular CelA secretion plasmids might be because of the extra cellular burden on *E. coli* Top10 cells when put under constitutive expression conditions along with subsequent initiation of strong secretion. It has been reported that PehC, PehB and Tek are particularly strong signal peptides in *R. solanacearum* [19] and thus, will be further examined under tightly regulated expression conditions, when the toxicity of the ligation products and the subsequent immediate expression and secretion of CelA can be repressed.

Following verification of the sequences of signal sequence and reporter gene, the CelA secretion plasmids were transformed into *E. coli* S17-1. However, only pKRSF1010-P_{tac}-pme-celA, pKRSF1010-P_{tac}-egl-celA, and pKRSF1010-P_{tac}-NosL-celA could be successfully taken up by *E. coli* S17-1, whereas the other CelA secretion plasmids seemed to be toxic for *E. coli* S17-1, and hence, resulting in no growth. The observed phenomenon, where CelA secretion plasmids could be transformed into *E. coli* Top10 but not *E. coli* S17-1, could be explained because of the integration of the mutant lac repressor, lac^q, into the genome of *E. coli* Top10 leading to the suppression of the expression. In *E. coli* S17-1 however, constitutive expression and simultaneous secretion of CelA has been initiated from the beginning, probably leading to the toxic accumulation of CelA in the periplasm of *E. coli* S17-1. The transfer of the particular CelA secretion plasmids could then be successfully achieved by triparental mating with the donor strain *E. coli* Top10, the helper strain *E. coli* HB101 [pRK2013] and the acceptor strain wild-type *R. eutropha* H16. In case of triparental conjugation, the *tra* genes are encoded on the helper plasmid pRK2013 and by triparental mating the conjugative transfer is initiated by the self-transmissible helper plasmid, which is first transconjugated into the donor strain *E. coli* Top10, which is carrying the CelA secretion plasmids. Secondly, the CelA secretion plasmids are mobilized by the helper plasmid and both are transferred into the recipient cell, wild-type *R. eutropha* H16. Furthermore, pRK2013 carries a colE1 replicon, which cannot replicate in *R. eutropha* H16 and therefore, after the triparental cell mixture was plated out on TSB plates with [200 µg mL^{-1}] kanamycin and [20 µg mL^{-1}] gentamycin, only *R. eutropha* H16 transconjugants carrying the CelA secretion plasmids, but not pRK2013 are able to grow.

To confirm the presence of the CelA secretion plasmids in *R. eutropha* H16, a Congo red assay with the whole cells was conducted. Following detection, the results of the assay already revealed diverse activity levels. *R. eutropha* H16 transconjugants carrying pKRSF1010-P_{tac}-pme-celA, pKRSF1010-P_{tac}-egl-celA, pKRSF1010-P_{tac}-RlpB-celA, and pKRSF1010-P_{tac}-iorB2-celA only showed weak activities compared to *R. eutropha* H16 harboring the remaining CelA secretion plasmids. The strongest activites could be achieved with the following CelA secretion plasmids: pKRSF1010-P_{tac}-F504_2793-celA, pKRSF1010-P_{tac}-cbhA-celA, pKRSF1010-P_{tac}-aac-celA, and pKRSF1010-P_{tac}-amiC-celA. The larger sizes of those halos already indicated a higher excretion of CelA into the extracellular medium under the influence of the signal peptides CbhA, Aac, F504_2793, and AmiC.

For quantitative comparison of the secreted CelA activity levels by the individual signal peptides, a pHBAH assay was conducted. Because the pHBAH assay measured the liberated reducing sugar concentrations after hydrolyzation of CMC by CelA, the subsequent fermentations for the secretion assays had to be performed in a glucose-free environment. Therefore, the main cultures were set up in LB media supplemented with 1 % glycerol and after 15 h incubation the O_{600} values were determined. The growth behaviour of the *R. eutropha* H16 transconjugants carrying the CelA secretion plasmids is in accordance to the growth of the empty vector control, pKRSF1010-P_{tac}-Δ49. The only CelA secretion plasmid, where significantly slower growth could be repeatedly observed, was pKRSF1010-P_{tac}-NosL-celA. The lower OD_{600} values (2.74 – 3.61 compared to 5.88 – 7.39) could be caused by too much cellular burden due to the presence of a strong signal peptide leading to cell lysis. However, in an effort to confirm cell lysis by visualizing the stressed shape of the *R. eutropha* H16 transconjugants, no abnormalities could be seen in either one of the *R. eutropha* H16 carrying one of the CelA secretion plasmids.

For the confirmation of CelA secretion by *R. eutropha* H16, the cell-free supernatants of the fermentation broths were then collected and the following assays were carried out: Bradford protein assay to determine the total protein amount in the supernatants, Congo red assay to confirm the presence of functional CelA in the supernatants, as well as, pHBAH assay to quantitatively compare the CelA levels based on the secretion efficiencies of the diverse signal peptides.

Based on the results of the Bradford protein assay, the total protein amount in the cell-free supernatants of *R. eutropha* H16 transconjugants carrying CelA secretion plasmids did not increase compared to the empty vector control [~ 15 µg mL^{-1}] and sometimes even lower protein concentrations were determined. In the second and third fermentation round nearly all supernatants had a protein concentration of 13.4 – 19.9 µg mL^{-1}. The only construct showing significantly lower protein concentrations in the supernatant, was pKRSF1010-P_{tac}-NosL-celA caused by the lower OD_{600} values of the fermentation broths and following OD_{600} normalization, the protein concentrations in the supernatant of pKRSF1010-P_{tac}-NosL-celA lies within the range of the protein concentrations (1.9 – 3.4 µg mL^{-1} OD_{600}^{-1}) of the other CelA secretion plasmids (data not shown). Furthermore, intracellular CelA could not be detected via a SDS-PAGE and therefore, it can be concluded that the amount of expressed and secreted CelA is very low and could not be efficiently detected by the Bradford protein assay or the SDS-PAGE.

To determine functional CelA in the cell-free supernatant of *R. eutropha* H16, first a Congo red plate assay was conducted with 100 µL supernatants and the activity was compared to the activity of 1.2 µg purified CelACcHis. The strongest activity could be achieved with the supernatant of *R. eutropha* H16 [pKRSF1010-P_{tac}-F504_2793-celA] (Tat-specific SP), where the lighter halo (indicating CelA activity) had a similar radius than the positive control (see Figure 28). Further signal peptides facilitated good secretion of functional CelA, such as *cbhA*, and *aac* for Sec-specific translocation, as well as, *amiC, RscNosZ*, and *F504_2437* for Tat-specific transolaction. The assay was also performed with pKRSF1010-P_{tac}-celAoCΔS and the supernatants revealed hardly any CelA activity. Thus, the possibility of CelA excretion due to cell lysis could be eliminated and the determined CelA activity levels were because of functional CelA secretion by *R. eutropha* H16. Furthermore, to quantitatively compare the secretion efficiency of the distinct signal peptides, the pHBAH assay was carried out with 30 µL of cell-free supernatants and the release of reducing sugars were measured after incubation with CMC. In regards to the results of the Congo red assay, similar activity levels could be observed within the same CelA secretion plasmids. The highest glucose concentrations could be measured in the enzyme reaction samples of *R. eutropha* H16 [pKRSF1010-P_{tac}-F504_2793-celA], followed by *R. eutropha* H16 [pKRSF1010-P_{tac}-F504_2437-celA], *R. eutropha* H16 [pKRSF1010-P_{tac}-cbhA-celA], *R. eutropha* H16 [pKRSF1010-P_{tac}-amiC-

celA], and *R. eutropha* H16 [pKRSF1010-P_{tac}-aac-celA]. By comparison of the amounts of released free reducing sugars following incubation with pKRSF1010-P_{tac}-F504_2793-celA (0.253 [mg mL^{-1}]) or 0.018 µg purified CelACcHis (0.325 [mg mL^{-1}]), the CelA concentration in the cell-free supernatant of *R. eutropha* H16 can be roughly estimated to be about 0.5 [µg mL^{-1}]. By calculating the enzymatic activity, as the amount of enzyme needed to release 1 µmol of reducing sugar per minute, the following units were determined: 1.56 [µmol min^{-1} mL^{-1}] for pKRSF1010-P_{tac}-F504_2793-celA and 1.215 [µmol min^{-1} mL^{-1}] for pKRSF1010-P_{tac}-F504_2437-celA. In comparison, Gupta et al. has selected the β-1,4-endoglucasnase, Endo5A (26 % similarity to CelA), for secretory production in *E. coli* and was able to measure endoglucanase activity levels of 0.15 [µmol min^{-1} mL^{-1}] in the extracellular fraction [83]. However, the 10-fold increase of activity in the supernatant of *R. eutropha* H16 depends mainly on the higher specific activity of CelA (~250 [U mg^{-1}] compared to ~20 [U mg^{-1}] Endo5A). Still, it can be stated that the constitutive secretory production of CelA in *R. eutropha* H16 can be compared to the expression in *E. coli* under tightly regulated expression conditions. Additionaly, the CelA activity levels can be compared to the activity levels of two another endoglucanase, TaCel5A, when secreted by *P. pastoris* under the control of the constitutive GAP promoter. In tube scale, the measured activities against CMC, varied from ~3.3 – 4.7 [µmol min^{-1} mL^{-1}] and further up-scaling of the cultivation led to an increase of ~10 [µmol min^{-1} mL^{-1}] [84].

In two-step secretion systems, the secretion efficiency depends on the secretion rate across the IM and on the secretion rate across the OM. Therefore, there is a chance that the overall protein secretion efficiency is limited due to inefficient translocation across the OM and recombinant protein might be accumulated in the periplasm. To exclude this possibility, the Congo red assay was also performed with the periplasmatic fraction of *R. eutropha* H16 transconjugants and the periplasmic fractions exhibited similar cellolytic activities as the extracellular fractions. Strong activity levels were revealed by pKRSF1010-P_{tac}-F504_2793-celA, followed by pKRSF1010-P_{tac}-F504_2437-celA, pKRSF1010-P_{tac}-cbhA-celA, pKRSF1010-P_{tac}-amiC-celA, and pKRSF1010-P_{tac}-aac-celA suggesting that the overall yield of secreted CelA could be increased by enhancing the membrane permeability of the OM (see 5 Conclusion and outlook). The periplasmic fractions of pKRSF1010-P_{tac}-pme-celA, pKRSF1010-P_{tac}-egl-celA, pKRSF1010-P_{tac}-iorB2-

celA, and pKRSF1010-P_{tac}-RlpB-celA were not qualified of hydrolysing a large amount of CMC and hence, no CelA activity could be detected in the periplasm. In correlation with the activity assays of the cell-free supernatant, which showed no CelA activities as well, it can be stated that those individual signal peptides were not capable of facilitating the first step of translocation across the IM.

In summary, the secretion of functional CelA by *R. eutropha* H16 could be achieved by a number of signal sequences. Furthermore, both the Sec- and the Tat- translocase were proven to be functional and good activity levels could be achieved. The best signal peptide for CelA secretion was the Tat- specific F504_2793. Similar CelA secretion levels could also be achieved by F504_2437, AmiC (both Tat- specific), CbhA and Aac (both Sec-specific). Furthermore, no preference for the native origin of the signal peptide can be observed as both NosZ signal peptides (from *R. eutropha* H16 and *R. solanacearum*) show similar CelA activity levels in the cell-free supernatant of *R. eutropha* H16 transconjugants. The amount of secreted CelA could not be detected and based on a roughly estimation is only about 0.5 [µg mL^{-1}] and thus, the improvement of the expression levels should be considered to be one of next steps (see 5 Conclusion and outlook).

4.3 Secretion of Lev by *Ralstonia eutropha* H16

Levanase isolated from *B. subtilis* has a molecular weight of ~73 kDa, and thus, is the largest reporter protein for the examination of the recombinant secretory production by *R. eutropha* H16. Furthermore, the expression of Lev, under the control of a *B. subtilis* promoter, has already been proven to be possible as functional Lev could be detected in the intracellular fraction of *R. eutropha* H16 cells [85]. The mutation rate during the construction of the Lev secretion was quite high, repeatedly exhibiting insertion or transposon elements in between of the signal sequence and the reporter gene and only 13 signal sequences (*pme, egl, tek, PqaA, F504_4738, F504_2783, NosL, F504_2199, RlpB, amiC, nasF, iorB2,* and *RscNosZ*) could be successfully cloned into the backbone of pCRSF1010-P_{tac}-levΔS after digestion with *Nde*I and *Spe*I. The unsuccessful ligation of Lev secretion plasmids containing the signal sequences *pehB, cbhA, aac, treA, F504_2437, F504_2793, ReH16NosZ* and *pehC* might be because of the extra cellular burden on *E. coli* Top10 cells when put under constitutive expression conditions along with

subsequent initiation of strong secretion. However, from the remaining signal peptides only the following two have been reported to be particularly strong signal peptides in *R. solanacearum*: PehB and CbhA. Furthermore, F504_2793 has shown great potential in the secretion of CelA. Therefore, to clarify if the unsuccessful construction of the particular Lev secretion plasmids is caused by strong secretion potential, the missing signal peptides will be examined under tightly regulated expression conditions leading to a decrease of cellular stress.

Following the positive sequence verification, the constructed Lev secretion plasmids were then transferred into *R. eutropha* H16 by conjugation with *E. coli* S17-1. However, transformation problems similar to the observations seen with the CelA secretion plasmids (see 4.2 Secretion of CelA by *Ralstonia eutropha* H16) occurred and not all Lev secretion plasmids were possible to be transformed into *E. coli* S17-1 and therefore, had to be transferred via triparental mating with the helper plasmid pRK2013 (Table 28). As described above, the unsuccessful transformation of *E. coli* S17-1 with some Lev secretion plasmids might be due to constitutive expression and higher simultaneous secretion of Lev that has been initiated from the beginning of growth, leading to the toxic accumulation of Lev in the periplasm of *E. coli* S17-1. In *E. coli* Top10 the integration of the lac^q into the genome leads to the suppression of the expression, thereby enabling the transformation of those particular Lev secretion plasmids into *E. coli* Top10.

To verify the secretion of Lev by *R. eutropha* H16, the setup of the secretion assays for Lev detection was in accordance to previous secretion assays for hGH and CelA. First, after 15 h incubation, the OD_{600} values of the main cultures were determined and the fermentation broths were then spun down and the cell-free supernatant was harvested. The growth behaviour of *R. eutropha* H16 transconjugants carrying Lev secretion plasmids varies considerably and the presence of constitutive expression and simultanous secretion of Lev might prohibit the growth of *R. eutropha* H16 due to increased cellular burden. By correlating the calculated total protein concentrations with the individual OD_{600} values, this claim could be encouraged as transconjugants showing slower growth, exhibit high concentrations of total proteins in the cell-free supernatant, suggesting that due to cell death the intracellular proteins are also released into the extracellular fraction. For further clarification, the cells should be investigated under the microscope. Another possibility for reduced growth might be the expression of

heterologous protein. However, none of *R. eutropha* H16 transconjugants which grew significantly slower displayed any Lev activity in the following experiments.

To determine if functional Lev could be exported into the extracellular fraction, the levanase activity assay was performed and the released glucose molecules were determined following incubation with sucrose. Only five signal peptides (NosL, F504_2199, AmiC, RscNosZ and F504_2783) were able to successfully secrete functional Lev, however only very low activity levels could be achieved when compared to the positive control, *P. pastoris* CBS 7435 mutS *aox1*::α-Lev-*HIS4*: 0.73 [µmol min^{-1} mL^{-1}] for *F504_2199*, 0.40 [µmol min^{-1} mL^{-1}] for *NosL*, 0.38 [µmol min^{-1} mL^{-1}] for *F504_2783*, 0.33 [µmol min^{-1} mL^{-1}] for *amiC*, and 0.21 [µmol min^{-1} mL^{-1}] for *RscNosZ*, whereas *P. pastoris* CBS 7435 mutS *aox1*::α-Lev-*HIS4* reached levels of 3.47 [µmol min^{-1} mL^{-1}]. From those five, only one signal sequence (*F504_2783*) was specific for the Sec translocase, while the others were specific for the Tat-pathway suggesting that Lev folds quickly in the cytoplasm of *R. eutropha* H16. Therefore, the translocation across the IM via the Sec-dependent pathway would have to be very efficient and fast.

In summary, the secretion of Lev could be achieved with some signal peptides specific for both the Sec- and the Tat- secretory pathway. However, the yield is still very poor and should be enhanced by the application of a stronger promoter under tightly regulated expression conditions. Furthermore, a tight regulation of expression seems to be necessary for the secretion of Lev as the immediate start of expression and secretion influences the growth of *R. eutropha* H16 in a considerable way.

In comparison of the successful secretion of CelA with the secretion of Lev, different signal peptides were able to secrete the individual reporter proteins, revealing that the interaction between reporter protein and signal peptide plays a key element in the successful translocation of the protein of interest [22]. However, the strongest signal sequences for both CelA and Lev secretion cannot be compared as it was not possible to clone them into the respective secretion plasmids.

5 Conclusion and outlook

Altogether, the functionality of the Sec- and Tat- translocase could be proven to be used for the secretory production of heterologous proteins of prokaryotic origin. It was also verified, that the observed excretion of the reporter proteins was truly due to protein secretion rather than being released by OM leakage, as negative secretion controls (reporter genes without signal sequence) were constructed and activity assays with the individual negative controls did not display any activities. Thus, the functionality of the T2SS machinery could also be confirmed for the utilization of secretory recombinant protein production. Therefore, a huge step in the establishment of *R. eutropha* H16 as an alternative secretory production host could be achieved, and further studies should focus on enhancing the protein levels in the extracellular fractions.

To increase the protein concentrations in the extracellular fraction, several strategies could be applied. The first and most obvious one, is the application of a stronger promoter. So far, P_{J5} has been the strongest promoter described in *R. eutropha* H16 [10]. However, beforehand a tightly regulated expression system should be developed, as otherwise, the stronger expression and simultaneous secretion from the beginning of growth, might lead to cell death due to cellular burden. Furthermore, when increasing the expression rate several other factors (e.g. inclusion body formation, folding errors etc.) have to be contemplated and harmonizing conditions should be applied.

The extracellular protein yield could also be increased by enhancing the periplasmic release at the end of the fermentation. This could be either achieved by using detergents or lysozyme to promote the leakage of the OM or by osmotic shock [13, 21]. Furthermore, in *E. coli* the co-expression of the *E. coli* bacteriocin release protein (BRP) could increase the overall yield of extracellular proteins [81]. BRP activates the OM protein phospholipase A leading to the formation of permeable zones in the OM. While *R. eutropha* H16 does not exhibit a similar protein to BRP, it does feature a similar protein to phospholipase A [H16_A1139] and other inducing triggers, such as temperature shock or polymixin B exposure, could be used to initiate the OM leakage [86].

Furthermore, the efficiency of the protein secretion can be amplified by the co-expression of translocase elements. Tat-specific translocation can be blocked by

cytoplasmic accumulation of the protein precursor, as well as, can be limited by the amount of TatC and TatB, which both act as bottlenecks in the efficient export of recombinant proteins. In *E. coli* the blockage of the TatABC translocase could the relieved by the coexpression of the phage shock protein (PspA) [87], whereas in *Corynebacterium glutamincum* the secretory yield of pro-PG by Tat-specific secretory production could be improved by a threefold by the overexpression of TatABC [29]. The yield of secreted human interleukin-6 (hIL) via the Sec-dependent translocation in *E. coli* could be increased by the co-expression of the Sec translocase elements, SecE and SecY [88].

Another improvement that could be executed, is the co-expression of molecular chaperones and other enzymes involved in disulfide bond formation. Thereby, the correct folding of the recombinant proteins can be supported and the spectrum of secreted proteins can be expanded to include more mammalian proteins [22].

In summary, within this work it could successfully be demonstrated that *R. eutropha* H16 is capable of recombinant secretory production of heterologous proteins and therefore, an important first step was established in making *R. eutropha* H16 a host for recombinant protein secretion.

6 References

[1] Makkar N.S., and Casida L.E. 1987. "*Cupiavidus necator* gen. nov., sp. Nov.: a nonobligate bacterial predator of bacteria in soul" *International Journal of systematic bacteriology* 37 (4): 323-326

[2] Pohlmann A., Fricke W.F., Reinecke F., Kusian B., Liesegang H., Cramm R., Eitinger T., Ewering C., Pötter M., Schwartz E., Strittmatter A., Voß I., Gottschalk G., Steinbüchel A., Friedrich B., and Bowien B. 2007. „Genome sequence of the bioplastic-producing „Knallgas" bacterium *Ralstonia eutropha* H16" *Nature Biotechnology* 24 (1): 1257-1262

[3] Lee S.Y. 1996. "Bacterial polyhydroxyalkanoate" *Biotechnology and Bioengineering* 49: 1-14

[4] Delamarre S.C., and Batt C.A. 2006. "Comparative study of promoters for the production of polyhydroxyalkanoates in recombinant strains of *Wautersia eutropha*" *Applied Microbiology and Biotechnology* 71: 668-679

[5] Friedrich B., and Schwartz E. 1993. "Molecular biology of hydrogen utilization in aerobic chemolithotrophs.," *Annual review of microbiology* 47: 351–83

[6] Burgdorf T., Lenz O., Buhrke T., van der Linden E., Jones A.K., Albracht S.P.J., and Friedrich B. 2005. "[NiFe]-hydrogenases of *Ralstonia eutropha* H16: modular enzymes for oxygen-tolerant biological hydrogen oxidation.," *Journal of molecular microbiology and biotechnology* 10 (2–4): 181–96

[7] Srinivasan S., Barnard G.C., and Gerngross T.U. 2002. "A novel high-cell-density protein expression system based on *Ralstonia eutropha*" *Applied and Environmental Microbiology* 68 (12): 5925 - 5932

[8] Barnard G.C., Henderson G.E., Srinivasan S., Gerngross T.U. 2004. „High level recombinant protein expression in *Ralstonia eutropha* H16 using T7 RNA polymerase based amplification" *Protein Expression and Purification* 38: 264-271

[9] Fukui T., Ohsawa K., Mifune J., Orita L., Nakamura S. 2011. "Evaluation of promoters for gene expression in polyhydroxyalkanoate-producing *Cupriavidus necator* H16" *Applied Microbiology and Biotechnology* 89: 1527-1536

[10] Gruber S., Hagen J., Schwab H., and Köfinger P. 2014. „Versatile and stable vectors for efficient gene expression in *Ralstonia eutropha* H16" *Journal of Biotechnology* 186: 74-82

[11] Bi C., Su P., Müller J., Yeh Y.-C., Chhabra S.W., Beller H.R., Singer S.W., and Hillson N.J. 2013. "Development of a broad-host synthetic biology toolbox for *Ralstonia eutropha* and its application to engineering hydrocarbon biofuel production" *Microbial Cell Factories* 12: 107

[12] Barnard G.C., McCool J.D., Wood D.W., and Gerngross T.U. 2005. “Integrated recombinant protein expression and purification platform based on *Ralstonia eutropha*” *Applied and Environmental Microbiology* 71 (10): 5735-5742

[13] Bernhard M., Friedrich B., and Siddiqui R.A. 2000. “Ralstonia eutropha TF93 is blocked in tat-mediated protein export” *Journal of Bacteriology* 182 (3): 581-588

[14] Kanehisa Laboratories. n.d. Kyoto Encyclopedia of Genes and Genomes (KEGG). Retrieved February 13, 2015 from http://www.genome.jp/kegg-bin/show_pathway?org_name=reh&mapno=03070&mapscale=&show_description=hide

[15] Poueymiro M., and Genin S. 2009. “Secreted proteins from *Ralstonia solanacearum*: a hundred tricks to kill a plant” *Current Opinions in Microbiology* 12: 44-52

[16] González E.T., Brown D.G., Swanson D.G., and Allen C. 2007. ”Using the *Ralstonia solanacearum* Tat secretome to identify bacterial wilt virulence factors” *Applied and Environmental Microbiology* 72 (12): 3779-3786

[17] M. Salanoubat M., Genin S., Artiguenave F., Gouzy J., Mangenot S., Arlat M., Billault A., Brottier P., Camus J.C., Cattolico L., Chandler M., Choisne N., Claudel-Renard C., Cunnac S., Demange N., Gaspin C., Lavie M., Moisan A., Robert C., Saurin W., Schiex T., Siguier P., Thébault P., Whalen M., Wincker P., Levy M., Weissenbach J., and Boucher C.A. 2002. “Genome sequence of the plant pathogen *Ralstonia solanacearum*” *Nature* 415: 497-502

[18] Liu H., Zhan S., Schell M.A., and Denny T.P. 2005. “Pyramiding unmarked deletions in *Ralstonia solanacearum* shows that secreted proteins in addition to plant cell-wall-degrading enzymes contribute to virulence” *Molecular Plant-Microbe Interactions* 18 (12): 1296-1305

[19] Zuleta M.C. 2007. “Identification of Ralstonia solanacearum exoproteins secreted by the type two secretion system using proteomic techniques” Master’s Thesis. University of Georgia: USA

[20] Tan N.S., Ho B., and Ding J.L. 2002. “Engineering of a novel secretion signal for cross-host recombinant protein expression” *Protein Engineering* 15 (4): 337-345

[21] Zhang G., Brokx S., and Weiner J.H. 2005. “Extracellular accumulation of recombinant proteins fused to the carrier protein YebF in *Escherichia coli” Nature Biotechnology* 24: 100-104

[22] Yoon S.H., Kim S.K. and Kim J.F. 2010. “Secretory Production of Recombinant Proteins in *Escherichia coli*” *Recent Patents on Biotechnology* 4: 23-29

[23] Low K.O., Mahadi N.M., and Illias R.Md. 2013. Optimisation of signal peptide for recombinant protein secretion in bacterial hosts. *Applied Microbiology and Biotechnology* 97: 3811-3826

[24] Mergulhao F.J., Summers D.K., and Monteiro G.A. 2005. “Recombinant protein secretion in *Escherichia coli*” *Biotechnology Advances* 23 (3): 177-202

[25] Fisher A.C., Kim J.-Y., Perez-Rodriguez R., Tullman-Ercek D., Fish W.R., Henderson L.A., and DeLisa M.P. 2008. “Exploration of twin-arginine translocation for expression and purification of correctly folded proteins in *Escherichia coli*” *Microbiological Biotechnology* 1 (5): 403 – 415

[26] Hahn H.P., and von Specht B.-U. 2003. „Secretory delivery of recombinant proteins in attenuated *Salmonella* strains: potential and limitations of Type I protein transporters“ *FEMS Immunology and Medical Microbiology* 37: 87-98

[27] Shaerlaekens K., Lammertyn E., Geukens N., De Keersmaeker S., Anné J., and Van Mellaert L. 2004. „Comparison of the Sec and Tat secretion pathways for heterologous protein production by *Steptomyces lividans*“ *Journal of Biotechnology* 112: 279-288

[28] Cusano A.M., Parrilli E., Marino G., and Tutino M.L. 2006. “A novel genetic system for recombinant protein secretion in the antarctic *Pseudoalteromonas haloplanktis* TAC125” *Microbial Cell Factories* 5: 40

[29] Kikuchi Y., Itaya H., Date M., Matsui K. and Wu L.-F. 2008. “TatABC Overexpression Improves *Corynebacterium glutamicum* Tat-Dependent Protein Expression” *Applied and Environmental Microbiology* 75 (3): 603-607

[30] Records A.R. “The type VI secretion system: A multipurpose delivery system with a phage-like machinery” *Molecular Plant-Microbe Interactions* 24 (7): 751-757

[31] Delepelaire P. 2004. “Type I secretion in gram-negative bacteria” *Biochimica et Biophysica Acta* 1694: 149-161

[32] Cornelis G.R., and Van Gijsegem F. 2000. “Assembly andfunction of type III secretory systems” *Annual Review of Microbiology* 54: 735-774

[33] Gosh P. 2004. “Process of protein transport by the type III secretion system” *Microbiology and Molecular Biology Reviews* 68 (4): 771-795

[34] Galán J.E., and Wolf-Watz H. 2006. “Protein delivery into eukaryotic cells by type III secretion machines” *Nature* 444 (7119): 567-573

[35] Fronzes R., Christie P.J. and Walksman G. 2009. “The structural biology of type IV secretion systems” *Nature Reviews Microbiology* 7 (10): 703-714

[36] Cascales E., and Christie P.J. 2003. “The versatile bacterial Type IV secretion systems” *Nature Reviews Microbiology* 1 (2): 137-149

[37] Burns D.L. 2003. “Type IV transporters of pathogenic bacteria” *Current Opinion in Microbiology* 6: 29-34

[38] Silverman J.M., Brunet Y.R., Cascales E. and Mougous J.D. 2012. “Structure and regulation of the type VI secretion system” *Annual Reviews in Microbiology* 66: 453-472

[39] Cascales E. 2008. “The type VI secretion toolkit” *EMBO reports* 9: 735-141

[40] Bingle L.E.H., Baily C.M. and Pallen M.J. 2008. “Type VI secretion: a beginner’s guide” *Current Opinion in Microbiology* 11: 3-8

[41] Jani A.J., and Cotter P.A. 2010. “Type VI secretion: Not just for pathogenesis Anymore” *Cell Host & Microbe* 8 (1): 2-6

[42] De Buck E., Anné J., and Lammertyn E. 2007. “The role of protein secretion systems in the virulence of the intracellular pathogen *Legionella pneumophilia*” *Microbiology* 153 (12): 3948-3953

[43] Filloux A. 2004. “The underlying mechanisms of type II protein secretion” *Biochimica et Biophysica Acta* 1694: 163-179

[44] Hederson I.R., Navarro-Garcia F., Desvaux M., Fernandez R.C., and Aldeen D.A. 2004. “The Type V protein secretion pathway: the autotransporter story” *Microbiology and Molecular Biology Reviews* 68 (4): 692-744

[45] Sandkvist M. 2001. “Biology of type II secretion” *Molecular Microbiology* 40 (2): 271-283

[46] Tseng T.-T., Tyler B.M., and Setubal J.C. 2009. “Protein secretion systems in bacterial-host associations, and their description in the Gene Ontology” *BMC Microbiology* 9 (Suppl I): S2

[47] Van Ulsen P., ur Rahman S., Jong W.S.P., Daleke-Schermerhorn M.H., and Luirink J. 2013. “Type V secretion: From biogenesis to biotechnology” *Biochimica et Biophysica Acta* 1843: 1592-1611

[48] Leo J.C., Grin I., and Linke D. 2012. “Type V secretion: mechanism(s) of autotransport through the bacterial outer membrane” *Philosophical Transactions of the Royal Society* 367: 1088-1101

[49] du Plessis D.J..F., Nouwen N., and Driessen A.J.M. 2011. “The Sec translocase” *Biochimia et Biophysica Acta* 1808: 851-865

[50] Natales P., Brüser T., and Driessen A.J.M. 2007. „Sec- and Tat-mediated protein secretion across the bacterial cytoplasmic membrane – Distinct translocases and mechanisms“ *Biochimica et Biophysica Acta* 1778: 1735-1756

[51] Lee P.A., Tullman-Ercek D. and Georgiou G. 2006. “The Bacterial Twin-Arginine Translocation Pathway” *Annual Review of Microbiology* 60: 373-395

[52] Ulbrandt N.D., Scotti P.A., and Bernstein H.D. 1997. “The *E. coli* signal recognition particle is required for the insertion of a subset of inner membrane proteins” *Cell* 88: 187-196

[53] Pugsley A.P., Francetic O., Driessen A.J., and de Lorenzo V. 2004. “Getting out: protein traffic in prokaryotes” *Molecular Microbiology* 52 (1): 3-11

[54] Pugsley A.P. 1993. “The complete general secretory pathway in Gram-negative bacteria” *Microbiological Reviews* 57 (1): 50-108

[55] Berks B.C., Palmer T. and Sargent F. 2005. “Protein targeting by the bacterial twin-arginine translocation (Tat) pathway” *Current Opinion in Microbiology* 8: 174-181

[56] Brüser T. 2007. “The twin-arginine translocation system and its capability for protein secretion in biotechnological protein production” *Applied Microbiology and Biotechnology* 76: 35-45

[57] Alami M., Lüke I., Deitermann S., Eisner G., Koch H.-G., Brunner J., and Müller M. 2003. „Differential interactions between a twin-arginine signal peptide and its translocase in *Escherichia coli*“ *Molecular Cell* 12: 937—946

[58] Albianik A.M., Matos C.F.R.O., Branston S.D., Freedman R.B., Keshavarz-Moore E., and Robinson C. 2013. “High-level secretion of a recombinant protein to the culture medium with a *Bacillus subtilis* twin-arginine translocation system in *Escherichia coli*” *Febs Journal* 280 (16): 3810-3821

[59] Moore W.V., Wohnlich L.P., and Fix J.A. 1983. “Role of disulfide bonds in human growth hormone binding and dissociation in isolated rat hepatocytes and liver plasma membranes” *Endocrinology* 112 (6): 2152-2158

[60] Junnila R.K., and Kopchick J.J. 2013. “Significance of the disulphide bonds of human growth hormone” *Endokrynologia Polska* 64 (4): 300-304

[61] Friedl M. 2014. “Characterization of the *Sorangium cellulosum* endocellulase CelA” Master’s Thesis. TU Graz: AT

[62] Wanker E., Huber A. and Schwab H. 1995 „Purification and Characterization of the *Bacillus subtilis* Levanase produced in *Escherichia coli*“ *Applied and Environmental Microbiology* 61 (5): 1953-1958

[63] Kunst F., Steinmetz M., Lepesant J.-A. 1977. „Presence of a third sucrose hydrolyzing enzyme in Bacillus subtilis: constitutive levanase synthesis by mutants of *Bacillus subtilis* Marburg 168“ *Biochimie* 59: 287-292

[64] Wanker E., Schörgendorfer K. and Schwab H. 1991. „Expression of the Bacillus subtilis levanase gene in *Escherichia coli* and *Saccharomyces cerevisiae*“ *Journal of Biotechnology* 18: 243-254

[65] Computational Genetics group, University of Thessaly. n.d. PRED-TAT. Retrieved November 16, 2014 from http://www.compgen.org/tools/PRED-TAT/#TOC-Run-PRED-TAT

[66] Bagos P.D., Nikolaou E.P., Liakopoulos T.D., and Tsirigos K.D. 2010. “Compined prediction of Tat and Sec signal peptides with Hidden Markov Models” *Bioinformatics* 26 (22): 2811-2817

[67] Figurski D.H., and Helinski D.R. 1979. “Replication of an origin-containing derivative of plasmid RK2 dependent on a plasmid function provided in trans” *Proceedings of the National Acadamy of Sciences*. USA 76: 1648-1652

[68] New Englands Biolabs® Inc. n.d. NEB Tm calculator. Retrieved January 5, 2015 from http://tmcalculator.neb.com/#!/

[69] Thermo Fisher Scientific Inc. n.d. DoubleDigest. Retrieved January 5, 2015 from http://www.thermoscientificbio.com/webtools/doubledigest/

[70] Bradford M. 1976. “A rapid and sensitive method for the quantification of microgram quantities of proteins utilizing the principle of protein-dye binding” *Analytical Biochemistry* 72 (1-2): 248-254

[71] Fic E., Kedracka-Krok S., Jankowska U., Pirog A., and Dziedzicka-Wasylewska M. 2010. “Comparison of protein precipitation methods for various rat brain structures prior to proteomic analysis” *Electrophoresis* 31: 3573-3579

[72] Wessel D., and Flügge U.I. 1984. “A method for the quantitative recovery of protein in dilute solution in the presence of detergents and lipids” *Analytical Biochemistry* 138 (1): 141-143

[73] Sazci A., Radford A., and Erenler K. 1986. „Detection of cellulolytic fungi by using congo red as an indicator: a comparative study with the dinitrosalicyclic acid reagent method“ *Journal of Bacteriology* 61: 559-562

[74] Teather R.M., and Wood P.J. 1982. “Use of congo red-polysaccharides interaction in enumeration and characterization of cellulolytic bacteria from the bovine rumen” *Applied and Environmental Microbiology* 43 (4): 777-780

[75] Mellitzer A., Glieder A., Weis R., Reisinger C., and Flicker K. 2012. „Sensitive high-throughput screening for the detection of reducing sugars“ *Journal of Biotechnology* 7: 155-162

[76] Cao Y., Tian B., Liu Y., Cai L., Wang H., Lu N., Wang M., Shang S., Luo Z., and Shi J. 2013. “Genome sequencing of *Ralstonia solanacearum* FQY_4, isolated from a bacterial wilt nursery used for breeding crop resistance” *Genome Announcements* 1 (3): e00125-13

[77] Becker G.W., and Hsiung H.M. 1986. “Expression, secretion and folding of human growth hormone in *Escherichia coli*” *FEBS Letters* 204 (1): 145-150

[78] Ecamilla-Trevino L.L., Viader-Salvadó J.M., Barrera-Saldana H.A., and Guerrero-Olazarán M. 2000. “Biosynthesis and secretion of recombinant human growth hormone in *Pichia pastoris*” *Biotechnology Letters* 22: 109-114

[79] Hahm M.S., and Chung B.H. 2001. “Secretory expression of human growth hormone in *Saccharomyces cerevisiae* using three different leader sequences” *Biotechnology and Bioprocess Engineering* 6 (4): 306-309

[80] Cheah K.-C., Harrison S., King R., Crocker L., Wells J.R.E., and Robins A. 1994. “Secretion of eukaryotic growth hormones in *Escherichia coli* is influenced by the sequence of the mature proteins” *Gene* 138: 9-15

[81] Hsiung H.M., Cantrell A., Luirink J., Oudega B., Veros A.J., and Becker G.W. 1989. “Use of bacteriocin release protein in *E. coli* for excretion of human growth hormone into the culture medium” *Biotechnology* 7: 267-271

[82] Hoffmann F., and Rinas U. 2004. „Stress induced by recombinant protein production in Escherichia coli“ *Advanced Biochemial Engineering and* Biotechnology 89: 73-92

[83] Gupta S., Adlakha N., and Yazdani S.S. 2012. “Efficient extracellular secretion of an endoglucanase and a β-glucosidase in *E. coli*” *Protein Expression and Purification* 88: 20-25

[84] Várnai A., Tang C., Bengtsson O., Atterton A., Mathiesen G., and Eijsink V.G.H. 2014. “Expression of endoglucanases in *Pichia pastoris* under control of the GAP promoter. *Microbial Cell Factories* 13: 57.

[85] Friehs K., and Lafferty R.M. 1989. “Cloning and expression of the levanase gene in *Alcaligenes eutrophus* H16 enables the strain to hydrolyze sucrose” *Journal of Biotechnology* 10: 285-292

[86] Snijder H.J., and Dijkstra B.W. 2000. “Bacterial phospholipase A: structure and function of an integral membrane phospholipase” *Biochimica et Biophysica Acta* 1488: 91-1001

[87] DeLisa M.P., Lee P., Palmer T., and Georgiou G. 2004. “Phage shock protein PspA of *Escherichia coli* relieves saturation of protein export via the Tat pathway” *Journal of Bacteriology* 186 (2): 366-373

[88] Pérez-Pérez J., Márquez G., Barbero J.-L-, and Gutiérrez J. 1994. “Increasing the efficiency of protein export in *Escherichia coli*” *Nature Biotechnology* 12: 178-180

7 Appendix

7.1 Amino acid sequences of model proteins

Lev 73,32 kDa

MADSSYYDEDYRPQYHFTPEANWMNDPNGMVYYAGEYHLFYQYHPYGLQWGPMHWGHAVSK
DLVTWEHLPVALYPDEKGTIFSGSAVVDKNNTSGFQTGKEKPLVAIYTQDREGHQVQSIAYSNDKGR
TWTKYAGNPVIPNPGKKDFRDPKVFWYEKEKKWVMVLAAGDRILIYTSKNLKQWTYASEFGQDQG
SHGGVWECPDLFELPVDGNPNQKKWVMQVSVGNGAVSGGSGIQYFVGDFDGTHFKNENPPNKV
LWTDYGRDFYAAVSWSDIPSTDSRRLWLGWMSNWQYANDVPTSPWRSATSIPRELKLKAFTEGVR
VVQTPVKELETIRGTSKKWKNLTISPASHNVLAGQSGDAYEINAEFKVSPGSAAEFGFKVRTGENQFT
KVGYDRRNAKLFVDRSESGNDTFNPAFNTGKETAPLKPVNGKVKLRIFVDRSSVEVFGNDGKQVITDI
ILPDRSSKGLELYAANGGVKVKSLTIHPLKKVWGTTPFMSNMTGWTTVNGTWADTIEGKQGRSDG
DSFILSSASGSDFTYESDITIKDGNGRGAGALMFRSDKDAKNGYLANVDAKHDLVKFFKFENGAASVI
AEYKTPIDVNKKYHLKTEAEGDRFKIYLDDRLVIDAHDSVFSEGQFGLNVWDATAVFQNVTKES*

CelAoC 33,01 kDa

MTDGTPVERHGRLRVMNGNIVGEHGSPVQLKGMSLFWSQWSNYYNGNVVNSLADNWESTVVR
AAMGIEGEDGYLQDAGAQKAKAKTIADAAIAKGIYVILDWHDHNAHQHLDLAKSYFREVAQAYKNT
PNVIFEVFNEPLNTNTWPAVKSYAEAVISEIRGQGANNLVIVGSPNWSQDVDIAADNPLSDQNVAYT
LHFYANTHKASLRDKAQKAINKKLALFVTEWGTCSADGNGQLNLGESQTWLDFLDSHNISWANWS
LGDKAEACSALRPNANQMGNWNDNDLTESGKWVKAKIAE*

hGH 22,55 kDa

MKRFPTIPLSRLFDNAMLRAHRLHQLAFDTYQEFEEAYIPKEQKYSFLQNPQTSLCFSESIPTPSNREET
QQKSNLELLRISLLLIQSWLEPVQFLRSVFANSLVYGASDSNVYDLLKDLEEGIQTLMGRLEDGSPRTG
QIFKQTYSKFDTNSHNDDALLKNYGLLYCFRKDMDKVETFLRIVQCRSVEGSCGF*

7.2 Amino acid sequences of signal peptides

The yellow highlights mark the changes to the published sequence.

pehB
MQWLRSMRVARHPDDPASPIAAASCFEKWRSAMRQRKMGRGAALLLAAMLAGALVACGSGEGD
GASGLSVSGGTAQTTAQTAGSTCSPVNVRATSGTRSTVPQHPCVPALA | YD

pme
MGTTPIHGAAVPYPRNAIAFHQLHIPIKQKSLTPGILLTGKITMQSKTLYLKATALLGGCTVFAATALA |
VT

egl
MKVIHLSFPSLSISPFFHFVMKSRFRIAAANRMHRCMPLVAASMAALMLAGCGGGDGDTALSTAAA
| TD

cbhA
MTARMPPIQHYREGRVNILQSKKRIWKKLEYVMAASLLAGGALSAPAVHA | EA

Tek
MQAQFKKRALVLGVSASAIAALVACGGGGGSESG | AS

Aac
MTHGFALRNTLAVAALAALTGCAGTAHG | SR

treA
MLDPRGLARPSRFCPRIIYAGTSHIRRATAAALLAASLCALPACA | DV

PqaA
MMKRPLVAMTLTAAMLACPLALA | RA

F504_4738
MSKLPSFKVIAILTSFNLGAFHVTAHG | QD

F504_2783
MKKSLLAMAVLGAFAGAAHA | QS

NosL
MNADRRRLLLAALAGCAGTIAVAACGRQDAA | AP

F504_2199
MLETKAAQKWVRMSRRAMVGLTAAVALLGGLGAGNASA | QA

F504_2437
MQAFDNNRRRWMRQAGALAAGSVAASSGVWPLASR | AT

RlpB
MPSRRRFVLALAAALPAAGLLSACGFHLRG | NN

F504_2793
MQRRSIIGWRATLVAGVLGMAAFGAQA | ET

amiC
MLIKHLPTDQPDDSHLPSQARRQWLSRMARAGAGTVVLSLAGPQIAFG | AN

nasF
MAAPSKTDTPINPKRRRVLATVAGGSAMALIDPLVRAGAWA | AG

iorB2
MTADATAPRRGRRRFLLGALGIGGALVVGWGVLPPRSRLGDA | AD

pehC
MPKQKHSSARHAGRQAPHRPQSPARRAFVMWSGASAGAALLGTLPGCGGDGGSSATA | AT

RscNosZ
MMSKHPHSPSTQQDETPSVPGRRRFMNSAALAGLATVVACTDKGASAGSAA | AT

ReH16NosZ
MSKEKASIGNGPGGIGRRQFLGTAALAGLAGVVACTDKGAAPAAA | AV

7.3 Linear standard curve for the determination of the protein concentration

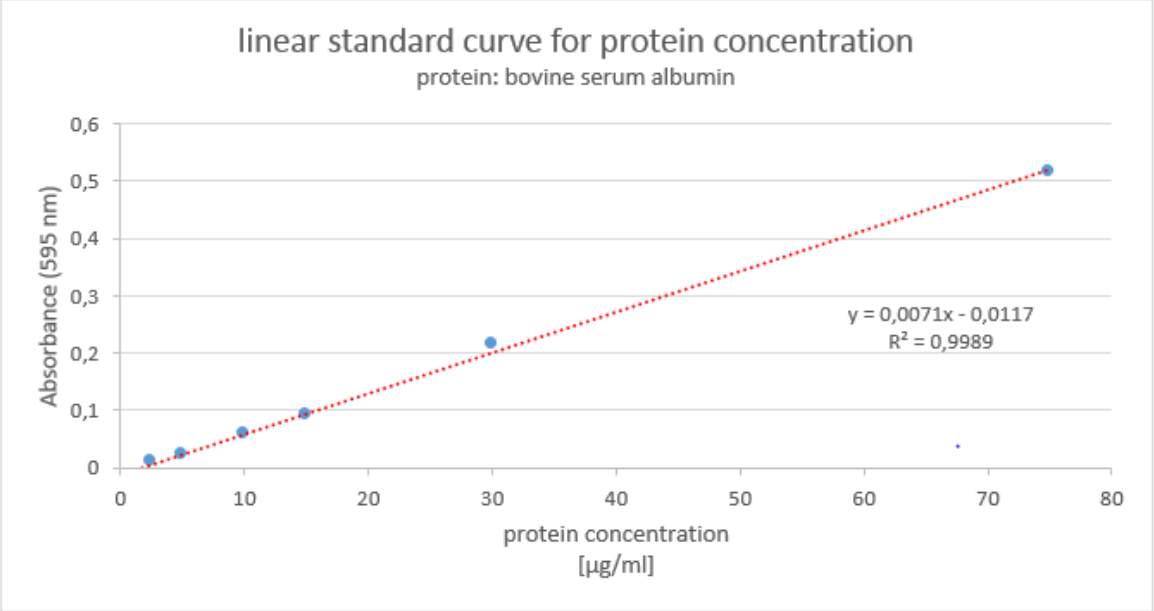

7.4 Linear standard curve for the determination of the glucose concentrations using the pHBAH assay

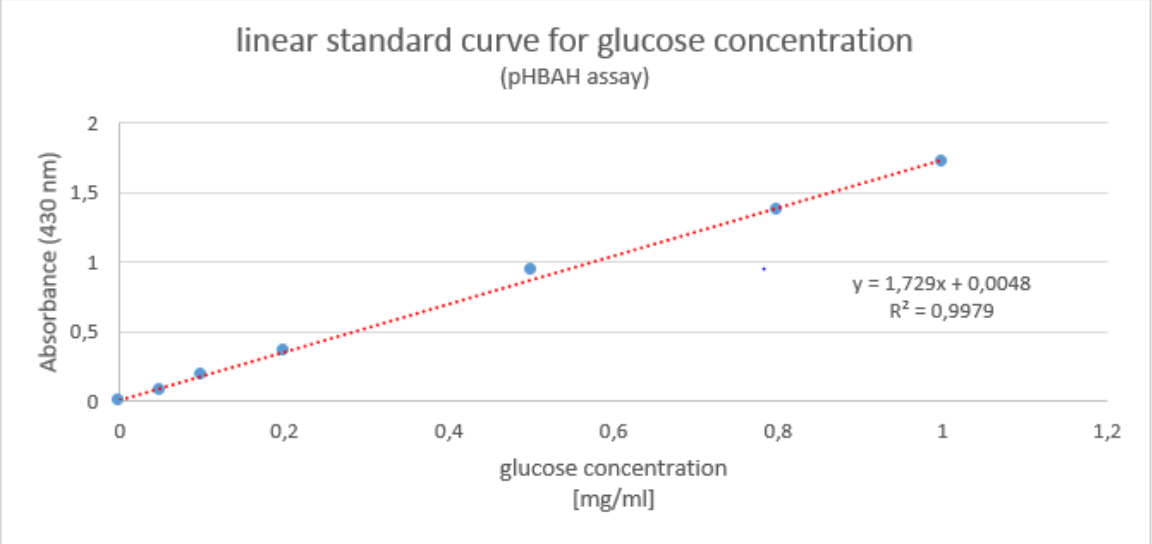

7.5 Linear standard curve for the determination of the glucose concentrations using the glucose-UV method